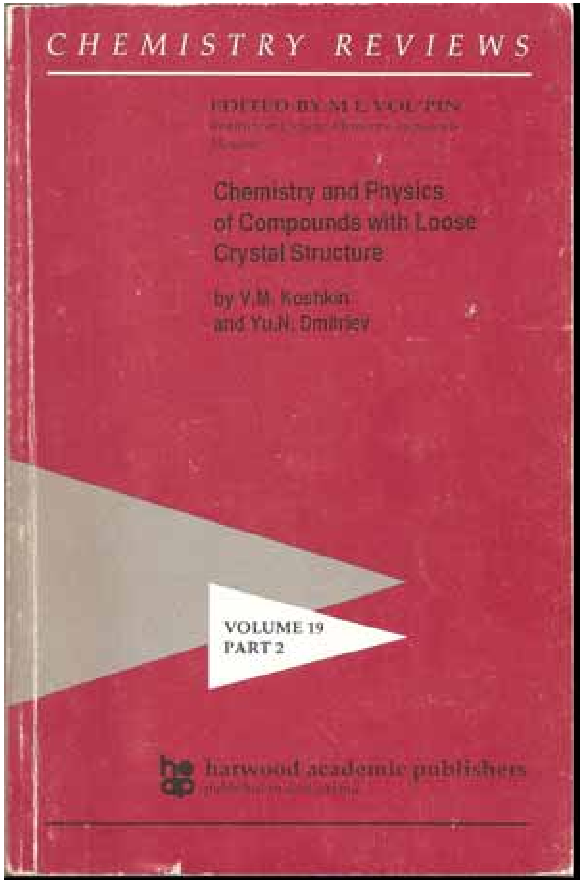

CHEMISTRY REVIEWS

EDITED BY M E VOL'PIN
[illegible]
[illegible]

Chemistry and Physics of Compounds with Loose Crystal Structure

by V.M. Koshkin
and Yu.N. Dmitriev

VOLUME 19
PART 2

harwood academic publishers
[illegible]

Chemistry Reviews
Volume 19

Edited by **M.E. Vol'pin**
Institute of Organo-Element Compounds, Moscow

Chemistry Reviews aims to highlight contributions from scientists in the former Soviet Union and topics will be chosen from a wide range of chemical themes with both fundamental and application emphasis, the sole criterion being that the topic represents an area of current scientific interest and activity.

Part 2:

Chemistry and Physics of Compounds with Loose Crystal Structure by **V.M. Koshkin and Yu.N. Dmitriev** systematically presents experimental data and theoretical models describing the unusual properties of crystalline compounds with loose structure. Falling into six categories these include (1) semiconductors and dielectrics with practically unlimited radiation stability, stoichiometric vacancies in crystalline compounds, general structural criterion of radiation stability of crystals; (2) features of chemical bonding in covalent semiconductors with loose structure; (3) semiconductor compounds, impurities in which are electrically and chemically inactive, theory of solubility of impurities localized in anion vacancies in the atomic state; (4) quantum dimensional effect and formation of miniband energy spectrum of electrons in intercalation layer inclusion compounds, intercalation thermodynamics; (5) new type of equilibrium lattice point defects, theory of instability zones of interacting defects in crystals; (6) [illegible] of various types of crystalline compounds with loose structure.

Forthcoming papers:

Anionic Polymerization of Dienes Induced by the Group I and the Group II Metals and their Complexes by A.A. Arest-Yakubovich

Polymerization of Dienes Induced by Titanium-Containing Catalytic Systems by V.S. Byrihin, V.B. Murachev and I.Sh. Guzman

harwood academic publishers
Published in Switzerland

ISBN: 3-7186-5548-9
ISSN: 1071-9114

CHEMISTRY REVIEWS

Aims and Scope

The aim of this series is to highlight contributions from scientists in the former Soviet Union to topics of current worldwide interest. The purpose is to increase awareness in the West of the extent of work being carried out in the former Soviet Union, and it is hoped that this may lead to fruitful collaboration between research groups. Topics will be chosen from a wide range of chemical themes with both fundamental and application emphasis, the sole criterion being that the topic represents an area of strong scientific interest and activity.

Ordering Information

Each volume is comprised of an irregular number of parts depending upon size. Issues are available individually as well as by subscription. 1994 Volume: 19

Orders may be placed with your usual supplier or directly with Harwood Academic Publishers GmbH in care of the addresses shown below. Journal subscriptions are sold on a per volume basis only. Claims for nonreceipt of issues will be honored free of charge if made within three months of publication of the issue. Subscriptions are available for microform editions; details will be furnished upon request.

All issues are dispatched by airmail throughout the world.

Subscription Rates

Base list subscription price per volume: ECU 125 (US $150).* This price is available only to individuals whose library subscribes to the journal OR who warrant that the journal is for their own use and provide a home address for mailing. Orders must be sent directly to the Publisher and payment must be made by personal check or credit card.

Separate rates apply to academic and corporate institutions. These rates may also include photocopy license and postage and handling charges. Special discounts are available to continuing subscribers through our Subscriber Incentive Plan (SIP).

(Continued on the inside back cover)

CHEMISTRY AND PHYSICS OF COMPOUNDS WITH LOOSE CRYSTAL STRUCTURE

CONTENTS

layer inclusion compounds. Intercalation thermodynamics. 5. New type of equilibrium lattice point defects — unstable vacancy–ion pairs at interstices. Theory of instability zones of interacting defects in crystals. Unstable pairs have a short lifetime and cannot be quenched. These very defects determine in particular the thermodynamics and transfer phenomena in superionic crystals. 6. Technical uses of various types of crystalline compounds with loose structure.

sold on a per volume basis only. Claims for nonreceipt of issues will be honored free of charge if made within three months of publication of the issue. Subscriptions are available for microform editions; details will be furnished upon request.

All issues are dispatched by airmail throughout the world.

Subscription Rates

Base list subscription price per volume: ECU 125 (US $150).* This price is available only to individuals whose library subscribes to the journal OR who warrant that the journal is for their own use and provide a home address for mailing. Orders must be sent directly to the Publisher and payment must be made by personal check or credit card.

Separate rates apply to academic and corporate institutions. These rates may also include photocopy license and postage and handling charges. Special discounts are available to continuing subscribers through our Subscriber Incentive Plan (SIP).

(Continued on the inside back cover)

Chemistry Reviews, Vol. 19, 1994, pp. 1–138

Printed in the USA

CHEMISTRY AND PHYSICS OF COMPOUNDS WITH LOOSE CRYSTAL STRUCTURE

VLADIMIR M. KOSHKIN and YURI N. DMITRIEV

Polytechnic Institute, Kharkov, Ukraine

ABSTRACT

Experimental data and theoretical models describing the unusual properties of crystalline compounds with loose structure are presented systematically for the first time. These include: 1. Semiconductors and dielectrics with practically unlimited radiation stability. Stoichiometric vacancies in crystalline compounds. General structural criterion of radiation stability of crystals. 2. Features of chemical bonding in covalent semiconductors with loose structure. 3. Semiconductor compounds, impurities in which are electrically and chemically inactive. Theory of solubility of impurities localized in lattice vacancies in the atomic state. 4. Quantum dimensional effect and formation of miniband energy spectrum of electrons in intercalation layer inclusion compounds. Intercalation thermodynamics. 5. New type of equilibrium lattice point defects — unstable vacancy–ion pairs at interstices. Theory of instability zones of interacting defects in crystals. Unstable pairs have a short lifetime and cannot be quenched. These very defects determine in particular the thermodynamics and transfer phenomena in superionic crystals. 6. Technical uses of various types of crystalline compounds with loose structure.

I was confirmed in the opinion, which I have always held, namely that emptiness is not something impossible, that nature is not at all fearful of emptiness, as many people think.

Blaise Pascal

In the final analysis the sense of curiosity about these empty places and their featureless landscapes is indeed art.

Joseph Brodsky

INTRODUCTION

Crystals exist that have been the subject of study by physicists for many decades. Such traditional materials in physics are few compared to the huge number of compounds known nowadays to chemists and crystallographers. To try and keep up with the flood of these new compounds is a hopeless and indeed scarcely inspiring task.

Nevertheless, the introduction of new chemical compounds into the sphere of interest of physics is essential, primarily on account of the extremely important materials technology task of producing a range of materials with widely differing combinations of physicochemical parameters so as to satisfy the ever-increasing demands of technology.

However, no less inspiring in the investigation of new, nontraditional materials is the high probability of detecting qualitatively new properties and phenomena.

Which of the huge number of new compounds is worth selecting for physical investigation in the hope of detecting unusual properties?

It is scarely possible to give general rules for such a choice — this is more a matter of skill and luck than logic and science, though, notwithstanding this, it is possible to formulate at least one of the rules.

Clearly, in the search for unusual phenomena in crystals attention should be directed above all to those that exhibit an unusual, and indeed *particular*, crystal structure.

This review describes the properties of materials whose uniqueness is entirely determined by their common structural feature, namely an unusually high concentration of structural vacancies.

The existence and concentration of these structural vacancies is determined exclusively by the fulfilment of valency conditions and does not depend, in contrast to Frenkel or Schottky defects, on the temperature or thermal prehistory of the sample. Such structural vacancies have accordingly been termed stoichiometric vacancies (SV). Stoichiometric vacancies are the structural component of a very broad class of materials, including semiconductors with principally covalent bonding (for example, In_2Te_3, $CdGa_2Se_4$, Sc_2S_3) and dielectric ionic crystals (for example, Y_2O_3, In_2O_3).

In In_2Te_3 type crystals, for example, the SV proportion is 16.6% of the total number of lattice sites, and all the SV are located in the cation sublattice. In $CdGa_2Se_4$ and other semiconductors of this type SV, distributed also only in the cation sublattice, comprise 12.5% of the total number of sites. In Y_2O_3 16.6% of SV are distributed in the anion sublattice.

The crystalline materials mentioned above and their numerous structural analogues belong to various crystallographic classes, though the presence of SV and the structural looseness associated with a high concentration of the latter predetermined, as investigations have shown, a number of common and extremely unusual properties in such materials.

Among such loose structures, In_2Te_3 type semiconductors have been investigated in more detail than others.

Hahn and Klingler [1] were the first to investigate materials of this type, and determined the structure of this group of substances.

Goryunova and coworkers [2] were the first to establish that In_2Te_3 type crystals are semiconductors.

The first comprehensive investigation of the particular features of the physicochemical properties of the semiconductor In_2Te_3 associated with the presence of SV in the lattice was carried out in 1958–1960 under the direction of Zhuze [3–6]. The wide-ranging work of Radautsan and coworkers played a significant role in establishing the physics of semiconductors of this type [7, 8]. Significant contributions in this direction were made by Woolley, Mushinskii, Newman, Pamplin, Tagiev and other investigators working in laboratories in various countries.

Interest in crystals with SV has continued unabated, and is connected with the discovery of a number of unusual physical properties of these materials. Experiments carried out in St Petersburg by Zhuse, Sergeeva and Shelykh [3] showed that, in contrast to all known crystalline semiconductors, impurities in the semiconductor In_2Te_3 have practically no effect on its electrical properties. Investigations carried out in Kharkov by Koshkin *et al.* [8–12] demonstrated that compounds with SV, including both semiconductors and dielectrics, have an anomalously high radiation stability compared with any other nonmetallic crystals. In the same work [8–12] it was also shown that unstable Frenkel pairs are the main type of equilibrium point defects in such structures and that, because of this, it is impossible for example to quench point defects, in contrast to other crystals.

In In_2Te_3 or Mn_2O_3 type crystals stoichiometric vacancies are distributed over the volume of the crystal. Loose crystalline structures in which SV are grouped in layers are extremely common. Crystals of the TiS_2, PbI_2, BiI_3 and Tl_2S type are examples of such crystals. In compounds of this type, the classical analogue of which is graphite, packets with strong ionic–covalent bonding are separated by SV layers since only a weak van der Waals interaction exists between the packets. Such layered structures also have very special physicochemical properties, the most notable of which is the ability to transform into so-called intercalated compounds when foreign atoms, ions or molecules penetrate the interlayer spaces, thereby creating new ordered structures.

The work of several groups (Gamble, Geball, Di Salvo, Vol'pin, Novikov, Wittingham, Schölhorn, Ioffe, Wilson, etc.) is devoted to investigations of layered intercalation compounds.

On the one hand, all these atypical phenomena have resulted in theoretical and experimental investigations with the aim of establishing their physical nature, while, on the other hand, the above-described unique properties of loose crystal structures have stimulated the development of a number of technical devices, based on the latter, that utilize these properties.

Accordingly, a voluminous literature exists including thousands of journal publications devoted to one or other aspect of the study of crystals with loose structure containing SV. However, up to now, no monographs exist that describe the principal mechanisms and regularities in the physics of loose crystal structures, which has led us to write this review.

We do not intend to provide a review of all investigations on the physics of such crystals, and this paper is not meant to serve as a manual in which information can be found on all currently known physical and physicochemical parameters of semiconductors and dielectrics with loose crystal structure.

Instead, our review aims to provide a systematic description of only the main current experimental data, theoretical models and ideas associated with the chemistry and physics of crystals, united by a common structural feature, namely looseness of the crystal lattice.

1. CRYSTAL CHEMISTRY AND PHYSICAL PROPERTIES OF COMPOUNDS WITH LOOSE LATTICE

1.1 Chemical Bonding and Structure of Inorganic Crystals

Chemical bonding in inorganic semiconductors and dielectric compounds is ionic–covalent (see, for example, [13]), which may be described with the aid of various quantum-mechanical approximation methods. The wave function of a system of two nonidentical atoms may be represented, for example in the Heitler–London method, as the superposition of covalent and ionic components. Since the total energy of the system under the superposition of the two states is reduced due to the existence of ionic–covalent resonance energy, all heteroatomic compounds have some degree of ionic bonding. The ionic bonding component produces an asymmetric electron density distribution in each bond, resulting in the formation of effective electrical charges on atoms in molecules and crystals.

In order to evaluate the degree of ionicity, Pauling [14] introduced the concept of electronegativity x, a quantity defining the capability of a given atom to accept an electron in a compound. The difference in the electronegativities Δx of elements participating in a chemical bond in the compound AB, $\Delta x_{AB} = x_A - x_B$, determines the contribution of the ionic component of the bond. There are several methods for determining x from various experimentally measured constants, electronegativity tables have been compiled, and several semiempirical expressions have been proposed for calculating the degree of ionicity λ from the difference in electronegativities.

The contribution λ of the ionic component of a bond in molecules and crystals may be calculated, and in fact fairly accurately, though it requires laborious quantum-chemical computations, and accordingly it is useful to be able to evaluate λ by the simple method of the difference in electronegativities:

$$\lambda = 1 - \exp[-C\Delta x_{AB}^2], \tag{1.1}$$

where C is a constant, which differs for compounds with various types of bonding orbitals determining a covalent bond. Despite the known imprecision of such a determination of the degree of ionicity, various macroscopic phenomena of ionicity may be described adequately with the aid of this equation: dipole moments, thermochemical parameters, ratio of high-frequency and static dielectric constants, magnitude of the effective charge measured from IR absorption data of the lattice and from X-ray spectroscopy data, magnitude of the isomeric chemical shift in NMR spectroscopy, contribution of Van Vleck polarization paramagnetism, etc. [14–16].

The bond energy is determined only by the ionic component in crystals, $E_{ion} = Aq^{*2}/d$, where q^* is the effective charge of the atom (ion), d is the interatomic distance, and A is the Madelung constant of the corresponding crystal structure, though the contribution of the ionic component in various semiempirical calculations is, following Pauling, fairly often determined only as an overall value, without separating E_{ion} and the resonance term.

The energy of a covalent bond is, as is known, determined by the overlapping of electron shells of neighbouring atoms, which in turn is determined by the relative spatial distribution of the wave functions of electrons participating in the bonding of the atoms. The radial part of the wave function of the valency electrons basically depends on the principal quantum number of the valency electrons in the atom.

The angular distribution of the wave functions is determined by the orbital quantum numbers: these are either 'pure' ψ-functions (spherically symmetrical s-function distributions, or p-functions oriented along three mutually orthogonal axes), or polygonal hybrid orbitals — sp, sp^2 or sp^3. The sp orbitals represent a 'stretched' dumb-bell, the sp^2 orbitals a triple-petal flat 'flower', and the angular sp^3 distribution a hybrid function with its maxima oriented towards the vertices of a tetrahedron, in the centre of which is located the atom in question. Elements in which the d- and f-orbitals have an energy slightly differing from the incompletely filled s- and p-states may form hybrid orbitals with the participation of d- and f-states [17].

In accordance with this, p-bonds are for example normally formed in crystal structures with a particular proportion of covalent bonding with a coordination number 6 (in PbTe, SnSe, and the like, which have a sodium chloride lattice). sp^3 bonds exist in crystal structures with a coordination number of 4 (diamond, germanium, silicon, GaAs, InSb and other crystals of the type $A^{III}B^{V}$, ZnS, CdTe and other $A^{II}B^{VI}$ compounds).

The crystal chemistry regularities of the atomic structure of solids enable a general description of the principal features of the structure of materials with different types of chemical bonding to be given.

The crystal chemistry approach is essentially based on a model that describes the packing of structural elements, to each of which is ascribed a crystal chemistry size that remains unchanged in different structures. This size is the so-called crystal chemistry radii of the chemical elements. The sum of the crystal chemistry radii r_i of two adjacent chemical elements in a crystal of the compound AB gives the interatomic distance d

$$d = r_A + r_B. \tag{1.2}$$

Several systems of crystal chemistry radii exist in accordance with the different types of chemical bonding in crystals, namely, ionic, metallic, atomic and covalent bonding [18].* The corresponding system of radii is employed to analyse and predict the structure of substances with ionic or covalent types of bonds. The use of such radii gives an indication of the most probable coordination number in the given compound, provides an evaluation of the lattice parameter of individual substances and solid solutions, and enables the bond to be characterized and the energy of the elastic substitutions to be calculated when impurities are introduced [20].

Various corrections are introduced that take into account the contribution, for example, of the ionic component of the bond in compounds with a predominantly covalent type of interaction. Thus, when calculating interatomic distances in compounds AB from the covalent radii the ionicity correction is taken into account by the Schomaker–Stevenson equation [21] by means of the difference in electronegativities

$$d = r_A + r_B - 0.09\Delta x_{AB}. \tag{1.3}$$

This equation is generalized [22] for the case of multicomponent covalent compounds with a tetrahedral coordination of atoms

$$\bar{d} = 2\sum_{i} r_i\eta_i - 0.09\sum_{i,k}|\Delta x_{ik}|\varepsilon_{ik}, \tag{1.4}$$

---

* This book basically deals with crystalline bodies the structural elements of which are only atomic ionic, and not molecular particles, van der Waals forces are the main type of intermolecular bonds. The crystal chemistry of molecular crystals has been developed by Kitaigorodskii [19]. Molecular crystals are not examined in the book.

where $\bar{d}$ is the average interatomic distance, r_i are the real covalent radii of the structural elements, η_i is the proportion of these structural elements in the stoichiometric formula of the compound, Δx_{ik} is the difference in electronegativities of atoms of types i and k, and ε_{ik} is the fraction of bonds between atoms of types i and k in the total number of bonds. Calculations of interatomic distances from crystal chemistry radii do not claim to be very accurate, the error normally being of the order of 0.02–0.04 Å. Calculations of interatomic distances for ionic–covalent crystals very often give results that are fairly close to one another and the experimental results when using a system of ionic radii as well as a system of covalent radii.

The use of crystal chemistry radii gives particularly graphic results in the known model of the closest packing of ion pairs [18, 23]. We shall discuss this model in more detail since it represents a convenient basis for a structural definition of the concept of a stoichiometric vacancy.

Closest packing of identical spheres may be accomplished in only two ways. One way is so-called three-layer packing, which corresponds to a face-centred cubic lattice (FCC packing). This is the structure of, for example, copper, silver and gold (Figure 1). The other method of closest packing is double-layer packing, corresponding to a hexagonal cell (HCP). This is the structure of, for example, zinc, beryllium and cadmium.

Unoccupied spaces, i.e. cavities, remain with such a closest packing of identical spheres (i.e. of identical atoms or ions constituting the structural elements of the crystal). In both cubic and hexagonal

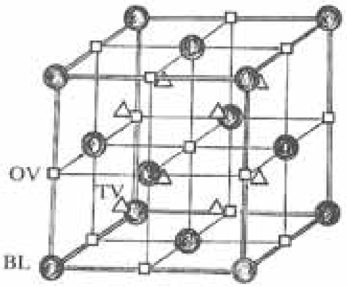

Figure 1 System of structural positions in cubic close packing.

close packing only two types of voids exist, namely tetrahedral (TV) and octahedral (OV). Each TV is surrounded by four atoms of the basic cell (tetrahedral coordination). Each OV is surrounded by six atoms of the basic cell (octahedral coordination). Two TV and one OV are associated with each sphere of the basic cell. Both octahedral and tetrahedral cavities in the FCC of a basic cell themselves form face-centred cubes from empty positions. The FCC from octahedral cavities is displaced relative to the FCC of the basic cell by half the edge of the cube and has, of course, the same lattice period as the basic cell. Tetrahedral cavities form two crystallographically equivalent cubes, the period of which also coincides with the period of the basic cell. FCC constructed from TV are displaced relative to the basic cell by one-quarter of the space diagonal of the cube of the basic cell. Hexagonal lattices — one of OV and two of TV — obtained in the HCP of the basic cell may be regarded in a similar way.

From the crystal chemistry point of view, the crystal structure of practically any inorganic material (assuming of course that there are no ligands of the type SO_4^{2-} or PO_3^{3-}, etc.) may be interpreted as constructed on the basis of the closest cubic or hexagonal packing of spheres with the filling of a certain number of tetrahedral and octahedral positions in this arrangement.

We shall examine several examples of such an arrangement. These arrangements are normally made for structures with a fairly high degree of ionicity. A cell consisting of ions with the largest ionic radius is chosen as the basic cell for examining binary (and more complex) compounds, although such a choice is arbitrary and the same result is obtained if a cell of small spheres is considered as the basic cell. For example, a structure of the sodium chloride type may be constructed based on a cell of large chlorine anions, each OV of which accommodates a sodium ion. The resultant structure is completely symmetrical as regards replacement of sodium ions by chlorine ions, and constitutes two structurally equivalent cation and anion sublattices (Figure 2a).

The hexagonal analogue of the cubic structure of sodium chloride is a lattice of the nickel arsenide (NiAs) type, constructed on the basis of a hexagonal cell of arsenic ions, the OV being fully occupied by nickel ions (Figure 2b).

A lattice of the zincblende type — sphalerite, ZnS — may be regarded as the result of the filling by zinc ions of one of the two TV families in the cubic basic cell of sulphur ions (Figure 2c). The

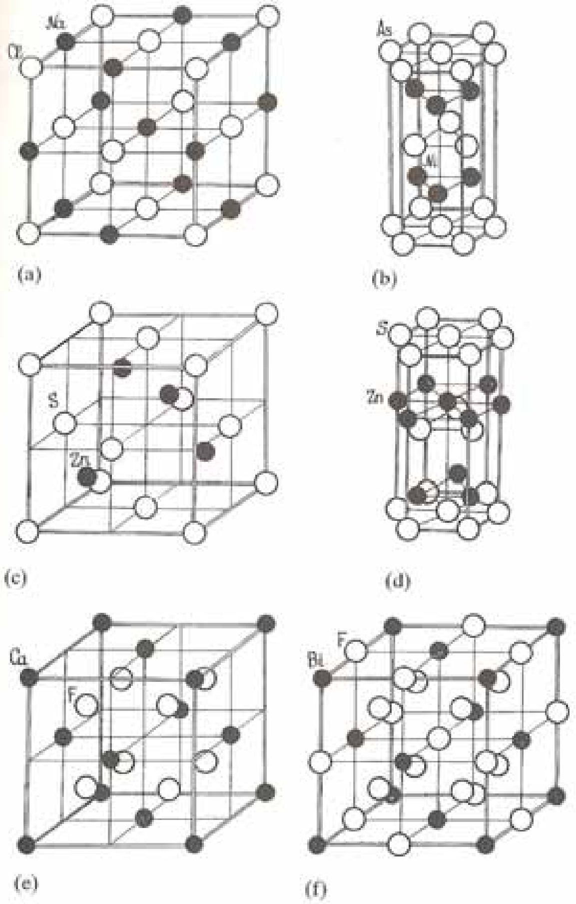

(a) (b) (c) (d) (e) (f)

Figure 2 Cubic and hexagonal close packing with different fillings of the tetrahedral and octahedral voids.

wurtzite type ZnS lattice is represented in a similar way: one of the two TV systems in the hexagonal basic cell of sulphur ions is filled with Zn ions (Figure 2d).

The fluorite (CaF_2) type structure (Figure 2e) may be represented as a cubic cell of calcium ions in which both TV families are occupied by fluorine ions. A rarely encountered structure type, BiF_3, exists, in which all the OV and TV in the basic cell of bismuth atoms are occupied by fluorine ions (Figure 2f).

Other types of cells may be considered in a similar way.

Of course, in BiF_3, for example, which is characterized by occupancy of all empty positions, new lattice 'voids' are 'formed' under such an occupancy, though naturally their geometrical dimensions are much smaller than those of the voids of the basic cell.

Finally, the characteristic sizes of the cavities in the basic cell (radius of the sphere inscribed in the OV $r_0^0=(\sqrt{2}-1)R$, and of the sphere inscribed in the TV $r_\tau^0=(\sqrt{6}/2-1)R$, where R is the radius of the spheres of the basic cell) are practically always less than the sizes of those atoms that are arranged in them, and the latter 'expand' the basic cell, since the distances between the atoms or ions in the latter increase. Accordingly, when talking of either OV or TV occupancy we do not characterize the filling of the space in the cell in terms of atomic volumes, and shall specify only the occupancy of the possible structural states in the cell. There are three choices of such structural states, namely two tetrahedral and one octahedral. Rock salt, sphalerite, and fluorite are examples of such structural types, in which each given state of the possible structural states is either completely occupied or completely free.

Structures exist however in which the positions of a given structural state are not fully occupied.

The following are examples of such structures:

(a) Sc_2S_3 is a sodium chloride lattice, although the OV of the basic cell of sulphur ions is only two-thirds occupied by cations (Sc^{3+}) (Figure 3a)

(b) In_2Te_3 is a sphalerite lattice, where in one TV family of the basic lattice of tellurium two-thirds of the cation sublattice sites are occupied, and the remaining one-third are vacant (Figure 3b)

(c) Mn_2O_3 is a fluorite lattice, where three-quarters of both TV families of the basic cell (Mn^{3+}) are occupied, and the remain-

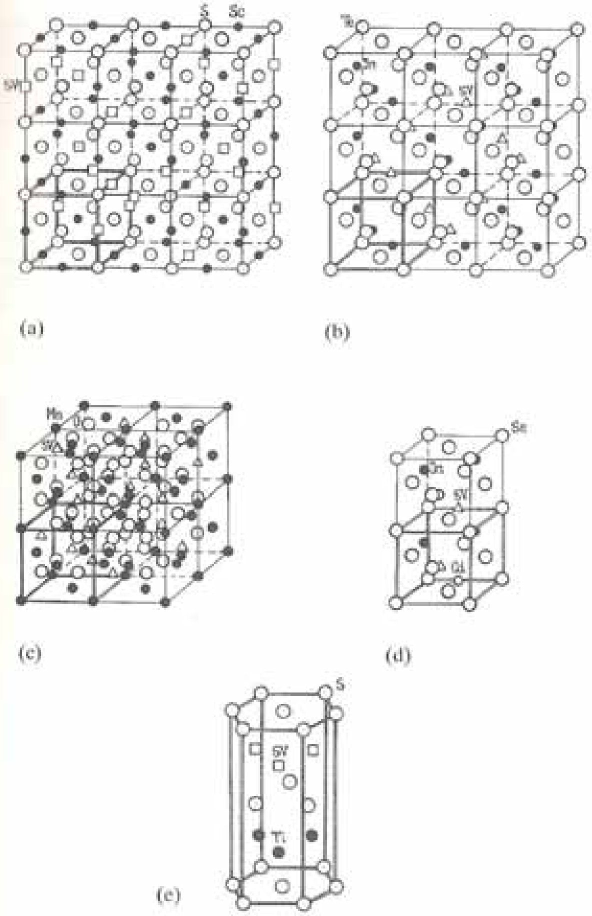

(a) (b) (c) (d) (e)

Figure 3 Some types of structure with stoichiometric vacancies.

ing quarter of the sites of the anion sublattice are vacant (Figure 3c)

(d) $CdIn_2Se_4$ is a thiogallate lattice similar to the sphalerite lattice with very slight tetrahonal distortion, and as in In_2Te_3 one of the TV systems in the basic selenium cell is only three-quarters occupied by cadmium and indium cations, and the remaining quarter of the cation sublattice sites are vacant (Figure 3d).

Layer hexagonal lattices of the CdI_2 or TiS_2 type may also be regarded as constructed on the basis of an anion cell with half the OV occupied. At the same time the vacant OV and OV occupied by cations are arranged in layers (Figure 3e). In SnI_4 one-quarter of one TV system in the main iodine cell is occupied.

When speaking of OV and TV occupancy in the basic cell it is understood, as it were, that the cubic or hexagonal symmetry of the basic cell, and consequently of the whole structure, is preserved. In actual fact, even if the symmetry of the basic cell is distorted, which occurs fairly frequently and mainly in crystals with a substantial covalent bond contribution, the choice of possible structural states remains the same. Crystallographically such structures with a distorted basic cell give new, more low-symmetry lattices, though the crystal chemistry occupancy rules remain in force. The crystallographic structural motifs are changed, though the crystal chemistry motifs remain unchanged.

The degree of occupancy of 'cavities' in the basic cell is ultimately determined not by the geometrical circumstances, which merely indicate the possibility of the existence of one or other coordination or one or other structural 'state'. The occupancy of TV and OV is determined exclusively by the valency relationships and preservation of the electroneutrality of the lattice as a whole, as can easily be seen, in particular, in the examples of the compounds given hereinafter ($Sc_2^{3+}S_3^{2-}$, $In_2^{3+}Te_3^{2-}$, $Mn_2^{3+}O_3^{2-}$, $Cd^{2+}In_2^{3+}Se_4^{2-}$, $Cd^{2+}I_2^{1-}$, etc.). Thus, the existence of partially occupied positions is determined by whether or not valency conditions are satisfied, i.e. by the stoichiometry of the crystal.

Vacant positions in the system of voids of the basic cell, which in accordance with the fulfilment of the valency conditions are only partially filled by atoms, are termed stoichiometric vacancies. For example, the concentration of stoichiometric vacancies (SV) in Sc_2S_3 and In_2Te_3 type cells is one-third of the positions in the cation sublattice, and in Mn_2O_3 type cells is one-quarter of of the positions in the anion sublattice; in ternary compounds of the type $CdIn_2Se_4$ the stoichiometric vacancies comprise one-quarter of the positions in the cation sublattice.

The existence and concentration of SV is determined only by the stoichiometric valency relationships, and does not depend, in contrast to thermally excited Schottky and Frenkel vacancies, either on the temperature or on the previous thermal history of the sample.

Stoichiometric vacancies are in this sense a structural and stoichiometric component of the crystal in the same way as atoms of chemical components.

The formulae of crystalline compounds with stoichiometric vacancies are written using the Riz–Ormont symbols [24], thus: $[Sc_2\square]S_3$, $[Ga_2\square]Se_3$, $[Zn\square In_2]Te_4$, $Y_2[O_3\square]$, $[CuIn_5\square_2]Te_8$, $[Pb\square]I_2$, etc. In the last of these examples, as in numerous other compounds of this type, the SV form flat layers.

Naturally the stoichiometric 'component' of a compound, i.e. a stoichiometric vacancy, exists only in the crystalline state. A necessary condition for the existence of stoichiometric vacancies in a crystalline compound is nonequivalence of the valencies of the anion and cation, i.e. of the structural elements comprising the basic cell and atoms occupying the empty positions.

In crystals where covalent bonding is substantial and interatomic interaction is not isotropic, the electron density distribution in the vicinity of the atoms, i.e. the structural components, cannot be considered even approximately as spherically symmetrical. It is clear therefore that in structures with a considerable proportion of covalent bonding, on account of the orientation of the bonds the electron density distribution makes the stoichiometric vacancies and voids in other systems of structurally permitted positions physically nonequivalent. We shall illustrate this below by specific examples.

1.2 Semiconductor Compounds with Stoichiometric Vacancies

Of the large number of crystals with stoichiometric vacancies, semiconductor compounds with tetrahedral coordination of the atoms in the lattice have without doubt been investigated most.

We shall examine the structure of this group of crystals in more detail. These crystals belong to a huge class of semiconductors discovered independently by Goryunova and Regel in St Petersburg in Russia and Welker in Germany, and termed diamond-like by Goryunova [25], since all crystals of this class, both binary and ternary crystals, have a lattice in which all the atoms are arranged tetrahedrally as in diamond. This class includes in particular compounds without SV, i.e. so-called 'normal' diamond-like phases: elementary (diamond, silicon, germanium, grey tin), binary compounds $A^{III}B^{V}$ (GaAs, InSb, GaP, AlSb, etc.), $A^{II}B^{VI}$ (CdTe, ZnSe, CdS, HgTe, etc.), some $A^{I}B^{VII}$ compounds (AgI, CuBr), as well as numerous ternary semiconductors $A^{II}B^{IV}C_2^{V}$ (for example $CdGeP_2$, $ZnSnAs_2$), $A^{I}B^{III}C_2^{VI}$ (for example $CuInTe_2$, $AgGaS_2$, $CuAlSe_2$, etc.), and $A_2^{I}B^{IV}C_3^{VI}$ (for example Cu_2GeSe_3, Cu_2SnS_3, etc.).

Chemical bonding in diamond-like crystals is covalent (in elementary semiconductors, e.g. diamond, silicon, germanium, α-tin) or ionic–covalent in semiconductor compounds. Covalent bonding in these crystals occurs as a result of overlapping of the electron shells of atoms existing in the sp^3-hybrid state [13, 26]. The degree of ionicity evaluated according to [14–16] naturally varies for different compounds, though in the majority of cases it is less than 50%, except for some sulphides and halides, in which the degree of ionicity is somewhat higher.

It can easily be seen that for all 'normal' phases with a tetrahedral coordination of the atoms, the average number of valency electrons belonging to one atom is four [25, 27, 28]. This corresponds to the formation of four two-electron bonds at each of the atoms involved in the 'normal' tetrahedral phase. As the degree of ionicity increases, the electron clouds are to some extent drawn towards the more electronegative of the components, which is termed the anion — a fairly arbitrary description in the case of compounds with predominantly covalent bonding.

Goldschmidt [29] (see also the generalization of Goldschmidt's rule [30]) has also made a very interesting observation, pointing out that the lattice parameters a of all 'normal' tetrahedral phases belonging to so-called isoelectronic series of compounds are practically identical. These are series of compounds in which all the components belong to the same period of the Mendeleev Periodic Table. Small differences in the lattice parameters are associated with a different degree of ionicity and are adequately described by expression (1.3). This is a consequence of the fact that covalent bonding, which predominates in these crystals and is determined by the overlapping of the wave function of valency electrons, depends under an identical hybridization character only on the radial distribution of the wave functions, which in turn is specified by the principal quantum number. The latter in isoelectron series of compounds is identical by definition.

A series of crystalline compounds with SV belong to this structural class of diamond-like compounds: $A_2^{III}\square B_3^{VI}$ (In_2Te_3, Ga_2Te_3, Ga_2Se_3, Ga_2S_3), $A^{II}B_2^{III}\square C_4^{VI}$ (for example $HgIn_2Te_4$, $CdGa_2Se_4$, etc.), $A^{I}B_3^{III}\square C_5^{VI}$ (for example $CuIn_3Te_5$), $A^{I}B_5^{III}\square_2 C_8^{VI}$ (for example $CuIn_5Te_8$), $A_2^{I}B^{II}\square C_4^{VII}$ (for example Ag_2HgI_4).

Only those diamond-like phases are known in which SV occur exclusively in cation positions. It has been shown that cations and SV may become ordered in the cation sublattice. The order–disorder transition in such crystals is a first-order phase transition [3, 4].

The identity of the crystal structure of 'normal' phases and phases with SV predetermines the existence of broad regions of solid solutions in systems of the type $A^{III}B^{V}-A_2^{III}B_3^{VI}$, $A^{II}B^{VI}-A_2^{III}B_3^{VI}$, $A^{I}B^{III}C_2^{VI}-B_2^{III}C_3^{VI}$. The concentration of SV in these systems changes from zero in 'normal' phases to 33.3% of all sites of the cation sublattice in $A_2^{III}B_3^{VI}$. The work of Radautsan [7] and Woolley [31–33] and their coworkers has made an important contribution to the study of these systems.

We shall examine bonding in a crystal of a typical compound with SV, namely the example of In_2Te_3 [34].

In the ordered phase of this compound the 'anionic' tellurium atoms may have two different environments: either indium atoms (cation) on three sides of the anion and a stoichiometric vacancy on one side, or two SV and two cations in the anion environment [35].

In those tetrahedral directions (see Figure 4a) along which a tellurium atom is adjacent to an indium atom, a normal sp^3 bond is formed since a pair of electrons belongs simultaneously to Te and In, as in crystals of the type $A^{II}B^{VI}$ or $A^{III}B^{V}$. In the direction of the SV in the tellurium atom there remains a sp^3-orbital with two electrons (lone pair). Four sp^3-hybrid double-electron clouds from each of the tellurium atoms surrounding the SV are accordingly directed towards the SV. The distribution of valency electrons in the In_2Te_3 cell is illustrated diagramatically in Figure 4(b).

The preservation of the balance of electrons can easily be followed from the 'molecular' scheme (Figure 4b) corresponding to this model. From the scheme it can be seen in particular that sp^3-cells filled with two electrons remain at the tellurium atoms. These cells correspond to the electron clouds examined above, directed towards the SV.

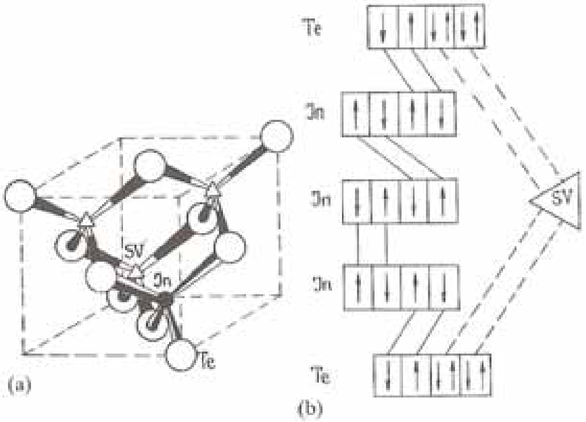

Figure 4 Stoichiometric vacancies in compounds of the In_2Te_3 type. (a) Spatial arrangement of bonds: ▭ two-electron sp^3 bond between In and Te atoms; ▭▬ lone pair on Te atom; (b) 'molecular' arrangement of chemical bonds.

If, following Suchet [28], we consider a SV as a full and equal structural element of a covalent crystal, it can easily be seen that the average number of valency electrons per one structural element (and not per one actual atom) is equal to four if we regard a SV as an atom with zero valency.

It is clear that the two-electron sp^3-hybrid clouds directed from the Te atoms towards the stoichiometric vacancy are completely filled, analogous to inert gas orbitals, and are not bonding orbitals. Covalent bonding via SV does not occur. In this sense an anion in crystals with SV is analogous to the terminal atom in 'molecular' chains of chalcogenic glasses. In the model of semiconductor glasses proposed by Street and Mott [36] the presence of a lone pair is also ascribed to such a terminal atom. Consequently a SV, being a structural component of the crystal, does not form a bond with its neighbours, which should be reflected in the energy parameters of crystals with SV.

Since the bonds in diamond-like crystals are substantially covalent, they are short-range and the interatomic interaction energy is practically entirely determined by bonds only with nearest neighbours.

It has been shown [37] that, as a result of the short-range nature of the forces in diamond-like crystals, the values of the physical parameters, which are determined by the lattice energy, are always lower in crystals with SV than in compounds without SV, the energy of each individual bond in which coincides with the energy of the individual bond in the phase with SV.

The concept of isoelectron and equivalent bonds was introduced in paper [37]. Bonds such as the two sp^3-bonds $A_1 \sim Z_1$ and $A_2 \sim Z_2$ (the symbol $\sim$ denotes a sp^3 bond, A_1, A_2 are cations, and Z_1 Z_2 are anions), in which the atoms A_1, A_2 and Z_1, Z_2 belong in pairs to the same row of the Periodic System, are termed isoelectron bonds. According to this definition, isoelectron bonds are, for example, the sp^3 bonds In ~ Te and Cd ~ Te; Cu ~ Se, Ga ~ Se and Zn ~ Se; Ga ~ S and Zn ~ S; etc. $\overline{A \sim Z}$ denotes a bond that is isoelectronic with the bond A ~ Z.

In one and the same type of orbitals, for example sp^3, participating in a covalent bond the covalent interaction energies in isoelectron bonds should be equal, which generally speaking follows directly from a consideration according to the molecular orbital method. It should be noted that the above concept of isoelectron compounds is naturally involved in the definition of isoelectron bonds.

As we have seen, the total bond energy depends also on the contribution of the ionic component of the bond. Two sp^3 bonds are termed equivalent if they are isoelectronic and the degree of ionicity of both is identical. Since an isoelectron state ensures equality of covalent bond energies, equality of the degree of ionicity of such bonds implies equality of the energies of the latter. Thus, the total energies of equivalent bonds are identical.

If the degree of ionicity of the bonds is evaluated according to one or other scale of electronegativities, it can be seen that elements of subgroups IIB and IIIB of the Periodic System have identical or extremely close electronegativity values. Accordingly, the sp^3-hybrid bonds Zn ~ Z and Cd ~ Z, Ga ~ Z and Zn ~ Z are equivalent (accurate, of course, to the assessment of the degree of ionicity from scales of electronegativities). $\overline{\overline{A \sim Z}}$ denotes a bond equivalent to the bond A ~ Z.

The introduction of the concept of isoelectron and equivalent bonds has enabled the internal energy of crystals with SV to be analysed. Since the number of bonds in a $A_2^{III}B_3^{VI}$ cell is one-third fewer than in a cell of the corresponding 'normal' phases, it is clear that if the bonds in $A_2^{III}B_3^{VI}$, $A^{II}B^{VI}$ are equivalent, the ratio of the internal energies of the corresponding crystals (provided the lattice periods are equal) should be close to two-thirds. Since few experimental data are available on lattice energies of crystals of the type $A_2^{III}B_3^{VI}$, ratios of the absolute melting points T_m (the melting points are adopted as a measure of the internal energy of the crystal) of compounds with SV to T_m of vacancy-free crystals $A^{II}B^{VI}$, in which $A^{II} - Z^{VI} = B^{III} - Z^{VI}$, were found in paper [37]. It turned out that this ratio is in fact close to the value two-thirds, which is direct confirmation that a SV does not contribute to the bond energy. At the same time this result shows that in crystals with predominantly covalent bonding, by virtue of the short-range nature of the latter each bond contributes additively to the internal energy of the crystal. This has led to the formulation of an additivity rule, which enables the melting points (and evidently also other parameters proportional to the internal energy of a crystal) of crystals with SV of different compositions to be calculated from the melting point data of 'normal' diamond-like compounds.

Consider a diamond-like compound of the general formula $A_{m_1}^{(1)}A_{m_2}^{(2)}\ldots A_{m_n}^{(n)}\square_n Z_k$, in which $n + \sum_{i=1}^{n} m = k$, where m_i, n, k are stoichiometric coefficients. If simple replacements by equivalent bonds are made, as in the simplest example given above, the expression for determining the melting point of the above compound is

$$T_m(A_{m_1}^{(1)}A_{m_2}^{(2)} \ldots A_{m_n}^{(n)}\square_n Z_k) = \sum_{i=1}^{n} \frac{m_i}{k} T_m\,(\overline{A^{(i)} - Z}), \quad (1.5)$$

where m_i/k is the proportion of $A^{(i)} - Z$ bonds in the total number of bonds in the crystal. As we have seen, in the case of bonds of atoms of Group III with chalcogens, replacement by the equivalent bond is easily performed; this is the isoelectron A^{II} – chalcogen bond.

In the case where replacement by an isoelectron bond is not simultaneously a replacement by an equivalent bond, a term that takes into account the correction for the change in the parameters in the isoelectron series under noncoincidence of the bond ionicity is introduced into expression (1.5). In this case

$$T_m\,(A_{m_1}^{(1)}A_{m_2}^{(2)} \ldots A_{m_n}^{(n)}\square_n Z_k)$$
$$= \sum_{i=1}^{n} \frac{m_i}{k} T_m\,(\overline{A^{(i)} - Z}) - \sum_{i=1}^{n} \frac{m_i}{k} \left(\frac{\partial T_m}{\partial x}\right)_i (\bar{x}_i - x_i) \quad (1.6)$$

where $\bar{x}_i$ is the electronegativity of the element chosen as isoelectronic element $A^{(i)}$, having an electronegativity x_i; $(\partial T_m/\partial x)_i$ is the derivative for the corresponding *i*th element of the isoelectronic series of compounds. The good agreement between theory and experiment shows that a SV, being a structural component, does not contribute to the internal energy of the crystals, and the melting point of the latter is proportional to the number of real covalent bonds in the lattice. In [37] it is shown that expressions (1.5) and (1.6) may be used to calculate the melting points of any phases with a diamond-like lattice in which a SV participates. This has been demonstrated for numerous ternary compounds of the type $(A^{II}B_2^{III}\square)C_4^{VI}$.

In this review we do not intend to provide reference information and details of loose structures that have been investigated in various publications up to the present. However, a large number of very common models of the physics and chemistry of loose structures have been experimentally verified, largely by the example of the compounds In_2Te_3, Ga_2Te_3 and Ga_2Se_3 with stoichiometric vacancies, and we therefore considered it necessary to give a brief summary of their physicochemical parameters. These data are collected in Table 1.

The data are obtained from original works by Abrikosov, Goryunova, Hahn, Koshkin, Mushinskii, Newman, Radautsan, Wooley, Zaslavskii, Zhuze and their coworkers.

1.3 Crystal-chemistry Radius of Stoichiometric Vacancy and Lattice Parameters of Crystals with SV

Zhuze, Sergeeva and Shelykh [3] have pointed out an interesting crystal-chemistry fact. It was found that in the isoelectronic series of diamond-like compounds characterized by identical lattice parameters, the values of the lattice parameters of compounds with SV obey the following rule: the values of crystals with SV are substantially less (*see* Table 2). As already mentioned above, chemical bonding in nonmetallic compounds is a superposition of covalent and ionic components, and accordingly it is productive to examine the crystal-chemistry patterns of such compounds by means of procedures using effective covalent radii according to (1.3) as well as by means of calculations involving the stacking of ion spheres. The description of structures without SV, i.e. with complete filling of these or other systems of cavities, gives fairly satisfactory agreement

Table 1 Principal physicochemical parameters of semiconductor compounds of the In_2Te_3 type

Compound	*Phase*	*Lattice parameter a (Å)*	*Melting point T_m (K)*	*Density $\rho \times 10^{-3}$ (kg/m³)*	*Microhardness $H\mu \times 10^6$ (N/m²)*	*Coefficient of thermal expansion $d \times 10^6$ (K⁻¹)*	*Coefficient of thermal conduction λ (J/m·s·K)*	*Energy gap*	
								Optical E_g(eV)	*Thermal E_{g0}(eV)*
In_2Te_3	α	18.40	940	5.79	—	10.1	1.13	1.11	1.08
	β	6.146	α→β* 843	5.73	1630	—	0.7	1.02	—
Ga_2Te_3	β	5.87	1063	5.57	2320	8.3	0.43	1.0	1.27
Ga_2Se_3	α	5.42	1293	4.92	3000	9.57	0.51	1.95	—

* Phase-transition temperature.

Table 2 Comparison of Structural and Thermal Parameters of Isoelectronic Crystalline Compounds [5, 39, 40]

	Compound	*Lattice parameter a (Å)*	*Thermal conduction λ (J/m·s·K)*	*Coefficient of linear expansion $d \times 10^6$ (K⁻¹)*
Isoelectronic germanium series	Ge	5.65	58.66	5.8
	GaAs	5.65	52.38	5.8
	ZnSe	5.66	13.83	7.0
	Ga_2Se_3	5.42	0.50	9.0
Isoelectronic α-tin series	α-Sn	6.46	—	5.2 (220 K)
	InSb	6.45	15.50	5.0
	CdTe	6.46	6.28	5.0
	In_2Te_3	6.15	1.13	7.3

between calculated and experimental data on interatomic distances using a system of ionic radii [18]. However, a similar examination on the basis of ionic radii for crystals with SV gives an extremely poor agreement with experimental values.

In [38] it is shown that if SV are regarded as a component of a crystal with 'ionic' radii r_T^0 and r_O^0, corresponding to the sizes of spheres inscribed in TV and OV, the agreement between the calculated and experimental data is extremely satisfactory. The average size of the structural element in TV and OV when some of the corresponding positions are occupied by atoms and some remain vacant was introduced in the calculations [38]

$$\bar{r}_T = r_T C_T + (1 - C_T)\, r_T^0 \qquad (1.7)$$

$$\bar{r}_O = r_O C_O + (1 - C_O)\, r_O^0, \qquad (1.8)$$

where r_T, r_O, C_T and C_O are the ionic radii and concentrations of the components in TV and OV positions. This corresponds to the assumption that Vegard's rule is satisfied for the statistical distribution of structural elements, including SV.

On introducing ions only into TV, the 'average' lattice parameter of a cubic crystal is

$$\bar{a} = \frac{4\sqrt{3}}{3}\,(R + \bar{r}_T). \qquad (1.9)$$

If ions are introduced only into OV, we have

$$\bar{a} = 2\,(R + \bar{r}_O), \qquad (1.10)$$

where R is the radius of ions of the basic cell.

It was shown during the course of this calculation that in the case of simultaneous occupancy of octahedral and tetrahedral positions the lattice parameter is determined by that ion which results in a large value of the lattice parameter, i.e. the lattice parameter is determined by that particular ion which 'expands' the basic cell more, in other words the size of the SV is less than the size of that structural element with which the SV occurs in identical structural positions, OV or TV.

Calculations of the sizes of SV according to (1.3) from lattice parameter data of a series of binary and ternary crystals with tetrahedral coordination of the atoms and SV with a cationic sublattice also show that the effective 'covalent' radius of the SV is less than the covalent radius of the cations [41], and that this decrease in the SV radius compared to the radii of the cations may range from 5% to 25%. A qualitative model explaining the nature of the SV 'compression' is given in [42].

Of course, numerical values of SV sizes obtained from the values of the ionic and covalent radii of the crystal elements should not, in principle, agree. However, the fact that the crystal-chemistry radius of a stoichiometic vacancy is less than the size of that structural element in the sublattice of which the SV is present is undoubtedly reliable.* This indicates that atoms adjacent to SV are displaced towards the latter.

Radautsan, while performing a fine X-ray structure analysis of $In_2\square Te_3$ crystals and having determined the coordinates of the atoms in this compound, showed that the tellurium atoms surrounding the SV are displaced towards the SV from the correct positions of the basic cubic cell [7].

The nature of the displacement of the atoms of the basic cell from their 'correct' positions is the same as in the case of any solid solutions, where there is a set of different interatomic distances and the decisive lattice parameter obtained from the X-ray data is an average value.

The aforementioned displacement indicates that the geometry of the sp^3 bonds in diamond-like crystals with SV is distorted, though it is clear that the change in the internal energy as a result of the distortion is fairly small compared to the energy of the chemical bond (cf. Section 1.2). The energy introduced by these displacements is, by and large, sufficiently well described as the elastic stress energy. This is examined in more detail in Section 2.

1.4 Peculiarities of Transport Phenomena in Semiconductors with SV

When diamond-like crystals are arranged in an isoelectronic series (Table 2), a striking anomaly appears that is characteristic of crystals with SV: their thermal conductivity is substantially lower than in other crystals of the same isoelectronic series (this was pointed out for the first time in [5]), and the value of the coefficient of thermal expansion in crystals with SV is anomalously large.

An interpretation of this fact was proposed in [41], based on the assumption that the anomalous thermal properties of diamond-like crystals with SV are determined by the anomalously large anharmonicity of the vibrations of atoms adjacent to SV.

In fact, the dependence of the potential energy of an atom adjacent to a SV on the magnitude of its deviation from the equilibrium position is substantially asymmetrical: if the deviation is in the direction of an adjacent atom, work is primarily expended against the rapidly increasing repulsive forces, whereas if the deviation is in the direction of the SV, work is primarily expended against the substantially more long-range attractive forces. Such a dependence of the potential energy E on the displacement u is described by a function substantially different from a quadratic function, for example to a first approximation by

$$E = \varkappa u^2 - g_v u^3, \tag{1.11}$$

where $\varkappa$ is a quasielastic force coefficient and g_v is a coefficient determining the degree of asymmetry of the potential curve and, simultaneously, the anharmonicity of vibrations of atoms adjacent to SV. Of course, the symmetrical vibrations of atoms whose nearest neighbours are not vacancies are described by means of the anharmonic term (g_0) in the expression for the energy:

$$E = \varkappa u^2 - g_0 u^3. \tag{1.12}$$

As is known [43], the coefficient of linear expansion of a crystal is

$$\alpha = \frac{3}{4}\frac{gk}{r_0\varkappa^2}, \tag{1.13}$$

---

* It should be noted that the crystal-chemistry dimensions of vacancies of thermal origin in metals and ionic crystals also correspond to the effective compression of the vacancy.

where r_0 is the interatomic spacing, k is the Boltzmann constant, g is the effective cubic anharmonicity of vibrations of atoms in the crystal; the thermal conductivity of solids is determined by the expression [44]

$$\lambda \sim \frac{\varkappa^{7/2}\,\overline{M}^{-1/2}}{g^2\,r_0 k\,T}, \tag{1.14}$$

where $\overline{M}$ is the average mass of the atoms in the crystal.

Thus, the coefficient of linear expansion α increases and the thermal conductivity λ decreases with a growth in the anharmonicity of vibrations in the crystal. Exactly such a behaviour of the parameters is observed in compounds with SV when they are compared with isoelectronic analogues without SV (Table 2). This result [41] was confirmed by the authors of article [45] in a description of thermal expansion in solid solutions with varying concentrations of SV.

It is important to point out that anomalously low thermal conduction occurs both under a statistical distribution of cations and SV and under ordering of the latter in the cationic sublattice, since under an ordered arrangement of SV, scattering of phonons does not occur in the harmonic approximation. It is clear that anomalously low thermal conduction of crystals with SV is determined by the anomalously large anharmonicity of vibrations of atoms adjacent to SV. It may be concluded from this that in fact the anharmonicity of vibrations of atoms in an asymmetric potential well is substantially greater than in a symmetric well. This fact determines the anomalous behaviour of the thermal parameters of crystals with stoichiometric vacancies.

In articles [46, 47] it is shown that in solid solutions (formed by fusing compounds with SV with isostructural materials without SV), where the concentration of SV may be changed as desired by the investigator by varying the composition of the alloy, the thermal resistance increases with a growth in the concentration of SV. It was shown [46] that this fact cannot be explained by so-called 'alloy' scattering according to Klemens–Ambegaokar [48], associated with variations in density in disordered solid solutions. The magnitude of the thermal resistance at comparatively small concentrations of SV (~3–4% of the total number of lattice sites) is suitably described by the generalized Kontorova equation [44]:

$$\lambda \sim \frac{\varkappa^{7/2}\,\overline{M}^{-1/2}}{r_0\,k\,T}\,[g_v^2 x - g_0^2(1-x)]^{-1}, \tag{1.15}$$

where x is the concentration of SV; g_v, g_0 are respectively the anharmonicity of vibrations of atoms adjacent to SV and remote from SV, obtained [46] assuming independent scattering of phonons at symmetrical and nonsymmetrical anharmonic lattice vibrations.

The results of Aliev *et al.* [47] on the investigation of the thermal conductivity of solid solutions with SV are also in good agreement with (1.15).

The scattering of charge carriers is also significantly determined by the presence of SV, which suppress mobility. The authors [49] have suggested that SV scatter the carriers like neutral centres, in which connection the scattering cross-section coincides with or is close to the crystal-chemistry cross-section of the SV in which permitted states for conductivity electrons are absent. Assuming that the velocities of the electrons are thermal velocities, the authors obtained the following expression for the mobility u

$$u = \frac{e}{\pi\,(3km)^{1/2}}\,\frac{1}{N_v\,r_v^2\,T^{1/2}} \tag{1.16}$$

where r_v is the crystal-chemistry radius of the SV; m, e are respectively the effective mass and charge of an electron; N_v is the number of SV per unit volume; r_v may be calculated according to [22]. This simple dependence enabled the mobilities to be calculated in $(In_2\square)Te_3$, $(Ga_2\square)Te_3$, $(Ga_2\square)Se_3$, $(CdIn_2\square)Te_4$ with a very satisfactory agreement with the experimental data. In article [50] the mobility of carriers in $(Hg_3In_2\square)Te_6$ was calculated fairly accurately by means of Equation (1.16), while in article [51] the change in the mobility of the carriers with a change in the concentration of SV in solid solutions of In_2Te_3–HgTe was calculated. The charge carrier mobilities in semiconductors with SV are rather small (for example, electron mobility in In_2Te_3 is close to the value 50 cm^2/V.S).

2. IMPURITIES AND DEVIATIONS FROM STOICHIOMETRY IN LOOSE CRYSTAL STRUCTURES

2.1 *Impurities in Semiconductor Crystals*

This short review of the behaviour of impurities in semiconductors is necessary for further description of the features of their behaviour in semiconductors with SV. A systematic discussion of the problems of doping conventional semiconductors may be found in the book [52].

There are two possible ways of arranging impurity atoms: in crystal lattice sites (substitution impurities) and in interstices (interstitial impurities). If the crystal-chemistry parameters of the impurity atoms (radius, electronegativity) do not differ greatly from those of the corresponding crystal component, the substitution mechanism is normally effective. If the radius of the impurity atom is sufficiently small (according to evaluations in [52] less than 0.6 of the radius of a matrix atom), the impurities are preferentially localized in the interstices. A comparison of diffusion processes in germanium, silicon and $A^{III}B^{V}$ compounds shows that the coefficients of diffusion of interstitial impurities at the same temperature are always several orders of magnitude greater than the corresponding values for replacement impurities. For example, lithium, iron and nickel, which are interstitial impurities in germanium, have coefficients of diffusion of the order of 10^{-9}–$10^{-10}\,\mathrm{m^2/s}$ at 1100 K, whereas the substitution impurities Zn, Ga, In, P, As and Sb have coefficients of diffusion of the order of 10^{-15}–$10^{-17}\,\mathrm{m^2/s}$ at the same temperature. Copper also diffuses extremely rapidly into Ge and Si, and EPR data indicate that, in the equilibrium state, a substantial proportion of copper atoms are localized in interstitial positions.

In germanium and silicon, substitution impurities whose valency differs by unity from the valency of the atoms of the matrix crystal organize sp^3-hybrid bonds with the latter. If the impurities are elements of Group V (donors in Ge and Si), the excess valency electron is localized on the hydrogen-like orbital centred on the impurity atom, whereas if the impurity is an element of Group III (acceptors in Ge and Si), the deficient electron (hole) is also localized on a similar orbital. According to Mott the energy of the ground state of such a system is

$$E_{\mathrm{el}} = \frac{m^*}{m_0}\frac{E_{\mathrm{H}}}{\varepsilon^2}, \tag{2.1}$$

and the radius of the electron orbit in the crystal is

$$r_{\mathrm{el}} = a_0\varepsilon\,\frac{m_0}{m^*}, \tag{2.2}$$

where E_{H}, a_0 are the energy and radius of the first Bohr orbit of the hydrogen atom, ε is the dielectric constant of the crystal matrix, m_0 is the mass of a free electron, and m^* is the effective mass of the

corresponding charge carrier in the crystal. These valuations according to (2.1) and (2.2) give values of the order of 10^{-2} eV for E_{el}, and ~15–40 Å for r_{el}. The hydrogen-like model adequately describes the experimental data for substitution impurities with a valency differing by unity from the valency of the atoms of the matrix material. This applies not only to germanium and silicon, but to compounds of the type $A^{III}B^{V}$ and $A^{II}B^{VI}$. Such impurities create permitted energy levels of electrons (donors) or holes (acceptors) in the forbidden energy gap. The evaluation of E_{el} given above shows that these fine levels are already ionized at very low temperatures, and that electrons move to the conduction band (or valency band) and determine the concentration of free carriers and the so-called impurity (in contrast to intrinsic) electron or hole conductivity.

Impurities whose valency differs by more than unity from the valency of the atoms they replace form somewhat deeper levels in the forbidden energy gap of the semiconductor, the number of which coincides with the difference in valencies [52]. For such impurities r_{el} is substantially less than for singly-charged impurities, and the approximation that regards the matrix as a continuous medium with a macroscopic value is inapplicable. We shall not dwell on the existing deep centre models cited in the reviews [53, 54], but would merely note that deep impurity levels may reach the range of permitted energy values (for example in the valency band).

Isovalent impurities (e.g. germanium, carbon, and tin in silicon) use all their electrons to form sp^3 bonds and do not contribute 'excess' charge carriers, though the local lattice distortions that they introduce naturally result in the appearance of permitted states in the forbidden energy gap of the levels of the electrons (holes), which in the equilibrium state at $T = 0$ K are not filled by electrons (or holes) since there are no excess carriers.

Inserted in interstices impurity atoms do not participate in the formation of chemical bonds in the crystal, though they may ionize, thereby donating or accepting an electron of the crystal matrix. A classic example of such an impurity is lithium in germanium and silicon, which ionizes, thereby introducing a fine donor level into the forbidden energy gap. Impurities exist (for example, copper) that are localized at lattice sites (in which case they produce a deep acceptor centre), as well as at interstitial sites (fine donor centre).

With an increase in the concentration of impurities the wave functions of the electrons at the impurity levels begin to overlap, creating an impurity band, which then merges with the conduction band or valency band. At relatively low doping levels the concentration of charge carriers increases linearly with an increase in the concentration of impurities. Such a type of dependence is preserved after the formation of the impurity band and after it has merged with any of the forbidden energy gaps. However, at very high doping levels the rise in the concentration of carriers on increasing the concentration of impurities stops. This is the result of interaction of impurity atoms, formation of complexes with one another, and at very large concentrations with the occurrence of advanced precipitation, of a drift of impurities to sinks (dislocations and packing defects). Not infrequently impurities that have formed a complex are electrically passive and do not contribute to the concentration of charge carriers, although all the other properties of the crystals (optical, mechanical, etc.) are essentially changed.

A compensation effect occurs when donor and acceptor impurities are simultaneously introduced into a semiconductor, so that the concentration of charge carriers becomes proportional to the difference in the concentrations of introduced donors and acceptors. If the concentrations of these impurities are equal to one another, there is no impurity conductivity and the semiconductor exhibits only intrinsic conductivity. However, of course, the compensated impurities determine the appearance of permitted states in the forbidden energy gap, which become attachment centres and traps, and the compensated donors and acceptors, being charged centres, very strongly scatter the charge carriers, thereby suppressing their mobility.

The charge state of the impurities, their localization position in the lattice and the dimensional factor determine the level of solubility of impurities in semiconductors. The temperature dependence of the solubility has a marked retrograde character: initially it rapidly increases with a rise in temperature, and then slowly falls.

The solubility of impurities in semiconductors is not large, though for different impurities it may vary within wide limits. In germanium, for example, the maximum solubility of iron is $10^{21}\,m^{-3}$, while the solubility of arsenic reaches $10^{26}\,m^{-3}$ (i.e. in the range $10^{-5}-1$ at.%). The solubility of isovalent impurities, for example tin in Ge and Si, is significantly greater. Silicon with germanium generally forms a continuous series of solid substitution solutions. This is connected with the total isomorphism of the lattices of these substances. The combined solubility of mutually compensating impurities is far greater compared to the solubility of each of them separately. The mechanism of such a combined dissolution is similar to the mechanism of the formation of isomorphous solid solutions, for example Ga and As in germanium [55].

Thus, impurity atoms in semiconductor crystals normally form chemical bonds with matrix atoms or ionize, exhibiting acceptor or donor properties depending on the localization site and chemical nature of the impurity. As a consequence, the equilibrium concentration of charge carriers in doped semiconductors differs from the intrinsic concentration. It should be emphasized in particular that the concentration of charge carriers and, consequently, the electrical conductivity of semiconductors is sensitive to the introduction of even extremely small concentrations of impurities, which greatly increase the conductivity of the semiconductor compared to the intrinsic conductivity. For example, the conductivity of silicon doped with boron (5×10^{-4} wt.%) increases by almost three orders of magnitude compared to undoped silicon at room temperature.

In binary and more complex semiconductors, as is known, there is a deviation from stoichiometry. With an excess of one of the components vacancies are formed in the sublattice of another component, which naturally of course are not stoichiometric vacancies, but instead are the consequence of non-preservation of the valency relationships as a whole over the crystal. These vacancies carry a charge and play the same role in the energy spectrum of the electrons as do impurities, i.e. lead to the formation of donor and acceptor electron states.

Another mechanism of deviations from stoichiometry is the insertion of excess atoms of one of the components in interstitial sites. The fate of these excess atoms is the same as for any impurity atoms in interstice positions. A modern review of the influence of deviations from stoichiometry is given in [56].

2.2 *Effect of Suppression of Electrical Activity of Impurities in Semiconductors with SV*

In contrast to the typical properties of doped semiconductors described in the previous section, the electrical parameters of doped semiconductors with SV are, in principle, different.

In 1960 an article was published by Zhuze, Sergeeva and Shelykh [3], in which the influence of chemically different impurities (belonging to different groups in the Periodic Table) on the electron properties of In_2Te_3 was investigated. The impurity elements Mg, Zn, Cd, Hg, Cu, Sb, Sn, Si and Ge were doped at 1 at.% into In_2Te_3. An investigation of the conductivity σ and Hall constant R of these crystals showed that both these parameters remained unchanged after introduction of the impurities.

An investigation of the temperature dependence of these parameters showed that they are strictly identical since they occur in undoped In_2Te_3. The temperature dependence of σ in the impurity-doped In_2Te_3 was that of the corresponding intrinsic conductivity, in which connection the value of the width of the forbidden energy gap obtained from the dependence $\sigma(1/T)$ coincides with that determined from the transmission spectra and photoconductivity spectra, taking into account the temperature dependence of the forbidden energy gap. Similar results were also obtained from an investigation of the Hall constant and concentration of charge carriers.

It was later [57, 58] demonstrated that impurities in the semiconductor Ga_2Te_3 exhibit the same property of electrical passivity. In these two references it was shown that the electrical conductivity and concentration of carriers in In_2Te_3 as well as in Ga_2Te_3 does not depend on the chemical individuality of the impurities or on their concentration within the limits of the solubility ranges of the corresponding impurities in these crystals (Figure 5), and remains intrinsic

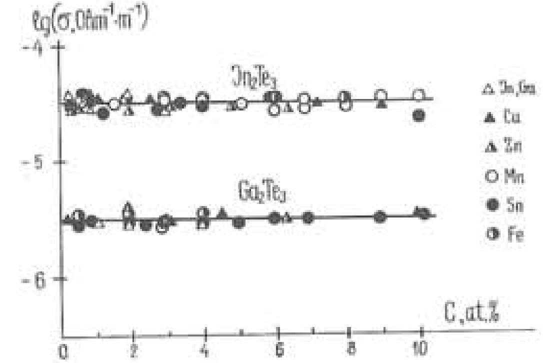

Figure 5 Independence of electrical conduction of compounds In_2Te_3 and Ga_2Te_3 on concentration and chemical individuality of impurities.

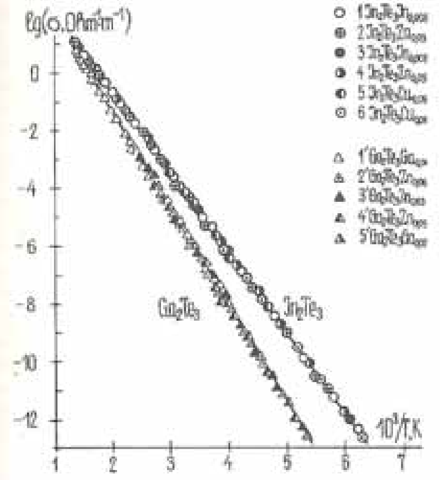

Figure 6 Temperature dependence of specific electrical conduction of doped compounds In_2Te_3 and Ga_2Te_3.

(Figure 6). It was revealed [59–62] that there is a deviation from stoichiometry in In_2Te_3 and Ga_2Te_3, in favour of excess of metal. It was established that the concentration of charge carriers and the conductivity of these crystals practically does not depend on the concentration of the excess component. It should be stressed that in semiconductors without SV, deviations from stoichiometry lead to the same consequences as the introduction of impurities, i.e. to an increase in the concentration of carriers and electrical conductivity values.

Details of a very informative experiment are given in article [63], where the impurity antimony was introduced in In_2Te_3 not along the section of the ternary system In_2Te_3–Sb, but along the section In_2Te_3–Sb_2Te_3. The authors showed that in this case antimony replaces indium while preserving the In_2Te_3 lattice and in complete accord with the fact that the valency of Sb does not coincide with that of the replaced indium, and the concentration of charge carriers increases, i.e. antimony forms a bond with tellurium and appears like a normal substitution impurity in the semiconductor.

We do not know of any specific investigations of the doping of the semiconductor compound Ga_2Se_3, which has the same structure as the above crystals, with the SV present in one-third of all the cationic positions. However, it was shown [64] that even when synthesized from reactants of a not very high degree of purity, so that the total concentration of impurities in the sample was not less than $10^{23}\,m^{-3}$, the Ga_2Se_3 samples exhibited an intrinsic conduction already at 450 K. It should be noted in this connection that at sufficiently low temperatures Ga_2Se_3 always exhibits an impurity conductivity, which, as we shall see below, may be substantial.

We showed that the mechanical parameters of In_2Te_3 and Ga_2Te_3 crystals change substantially under doping [60–62, 65, 66]. In particular, the microhardness values H_μ (indentation of a diamond pyramid) increase with a rise in the concentration of impurities. We shall deal later with the interpretation of this dependence, but would note here that its investigation provides a good possibility of determining the solubility of impurities in In_2Te_3 and Ga_2Te_3, in which electrical methods of determination, which are so convenient and are widely used in investigating conventional semiconductors, are in principle unsuitable in this case due to the 'insensitivity' of the electrical conductivity of crystals with SV to the concentration of impurities.

The investigation of the narrow-gap ternary semiconductor $Hg_3In_2\square Te_6$ having a lattice similar to that of sphalerite and with one-sixth of the cationic positions occupied by SV provides very interesting results. Data [50] show that conductivity in these crystals is intrinsic conductivity, and the impurities Sn, Mn, Fe and Cu specially introduced into a crystal at 1 at.% left the electrical properties of the above semiconductors virtually unchanged [67].

A number of authors have investigated solid solutions of $(A^{III}B^{V})_{1-x}-(B_2^{III}C_3^{VI})_x$, $(A^{II}C^{VI})_{1-x}-(B_2^{III}C_3^{VI})_x$, $(A^{I}B^{III}C_2^{VI})_{1-x}-(B_2^{III}C_3^{VI})x$ (see for example [31, 64, 68–70], in which tetrahedral coordination of atoms and a lattice close to the sphalerite lattice is preserved, and the concentration of SV changes from zero to one-third of the number of cationic positions. In all alloys without exception, containing a substantial amount of uncontrollable impurities, it is found that the concentration of charge carriers rapidly decreases with a rise in the SV concentration, and approaches the intrinsic concentration irrespective of whether or not the width of the forbidden energy gap increases or decreases with an increase in x. This indicates that the presence of SV in fact leads to a suppression of the impurity conduction.

Some possible interpretations of the phenomenon, unique for crystalline semiconductors, of the absence of impurity conductivity dependence on introducing impurities have been proposed.

(a) It was suggested in [33] that an impurity conduction compensation mechanism exists because of the change in the number of SV

(b) Another variant of the compensation mechanism was proposed in [71, 72], involving a possible change in the valency of indium and gallium from 3 to 2 during the dissolution of impurities exhibiting their normal valencies

(c) The possibility of insertion of impurity atoms in SV in an unionized atomic state was suggested in [61, 73, 74].

Any of the above three mechanisms requires a knowledge of the localization site of the impurity and the determination of its valency state. We shall carry out a preliminary crystal-chemistry analysis of the possibilities of dissolution of impurities in In_2Te_3 without the formation of excess electrons, i.e. excess electrons for sp^3 bonds in this crystal, and without the formation of holes, i.e. a deficiency of electrons in the sp^3 bonds [60]. If we assume that the sphalerite lattice is preserved during the dissolution of impurities, then the number of cationic sites in such a lattice, including SV, should remain equal to the number of anionic positions. This is the 'structural' condition. The second condition ('electronic' condition [25, 28]) is that the number of valency electrons belonging to one structural element of the crystal (including SV) should be equal to four. Let us examine from this aspect, for example, the first of the proposed mechanisms of the phenomenon. The structural-chemical formula of the alloy in the case where m SV atoms are 'replaced' by X atoms with valency M with a simultaneous change in the number of SV of v is $\square_{1+v}In_2X_mTe_3$. The 'structural' condition gives $v+m=0$, and the 'electronic' condition $2\times 3+6\times 3+m\times M/1+v+m+2+3=4$, which gives $m\times M=4(v+m)$, i.e. $M\times m=0$, which corresponds to either zero solubility or zero valency during such a replacement. From this it follows that the mechanism for compensating the change in the number of SV is hardly implemented. The assumption concerning inserted impurity atoms in the unionized atomic state is naturally not subject to any restrictions from the point of view of such a crystal-chemistry analysis.

If we assume the possibility of compensation involving charge transfer of some of the indium atoms, two variants of the localization of impurities would be likely: in the first variant the impurities are localized in the SV or interstices, ionize, and some of the indium atoms remaining at the lattice sites change their valency. In the second variant the impurities replace In, and the expelled indium atoms are localized either in the SV or the interstices.

Thus, irrespective of which physical mechanism is involved in suppressing the electrical activity of impurities in In_2Te_3, it should be associated with the insertion of atoms or ions in SV or interstices.

2.3 *Valency Electrons in Interstitial Impurities*

In the investigation of the thermodynamics of dissolution, impurity atoms introduced into the crystal lattice are examined fairly successfully in the continuous elastic model [20]. In this connection it is assumed that the crystal matrix constitutes an elastic medium with a spherical cavity of radius R_0 corresponding either to the crystal-chemistry radius of the replaced matrix atom, or to the geometrical 'void' in the packing of matrix atoms in the case where interstitial impurities are involved. The introduction into a cavity of radius R_0 of an impurity atom, i.e. a sphere of radius $R > R_0$, leads to the appearance of elastic stresses in the matrix and to an increase in its internal energy U. At the same time the elastic medium 'compresses' the impurity atom, resulting in an increase in its internal energy. Such a simple description of the 'mutual' elastic compression of the matrix and impurity atom is completely satisfactory from the point of view of the thermodynamics of solid solutions of metals. When semiconductors are examined according to a similar procedure, the above approximation may be used to evaluate the elastic energy of the matrix. The description of the energy of the impurity atom in such a model does not of course enable us to determine the electron state of the impurity, which is in principle important.

The simplest model describing the electron state of an inserted impurity atom that does not form a chemical bond with the matrix atoms is given in article [75], where a hydrogen-like atom with a spherical cavity of radius R_0 is considered. It is assumed that the spherical potential well has infinitely high walls, and a charge Z^* placed at its centre is the Slater effective charge of the nucleus, taking into account screening by all the electrons of the internal shells of the atom, which are assumed to be undeformed during 'compression' of the atom by the matrix. Using atomic energy units $mZ^{*2}e^2/\hbar^2$ and atomic length units $\hbar^2/mZ^*e$, where m, e are respectively the mass and charge of the electron and $\hbar$ is Planck's constant, we shall write the Hamiltonian in Schrödinger's equation in the form

$$\hat{H} = -\frac{1}{2}\frac{d^2}{dr^2} - \frac{1}{r}\frac{d}{dr} - V(r) \tag{2.3}$$

where the potential

$$V(r) = \begin{cases} -1/r, & \text{for } r < R_0 \\ \infty, & \text{for } r > R_0 \end{cases} \tag{2.4}$$

The S-state of electrons with an orbital quantum number equal to zero is investigated. The energy eigenvalues are similar to those for a free hydrogen atom $E = -1/2n^2$, where n is the principal quantum number. The wave function should satisfy the boundary condition $\psi(R_0) = 0$, the normalization condition $\int_0^R \psi^2(r)r^2\,dr = 1$, and should have a finite value. A numerical calculation of n and $\psi^2(0,R)$ gives the result shown in Figure 7. As was to be expected, for $R_0 \to \infty$ the value of n corresponding to the lower energy state of the electron in the atom tends to unity, i.e. the energy of an electron at $R_0 \to \infty$ approximates to the energy value for the free atom. With a decrease in R_0 the value n rapidly increases. The other asymptote of the curve $n(R)$ is the straight line $R_0(\text{as}) = 1.83$. At $R_0 \to R_0(\text{as})$ the value of n increases without limit, which means that for $R_0 < 1.83$ and the form of the potential (2.4) states with a negative energy do not exist at all on the impurity atom.

The physical meaning of this result is that compression of the electron shell of the atom and an increase in the electron density (see Figure 7) very rapidly raise its energy, and if the walls of the potential well were not assumed to be infinitely high or if the possibility of other electron states were taken into account in the problem (for example the occurrence of chemical bonding or ionization), the electron would move to a lower one of the possible energy states.

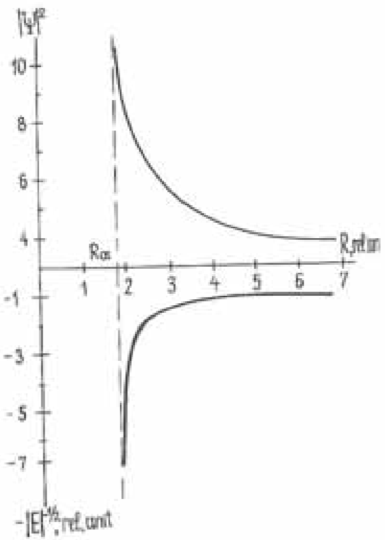

Figure 7 Dependence of electron cloud density $|\psi|^2$ and energy E_{el} of s-electron on radius R of cavity in which neutral atom is situated (infinitely high potential walls).

In article [76] a model is examined that takes account of the finite value of the energy wall at the boundary of the cavity and the possibility of ionization of an impurity atom and the escape of its valency electron to the conduction band of the crystal matrix, where its energy in the ionized impurity field may be described in the Mott form $(-1/\varepsilon r)$, where ε is the dielectric constant of the matrix. It is evident that at $r = R_0$ the potential $(-1/r)$ should continuously transform to the potential $(-1/\varepsilon r)$. The condition of such a 'join' gives the following form of the potential $V(r)$ in the Hamiltonian (2.3):

$$V(r) = \begin{cases} Z^*/r + (Z^* - 1/\varepsilon)/R_0 & \text{for } r \leqslant R_0 \\ -1/\varepsilon r & \text{for } r \geqslant R_0 \end{cases} \tag{2.5}$$

The condition of continuity of the wave function and its derivative for $r = R_0$ leads to the equation defining the spectrum of permitted energies of an electron. The result of a numerical computation of the energy of the lowest state of an electron as a function of the size of the cavity R_0 is given in Figure 8. Naturally, for $R_0 \to \infty$ the energy of an electron corresponds to its energy in a free atom of the impurity, and for $R_0 \to 0$ it corresponds to the energy of an electron in a Mott orbit, localized in the matrix material in the ionized impurity field. A calculation shows that there is a critical value of the size of the cavity $R_0 = R_0(\mathrm{cr})$ such that, for $R_0 < R_0(\mathrm{cr})$, the ground state of an electron is close to the Mott state (ionization of the impurity occurs), while for $R_0 > R_0(\mathrm{cr})$ the dependence of the energy of the electron on R_0 changes sharply and, with a further increase in R_0, rapidly decreases, approximating to the value of the energy of an electron on the impurity in the atomic state. There is an evident natural connection between the values $R_0(\mathrm{as})$ (Figure 7) and $R_0(\mathrm{cr})$ (Figure 8): if the energy barrier for the escape of an electron to the conduction band of the matrix is not infinitely high, then when the energy of an electron becomes close to the ionization

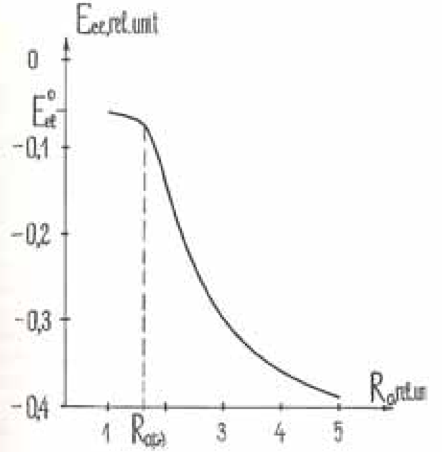

Figure 8 Dependence of energy of electron in atom on radius R_0 of cavity in which atom is situated. Numerical calculation for potential of form (2.5).

potential of the impurity the latter advantageously ionizes. At the same time, the electron occurs in the Mott orbit.

We shall investigate the total change in energy that occurs due to insertion of an impurity atom. When an atom of radius R is accommodated in a cavity of radius R_0, the atom expands the cavity by ΔR and at the same time is itself compressed under the action of the elastic forces of the matrix. In the classic work by Pines [20], where the theory of solid solutions of metals was formulated for the first time, the total energy of the lattice and compressed impurity atom, due to one atom, in an alloy with a concentration of dissolved material $x \ll 1$ is calculated within the framework of the theory of elasticity

$$U = 8\pi\,(\Delta R/R_0)^2 R_0^3 x(1 - x)(1 + lx/S), \qquad (2.6)$$

where $S = 3/4G_0 + \chi_i$; $l = 3/4G_i + \chi_0 - 3/4G_0 - \chi_i$; G_0, G_i are the shear moduli; χ_0, χ_i are the compressibility factors of, respectively, the matrix and impurity material.

As discussed above, the continuous description of the change in internal energy of the matrix adopted in the study of semiconductors is totally satisfactory, though the change in the internal energy of an impurity atom requires examination of the changes in its electron state as a function of the real size of the cavity in which it is localized.

The total energy of an impurity atom and matrix is [76]:

$$U(R_0, \Delta R) = \frac{8\pi}{3} G_0(\Delta R/R_0)^2 R_0^3 + E(R_0 + \Delta R), \qquad (2.7)$$

where the first term describes the energy of an elastically stressed matrix in the vicinity of an interstitial impurity atom of radius $r = R_0 + \Delta R$, and the second term describes the change in energy of an electron in a compressed interstitial impurity atom. It is clear that the latter should essentially be determined by the type of relationship between the sizes of the cavity R_0 and the value of the critical radius $R_{0(\mathrm{cr})}$, defining the transition from the atomic state of the electron to the ionized state existing in the Mott orbit.

The dependence $U(\Delta R)$ at different ratios of R_0 and $R_{0(\mathrm{cr})}$ is illustrated in Figure 9. In the case of large values of R_0 or a soft matrix (small value of G_0) the inserted atom is weakly 'compressed', its electron states are close to the atomic states, and the single energy minimum of the system corresponds to a quantitatively comparatively large ΔR (and relatively small elastic stresses in the matrix), the electron on the interstitial impurity being preserved in a state close to the atomic state. This corresponds to a neutral, unionized impurity atom localized in a cavity (Figure 9, curve 1). In another limiting case, namely where the size of the cavity R_0 is small compared to the crystal-chemistry size of the inserted atom or the matrix is very rigid (G_0 is large), the single minimum of the total energy of the impurity–matrix system corresponds to an ionized atom with an electron in the Mott orbit (Figure 9, curve 4). In the intermediate case the system has two energy minima, U_1 and U_2; one minimum corresponds to a neutral atom with an elastically deformed lattice, and the other to an ionized impurity, though with lesser elastic stresses in the matrix. Depending on the value of R_0 and G_0, both the first and second minima may be deeper (Figure 9, curves 2, 3). It should be noted that, in the case where the inserted atom is ionized, the contribution of the polarization of the lattice, which slightly reduces the energy of the system in the case of an ionized

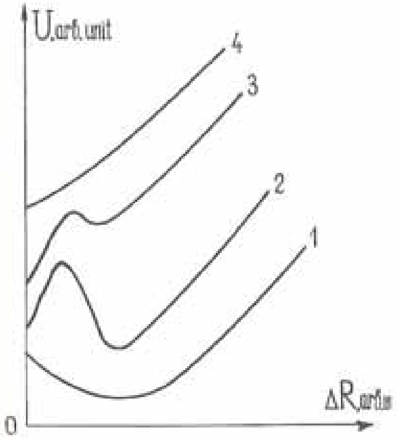

Figure 9 Total energy of system comprising elastic matrix and inserted atom as function of difference ΔR of atomic radius of impurity and radius of cavity (for explanation see text).

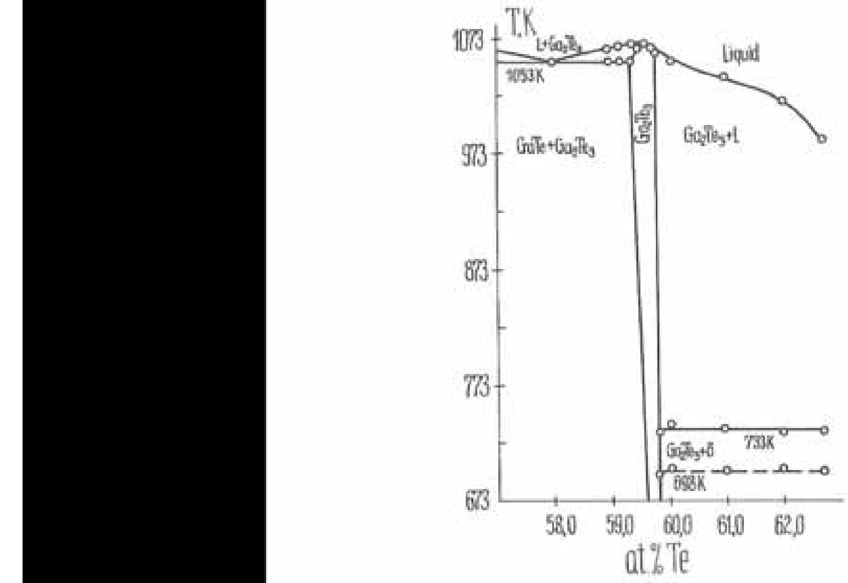

Figure 11 Phase diagram of system Ga–Te in vicinity of compound Ga_2Te_3.

limits of the homogeneity range are high-resistance alloys and have a conductivity and charge-carrier concentration corresponding to intrinsic conduction. The deviation from stoichiometry in Ga_2Te_3 has also been mentioned in [59], where it was also pointed out that the strictly stoichiometric composition has a low resistance.

The systems In_2Te_3–Sb, –Bi, –Mg, –Cd, –Zn, –Cu, –Fe, –Sn were investigated by the same methods and the sections of their phase diagrams in the composition ranges adjacent to the compound In_2Te_3 were also plotted [66, 78–81]. The behaviour of the impurity Mn in In_2Te_3 at various temperatures was also investigated [58, 82]. The general procedure for producing the alloys consisted in preparing a In_2Te_3 melt with the corresponding impurities. The melt was held at a temperature exceeding the melting point by 200–300 K for 24–36 hours, and was then quenched in air or in iced water. The obtained samples were then annealed for 600–1200 hours at temperatures of 823 K and 923 K in order to convert the alloys into the equilibrium state at these temperatures. The state of equilibrium of the alloys was monitored by studying the kinetics of the change in various parameters during annealing (microhardness, electrical conduction, thermo-e.m.f.) combined with X-ray phase analysis.

The solubility of the impurities Bi, Sb, Cd, Zn, Cu, Sn, Fe and Mn in Ga_2Te_3 at various temperatures was investigated by the same methods [58, 66, 78, 80]. Examples of the phase diagram are shown in Figure 12. All these phase diagrams are qualitatively similar to one another and to the section of the diagram In_2Te_3–In. From this it follows that the behaviour of impurity atoms in In_2Te_3 and of superstoichiometric In are thermodynamically similar. The *E* point on these diagrams is apparently close to the singularity point. Bearing in mind the general topological rules, this point should be represented on the phase diagrams as shown in the inset diagrams in Figure 12, though the accuracy of the experimental determinations does not enable this division to be fixed.*

The following particular features of the compounds In_2Te_3 and Ga_2Te_3 as regards their deviation from stoichiometry and dissolution of impurities may be noted:

(a) both compositions are binary with strict stoichiometry, i.e. the strictly stoichiometric compounds In_2Te_3 and Ga_2Te_3 do not exist. The dissolution of superstoichiometric In (or Ga) and dissolution of metallic impurities of any chemical nature stabilizes the In_2Te_3 and Ga_2Te_3 lattice. The concentration C_0 resulting in stabilization is at least less than 0.4 at.%

(b) in all the phase diagrams a composition C_{ext} exists, differing from the stoichiometric composition but presenting within the limits of the homogeneity range based on the In_2Te_3 and Ga_2Te_3 lattice, to which the solidus maximum corresponds

(c) on comparing the solubilities of impurities in the semiconductors In_2Te_3 and Ga_2Te_3 with similar values in other covalent semiconductors — germanium, silicon, gallium arsenide, etc. [52, 83] — we arrive at the conclusion that for

---

* In the homogeneity region of the α-phase of In_2Te_3, under very long annealing times the solution may decompose with the formation of extremely similar crystal-chemistry phases.

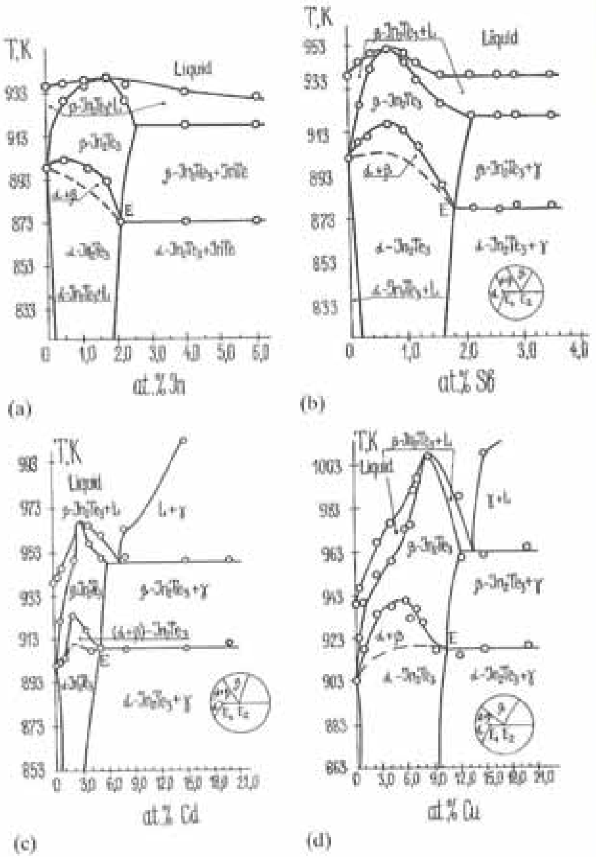

Figure 12 Examples of phase diagrams of systems In_2Te_3—Me; Me: (a) indium, (b) antimony, (c) cadmium, (d) copper.

all impurities, without exception, in crystals with SV the values of the limiting solubility C_m are large but are in general of the same order of magnitude as the maximum solubility of the most soluble impurities in Ge and Si.

We would emphasize once again that, in contrast to all other semiconductors, dissolution of impurities in $B_2^{III}C_3^{VI}$ does not result in the appearance of impurity conduction. The total similarity between the $B_2^{III}C_3^{VI}$ — superstoichiometric B^{III} phase diagram — and the $B_2^{III}C_3^{VI}$ — impurity phase diagram — and the fact of the electrical passivity of the impurities and superstoichiometric atoms leads to the conclusion that the dissolution mechanisms of impurities and deviations from stoichiometry are identical.

Confirmation of this is also provided by experiments on differences in solubility of impurities in In_2Te_3 of stoichiometric composition and in In_2Te_3 containing 0.5 at.% superstoichiometric In [84]. The equilibrium solubility of antimony and cadmium was investigated at 823 K. Whereas the solubility C_m of antimony and cadmium in stoichiometric In_2Te_3 is 1.6 at.% and 3 at.% respectively, the solubility of these impurities in $In_2Te_3In_{0.05}$ is 1.24 at.% (Sb) and 1.90 at.% (Cd). Thus, it was found that the solubility of the impurities decreases if there are already superstoichiometric atoms in In_2Te_3. This indicates that impurities and superstoichiometric atoms compete for a place in the lattice, which confirms the identity of the mechanisms of their localization in the lattice during dissolution.

2.5 *Theory of Solubility of Impurities in Semiconductors with SV*

The analysis of the possible mechanisms of disolution of impurities in crystals with SV given in Section 2.3 showed that one of the probable localization mechanisms of impurity atoms is insertion of such atoms in SV in the unionized, atomic state.

The Helmholtz free energy F of a system with N_v stoichiometric vacancies and N_{imp} impurity atoms per unit volume ($C = N_{imp}/N_v$ is the concentration of impurity atoms localized in SV) was investigated in article [73] assuming that this localization mechanism takes place:

$$F = F_0 + \Delta F = F_0 + \Delta U - T\Delta S, \qquad (2.11)$$

where F_0 is the free energy of the crystal without impurities, and the change in entropy due to localization of N_{imp} impurity atoms in N_v stoichiometric vacancies is

$$\Delta S = k \ln \frac{N_v!}{(N_v - N_{\mathrm{imp}})!\, N_{\mathrm{imp}}!} \qquad (2.12)$$

ΔU denotes the change in internal energy of the crystal under dissolution of the impurities.

As demonstrated above, if the impurities are neutral they produce only elastic stresses in the lattice, the energy of which is determined by the difference in the crystal-chemistry radii of the cavity in which the impurity atoms are localized and the actual crystal-chemistry sizes of the latter. Accordingly, the elastic distortion energy of the lattice due to insertion of one impurity atom in a SV is

$$U_{\mathrm{imp}} = \frac{8\pi}{3} G_0 \left(\frac{\Delta R}{R_0}\right)^2 R_0^3, \qquad (2.13)$$

where R_0 is the effective crystal-chemistry size of the SV, R is the radius of an impurity atom, $\Delta R = R - R_0$ and G_0 is the shear modulus of the material of the matrix (cf. (2.7)). It is obvious, of course, that due to 'replacement' of a stoichiometric vacancy by an impurity atom, the corresponding number of SV 'disappears'. Each SV should make its own contribution to the internal energy of the crystal U_{SV}. If the SV and cations are disordered in the cation sublattice, then U_{SV} may also effectively be described as the elastic stress energy, bearing in mind the fact mentioned in Section 1.3, namely that atoms of anions are shifted towards the SV since its crystal-chemistry size is less than the size of the cation. Generally speaking, the energy of elastic interactions of impurity atoms and SV must be taken into account. Employing the theory [85] describing this type of interaction, it can easily be demonstrated [73] that the energy of such interactions is one-and-a-half to two orders of magnitude less than the energy U_{imp} or U_{SV}. In fact, it is exactly this interaction that is responsible for the formation of clusters of impurities, for the ordering of SV and the ordering of impurities, though its contribution to the total free energy is immeasurably less than the contribution of the elastic stresses introduced by the impurity into the matrix. With the object of establishing the solubility characteristics in the expression for the free energy of the crystal, we shall to a first approximation ignore the contribution of elastic interactions of impurities and SV. Substituting (2.12) into (2.11) after expansion according to Stirling's formula, we have:

$$F - F_0 = \Delta F = N_{\mathrm{SV}}(U_{\mathrm{imp}} - U_{\mathrm{SV}})C + kTN_{\mathrm{SV}}[C\ln C + (1 - C)\ln(1\text{-}C)], \qquad (2.14)$$

where U_{imp} and U_{SV} are respectively the elastic stress energies of the lattice produced by one impurity atom and one SV. The minimum of the free energy of the phase with dissolved impurity is obtained at a concentration C_{ext}, which is the root of the equation $\partial F/\partial C = 0$:

$$C_{\mathrm{ext}} = \{1 + \exp[(U_{\mathrm{imp}} - U_{\mathrm{SV}})/kT]\}. \qquad (2.15)$$

Thus, at an impurity concentration C_{ext} the free energy of the crystal is a minimum, i.e. a crystal with SV under dissolution of such a concentration of impurities localized in the SV is thermodynamically more stable than a crystal without such impurities.

In order to determine the solubility of the impurities it is necessary to solve the problem of the minimum of the free energy of a system consisting of two phases, namely the phase in question with SV with a maximum concentration of impurity C_m at the given temperature, and a second phase that appears in the system when the limiting concentration C_m is reached.

The free energy of such a two-phase system is [20]:

$$\Phi = pF(C_m) + (1 - p)F_2(Z_m), \qquad (2.16)$$

where p and $(1 - p)$ are the concentrations of the specified two phases in the alloy with a given concentration a; $F_2(Z_m)$ is the free energy of the second phase, where the concentration Z_m corresponds to the limit of the region of existence of the second phase with free energy F_2 on the F phase side. From the equilibrium conditions $\partial\Phi/\partial C|_{C_m} = \Phi'_{(C)} = 0$ and $\partial\Phi/\partial Z|_{Z_m} = \Phi'_{(Z)} = 0$, and using the lever rule to determine p through a and the limiting concentrations C_m and Z_m in these phases existing at equilibrium, we obtain the following two equations

$$F'_{(C)}(C_m) = F'_{2(Z)}(Z_m) \qquad (2.17)$$

$$F(C_m) - F_2(Z_m) = C_m F'_{(C)}(C_m) - Z_m F'_{2(Z)}(Z_m) \qquad (2.18)$$

A strict solution of the determination of C_m, as can be seen from Equations (2.18) and (2.17), requires the formulation of a model of the free energy not only of the phase with SV but of the second phase, which appears after the limiting concentration of impurities in the phase F is reached, and which is complicated by the fact that, for the various phase systems, F_2 is generally of a completely different nature.

It is simpler to determine the concentration C_{m} corresponding to the start of instability of the solution of impurities in the phase F.

The free energy of the boundary alloy still present in the solubility range of the impurity may be written in the form (2.11). A certain amount of a second phase with free energy F_2 appears on the other side of the solubility boundary. The phase F becomes unstable when the value of the free energy $F_2(Z_{\text{m}})$ becomes less than the free energy $F = F(C_{\text{m}})$. At the stability boundary of the phase F the free energies of the interacting phases should be equal

$$F_0 + \Delta F_0(C_{\text{m}}) = F_2(Z_{\text{m}}). \tag{2.19}$$

Generally speaking, the values C_{m} and C_{m}^0 do not coincide, though it is easy to determine the condition under which these values are similar. In actual fact, by substituting (2.17) in (2.18) we have

$$F(C_{\text{m}}) = F_2(Z_{\text{m}}) - (Z_{\text{m}} - C_{\text{m}})F'_{(C)}(C_{\text{m}}). \tag{2.20}$$

It is clear that Equation (2.20) coincides with (2.19) if $(Z_{\text{m}} - C_{\text{m}})F'_{(C)}(C_{\text{m}}) \ll F_2(Z_{\text{m}})$, which corresponds to a small value of the derivative $F'_{(C)}(C_{\text{m}})$, i.e. to a relatively weak change in the thermodynamic potential under a change in the concentration of impurities. Unfortunately, it is not possible to evaluate analytically the applicability of the above inequality in the systems under consideration, though, as we shall see later, Equation (2.20) satisfactorily describes the experimental data.

Substituting ΔF from (2.14) in (2.19) and denoting $F_2(Z_{\text{m}}) = F_2$, we obtain the equation for the concentration

$$(1 - C_{\text{m}})\ln(1 - C_{\text{m}}) + C_{\text{m}}\ln C_{\text{m}} = \frac{F_2 - F_0}{N_{\text{SV}}kT} - \frac{U_{\text{imp}} - U_{\text{SV}}}{kT}C_{\text{m}}. \tag{2.21}$$

A full investigation of the solutions of this equation for various ratios of the constants appearing in the latter is given in article [73]. Here we shall discuss in more detail one of the possible variants of the solution, corresponding, as we shall see, to the real situation in phases with SV. For $F_2 - F_0 < 0$, which corresponds to a large thermodynamic stability of the phase F_2 compared to the phase F, where impurities are absent, and for $U_{\text{imp}} - U_{\text{SV}} > 0$ two solutions of Equation (2.21) exist, which are illustrated in Figure 13. The first solution corresponds to the fact that the phase F, which is unstable in the absence of impurities, is stabilized by impurities with concentration C_0, corresponding to the appearance of the stable phase F.

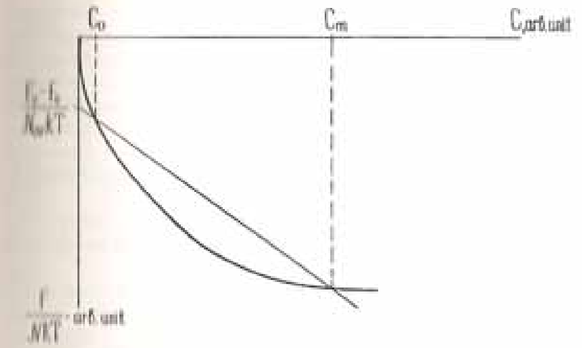

Figure 13 Solution of Equation (2.21).

The second solution corresponds to the limiting concentration C_{m}, above which the second phase F_2 appears. From Figure 13 it is clear that at a constant value of U_{SV}, i.e. for the given crystal with SV, the solubility falls with an increase in U_{imp}.

Thus, the theory of the dissolution of impurities in crystals with SV assuming that the impurities are localized in the SV in a unionized, atomic state leads to the following conclusions [73, 74, 80, 81, 86]:

(a) a strictly stoichiometric composition of compounds with SV may be unstable, and is stabilized only by deviations from stoichiometry or by dissolution of impurities

(b) within the limits of the solubility range the free energy of the phase with SV reaches a minimum at a concentration C_{m}^0, corresponding to the greatest thermodynamic stability of the phase

(c) the solubility of impurities C_{m} should increase with a rise in temperature

(d) the limiting solubility C_{m} of the impurities is determined by the energies of the elastic stresses on the impurity atom U_{imp} and the elastic stresses (U_{SV}) on the vacancy. For a given crystal $U_{\text{SV}} = \text{const.}$, and the value of C_{m} should increase with a decrease in the size of the impurity atom.

To start with we shall compare qualitatively these theoretical conclusions with the experimental data. All the In_2Te_3-impurity phase diagrams show (*see* Section 2.4) that the strictly stoichiometric composition In_2Te_3 is a two-phase composition, and only the introduction of a certain concentration of impurities stabilizes the lattice and the corresponding alloys become single-phase. Superstoichiometric In acts like any other impurity in In_2Te_3. The compound Ga_2Te_3 exhibits a similar behaviour. This confirms the first conclusion of the theory.

If the solidus temperature is taken as a measure of thermodynamic stability, then the presence of a solidus maximum should be regarded as confirmation of point (b) of the theory.

In accordance with conclusion (c) of the theory the value of C_m for all impurities in In_2Te_3 and Ga_2Te_3 increases with a rise in temperature.

Dependences of the limiting solubility C_m of various impurities in In_2Te_3 and Ga_2Te_3 on the crystal-chemistry sizes of the impurity atoms are shown in Figure 14 (the values of the atomic radii [18] are shown relative to a coordination number of four). It is evident that, in complete conformity with conclusion (d) of the theory, the limiting solubility of impurities in In_2Te_3 and Ga_2Te_3 rapidly decreases with an increase in the radii of the impurity atoms. The dependences of C_m on the atomic volumes of impurity atoms, taken from [87], are illustrated in Figure 15. The decrease in C_m with an increase in atomic volume is also evident. Finally, it is known that, according to the well-known Bachinskii–Frenkel–Andrade formula, the value of the reciprocal kinematic viscosity 1/v is proportional to the volume of the atoms in the melt. Using experimental data [88] on the viscosity of melts of various metals, it can be shown that the limiting solubility C_m of impurities decreases with an increase in the reciprocal viscosity of melts of metals corresponding to the impurity material [89].

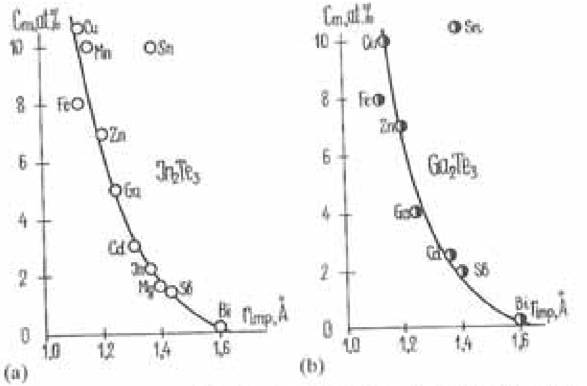

Figure 14 Dependence of limiting solubility C_m on atomic radius of impurity: (a) In_2Te_3 (at 823 K); (b) Ga_2Te_3 (at 923 K).

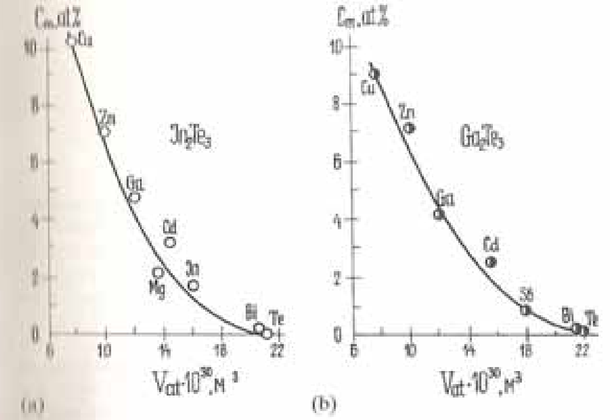

Figure 15 Dependence of limiting solubility C_m on atomic volume of impurities: (a) In_2Te_3 (at 823 K); (b) Ga_2Te_3 (at 923 K).

All these dependences conclusively confirm conclusion (d) of the theory, namely that the solubility of impurities is principally determined by the energy of the elastic stresses introduced by the latter into the lattice with impurity atom localization in the SV, which results in a decrease in solubility with an increase in the size of the impurity atom.

Thus, there is complete qualitative agreement between the experimental data and the theoretical conclusions.

We shall now examine the quantitative agreement between experiment and theory [80, 81, 86].

From (2.21) it follows that the quantity

$$Z = \frac{-kT}{C_m}[1 - C_m)\ln(1 - C_m) + C_m\ln C_m]$$

for different impurities should depend linearly on

$$U_{\text{imp}} = \frac{8\pi G R_0^3}{3}\left(\frac{R}{R_0} - 1\right)^2$$

These dependences are illustrated in Figure 16 for various impurities in In_2Te_3 and Ga_2Te_3. It is clear that they are in fact linear, in total agreement with theory. Eleven impurities differing in crystal-chemistry sizes and chemical properties were investigated. The solubilities of ten of these are completely quantitatively described by the theory. Only the solubility of tin in both In_2Te_3 and Ga_2Te_3 does not satisfy Equation (2.21). This is probably associated with the inpracticability for the systems In_2Te_3–Sn and Ga_2Te_3–Sn of the approximation (2.20), which is based on the fairly rigid and difficultly verifiable condition imposed on the free energies F and F_2. However, a thermodynamic analysis of the dissolution mechanism is possible and with the aid of Equation (2.14), where the characteristics of the second phase are absent, the expression for the concentration C_{ext} corresponds to the minimum of the free energy and to the experimentally determined solidus maximum in the limits of the phase F. From (2.14) it follows that

$$-kT\ln C_{\text{ext}} = U_{\text{imp}} - U_{\text{SV}} = \frac{8}{3}\pi G_0 R_0^3\left(\frac{R}{R_0} - 1\right)^2 - U_{\text{SV}} \quad (2.22)$$

and, consequently, the dependence of $kT\ln C_{\text{ext}}$ on $\left(\frac{R}{R_0} - 1\right)^2$ should be linear. This dependence was plotted [58, 81] using phase diagram data based on In_2Te_3, including the diagram for In_2Te_3–Sn, and is found to be linear, in full agreement with the theory (Figure 17). Accordingly, it may be regarded as proven that the dissolution mechanism for tin, as well as for Fe, Cu, Mn, Zn, Cd, Mg, Sb and Bi and superstoichiometric In and Ga in Ga_2Te_3, consists in the localization of these impurities in the SV. It should be noted that the linear dependences (Figures 16 and 17) are preserved within a wide range of changes of the parameter R_0 (at least in the limits 0,6–1,1 Å) and the choice of this parameter practically has no effect on the nature of the dependences. However, using the experimental

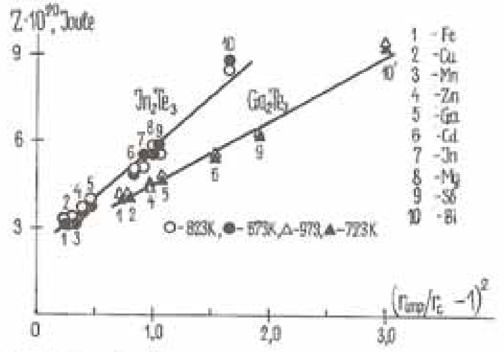

Figure 16 Correspondence between experimental data on solubility C_m of impurities in In_2Te_3 and Ga_2Te_3 and theoretical Equation (2.21) (for explanation see text).

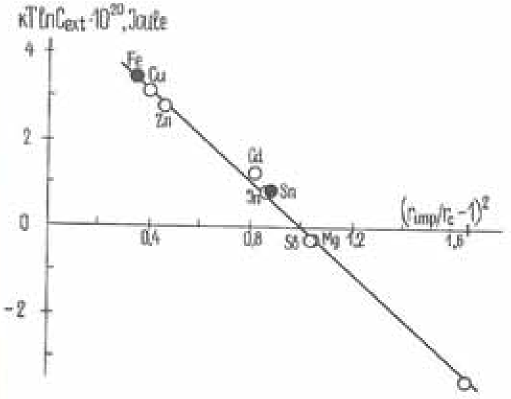

Figure 17 Correspondence between experimental data on C_{ext} in In_2Te_3 and theoretical Equation (2.22) (for explanation see text).

value of the shear modulus G_0 for In_2Te_3 ($9.30 \times 10^{11}\ \text{N/m}^2$) a more accurate estimate of the effective crystal-chemistry size of the SV with respect to the insertion of impurity atoms was obtained, $R_0 = 0.8$ Å. The most probable size of the SV in Ga_2Te_3 is 0.6–0.7 Å. The value of U_{imp} for various impurities, calculated from the independent theoretical Equations (2.14) and (2.20) and using independent experimental determinations of C_m and C_{ext}, give practically identical values, which demonstrates the consistency of the model. By comparing data on the solubility of the same impurity in different crystals with SV, it is possible with the aid of the theoretical equations to estimate the effective elastic stresses on SV [90].

2.6 *Electron States of Impurities in Semiconductors with SV*

The data on the thermodynamics of dissolution of impurities in In_2Te_3 and Ga_2Te_3 discussed in the previous section enable very precise information to be obtained on the electron state of impurity atoms.

The application of the crystal-chemistry analysis method to determine the type of bonding in crystalline compounds consists in comparing the parameters of these compounds with various systems of crystal-chemistry radii of the elements, i.e. covalent, ionic or atomic radii. If correlations are found between any of the parameters and one or other system of radii, conclusions may be drawn concerning the type of bonding that exists in the given compound. An investigation of the thermodynamic parameters of impurity metals in In_2Te_3 (C_{ext} and C_m) and Ga_2Te_3 (C_m) revealed the following [80, 81, 86, 91]:

1. There were no correlations whatsoever between these values and the values of the covalent tetrahedral radii [18, 22] of the impurities. This indicates the absence of covalent bonding between impurity atoms and matrix atoms.
2. It was shown that there is no correlation between the values C_m and C_{ext} and the values of the ionic radii of the impurities, whatever assumptions were made concerning the degree and nature of the ionization. This indicates that the impurity atoms are not ionized.
3. A regular uniform decrease in C_m and C_{ext} is observed in fact only with an increase in atomic radii and atomic volumes of impurity atoms (Figures 14 and 15). Furthermore, the calculations given in Section 2.5 showed that all the thermodynamic characteristics of solutions of impurities in In_2Te_3 and Ga_2Te_3 are satisfactorily quantitatively described using just the atomic radii of the impurities. All these facts indicate that impurity atoms in crystals of In_2Te_3 and Ga_2Te_3 do not ionize, do not participate in chemical bonding with matrix atoms, and are in the atomic state. The thermodynamics of solutions of impurities in In_2Te_3 and Ga_2Te_3 can, as shown above, be completely quantitatively described taking account only of the energy of the elastic stresses in the lattice produced by the insertion of impurity atoms in SV, which also confirms the fact that impurities in these crystals are not ionized.
4. Both the electrical conduction and thermodynamic parameters of doped crystals are entirely independent of the chemical individuality of the impurities. Impurity metals of Group I of the Periodic System (Cu), Group II (Mg, Zn, Cd), Group III (In, Ga), Group IV (Sn), Group V (Sb and Bi), Group VI (Mn), and Group VII (Fe) do not exhibit any features of chemical differences in $A_2^{III}B_3^{VI}$, and only their atomic sizes determine the thermodynamic parameters of the doped crystals.

Essential information on the state of the impurities may be obtained from measurements of the microhardness H_μ (impression produced by a diamond tip). It was shown [92] that the microhardness of crystals with predominantly covalent bonding is determined by the mobility of the dislocations, to be more precise by the magnitude of the Peierls barrier. When doping In_2Te_3 and Ga_2Te_3, as already mentioned above, the values of H_μ increase with a rise in the concentration of impurities. These dependences were investigated in article [65]. It was found that at a concentration equal to the limiting solubility C_m, the value of H_μ reaches a magnitude that is practically identical for all impurities in each of the specified materials (limiting hardening). In this connection, it is obvious that the specific increase in microhardness per unit concentration ($\Delta H_\mu/C$) differs for different impurities and is determined by their atomic size. The magnitude of H_μ is determined by the plastic deformation of the material during impression, i.e. by the generation and mobility of dislocations, and accordingly in [65] the increase in H_μ due to doping is regarded as the result of pinning of dislocations on the impurities. As is known, the hardness of a material is a quantity proportional to the critical mechanical stress necessary to move the dislocations; $H\mu$ is described by the expression

$$H_\mu = A\exp(E/kT), \qquad (2.23)$$

where A is a constant and E is the energy barrier that the dislocation has to overcome in order to execute free movement. The pinning of dislocations with doping and, consequently, the specific increase should be determined by the energy of the deformation on the impurities, these values being calculated from the thermodynamic data given above. In [65] it is shown that

$$\Delta H_{\mu} = BC\exp[\alpha(U_{imp} - U_{SV})/kT], \tag{2.24}$$

where α and B are coefficients. The dependences of $\log[\Delta H\mu/c]$ on $|U_{imp} - U_{SV}|$ for In_2Te_3 and Ga_2Te_3 doped with different impurities at various equilibrium temperatures are shown in Figure 18. The assumption concerning the stopping of dislocations at elastic deformations of the lattice produced in fact by neutral impurities is confirmed.

An analysis of the thermodynamic data thus confirms the assumption that impurity atoms in In_2Te_3 and Ga_2Te_3 are localized in stoichiometric vacancies, and remain in an unionized, atomic state and do not participate in chemical bonding with matrix atoms. A neutral stoichiometric vacancy is as it were 'replaced' by a neutral impurity atom.

In addition to thermodynamic data and data on the preservation of the intrinsic nature of the conduction in strongly doped In_2Te_3 and Ga_2Te_3 semiconductors, a whole range of other evidence has

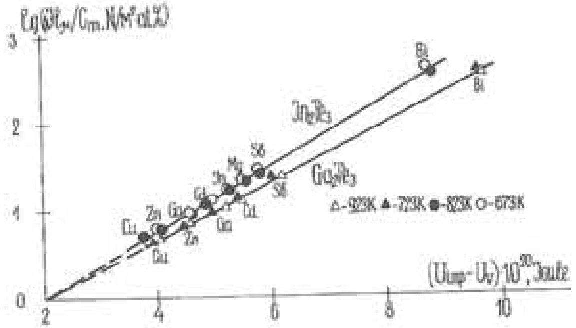

Figure 18 Correspondence between experimental data on microhardness H_μ of doped crystals of In_2Te_3 and Ga_2Te_3 and expression (2.24) (for explanation see text).

been obtained which shows that impurities in these crystals are in an atomic state. An investigation of the mobility of electrons in doped In_2Te_3 showed that, in both polycrystalline and monocrystalline samples, this quantity is practically identical and has a value of $(45 \pm 25) \times 10^{-4}\,m^2/V.s$. The concentration of impurities reaches values exceeding $10^{26}\,m^{-3}$, and if it is assumed that the impurities are ionized, then an evaluation of the mobility according to the known Conwell–Weisskopf model [93] gives a value of the mobility of the order of $10^{-4}\,m^2/V.s$, i.e. at least one order of magnitude less than is actually observed. This points to the absence of the electrical compensation effect of impurities by charge transfer of In atoms, suggested in article [71]. The absence of the compensation effect is also demonstrated by experiments on the joint solubility of In and Sb and In and Cd in In_2Te_3 [84], which are described in Section 2.5.

A series of investigations has been devoted to a study of nuclear gamma resonance (NGR) spectra in the impurities ^{119}Sn and ^{57}Fe in In_2Te_3 and Ga_2Te_3 [72, 75, 94–96]. The experiments showed that impurity ^{119}Sn gives identical values of the chemical shift with respect to the source $Ba^{119}SnO_3$ in both In_2Te_3 and Ga_2Te_3 ($\delta = (3.58 \pm 0.05) \times 10^{-3}\,m/s$ at $T = 300\,K$ and $\delta = (3.75 \pm 0.04) \times 10^{-3}$ at $T = 30\,K$), the intensity of the absorption peaks increasing with a rise in the concentration of implanted tin. This indicates that a single mechanism is involved in the dissolution of tin in In_2Te_3 and Ga_2Te_3.

In the NGR spectra of alloys of In_2Te_3 and Ga_2Te_3 with iron-57 at room temperature, an intense twin doublet is observed, the centres of gravity of these doublets coincide, and the identical value of the isomeric shift with respect to $^{57}CoPd$ for In_2Te_3 and Ga_2Te_3 ($\delta = (0.40 \pm 0.04) \times 10^{-3}\,m/s$) also indicates that the mechanisms of dissolution of impurities in these semiconductors are identical. The large value of the quadrupole splitting characteristic of the iron states $Fe^{2+}(3d^6)$, $Fe^0(3d^7 4s)$ and $Fe^0(3d^6 4s^2)$ in a crystal field of symmetry less than cubic symmetry [97, 98] indicates the local destruction of tetrahedral symmetry in crystals with SV. The presence of two doublets with one centre of gravity shows that the iron atoms are localized in two crystallographically nonidentical positions, although the electron states of the impurity in both positions are identical, judging from the coincidence of the magnitude of the isomeric shift. A similar situation exists for example in the case of neutral ion atoms Fe^0 frozen in a matrix of solid CO_2 [97]. On lowering the temperature the 'internal' iron doublet in In_2Te_3 and Ga_2Te_3 coalesces with the external doublet [96], which indicates that the values of the internal energies corresponding to these two states of the impurity atom are extremely close, and that the transition barrier from one state to the other is small. According to evaluations [96] this barrier is $\sim 10^{-2}$ eV. An investigation of the quadrupole splitting of NGR spectra of iron in In_2Te_3 and Ga_2Te_3 showed that the intensity of the 'internal' doublet with less splitting in the Ga_2Te_3 disordered phase decreases, whereas in the β-phase of In_2Te_3 this doublet is completely absent [96]. It may therefore be assumed that the non-equivalence of the positions of the iron impurity atoms is manifested only under ordering of the SV.

The presence of two nonequivalent positions of impurity atoms of both iron and manganese in In_2Te_3 and Ga_2Te_3 is detected in the EPR spectra [58]. In the EPR spectra of manganese that have been investigated more fully, two broad isotropic signals are observed with a g-factor of 2.0 and width 1 kOe (7.96×10^4 A/m) and $g = 4.3$ and width 0.4 kOe (3.18×10^4 A/m), and the relative integral intensity of the signal with $g = 2$ is one to two orders of magnitude greater than the intensity of the signal with $g = 4.3$. The intensity of both increases with an increase in the manganese concentration. The fine structure of the spectra is not resolved. Practically such manganese EPR spectra with respect to all parameters were discovered in various semiconductor glasses [99, 100], which is associated with the presence in the glass net of two nonequivalent positions, in one of which the impurity is in a weak crystal field of tetrahedral symmetry (g-factor equal to 2.0) and in a strong field of axial symmetry ($g = 4.3$).

The NGR spectroscopy data may provide information on the electron state of the impurities since, as is known, the magnitude of the chemical shift δ characterizes the density of s-electrons at the nucleus of the atom.

However, a direct determination of the electron state of impurities in In_2Te_3 from the NGR spectra proved fairly complex. The value of the isomeric shift for tin in In_2Te_3 and Ga_2Te_3 ($\delta = (3.58 \pm 0.05) \times 10^{-3}$ m/s) was found to be close to the value of δ for tin in the compound SnTe, which led the authors [71, 72] to suggest that the impurity tin forms a chemical bond with tellurium atoms in the In_2Te_3 matrix. Meanwhile, the isomeric shift scale for tetrahedrally coordinated tin constructed in [94], where the dependence of the magnitude of the shift on the real value of the electron density on the nucleus is obtained (taking into account the charge transfer in the chemical bond according to [16] and also taking into account the screening action of the valency electrons according to [101] with relativistic corrections, which are substantial for heavy atoms), gives good agreement between the experimental value of the isomeric shift and the calculated value for a neutral tin atom. This value is also close to the evaluation [102] of the shift for a neutral atom in fairly rigid crystal matrices. The difference between the value of δ in In_2Te_3 and Ga_2Te_3 and that for tin in solidified inert gases [103, 104] is associated in [75] with the effect of 'compression' of the electron shell of implanted neutral atoms in matrices of high rigidity when the density of electrons on the nucleus increases (*see* Section 2.3 and Figure 9). However, the results given in [105] may well be the most informative, where in one experiment the value of δ was determined for Sn in In_2Te_3 and tin in SnTe, where a significant difference in the values was found ($\delta = (0.80 \pm 0.05) \times 10^{-3}$ m/s for SnTe and $\delta = (0.90 \pm 0.05) \times 10^{-3}$ m/s for tin in In_2Te_3).

When investigating the NGR spectra of iron in In_2Te_3 and Ga_2Te_3 it was discovered [95] that the value of δ is close to that for Fe^{2+} ions. The authors of article [72] suggested that iron in these crystals is present in a state of chemical bonding with Te atoms in In_2Te_3 and Ga_2Te_3. Meanwhile iron introduced in a CdTe crystal, which is of similar structure, and situated in the latter in a cadmium substitution position under a practically identical degree of charge transfer, differs from the value of the Fe isomeric shift in In_2Te_3 ($\delta = 0.33 \times 10^{-3}$ and 0.42×10^{-3} m/s respectively at $T = 300$ K). This is hardly in agreement with the assumption made in [72]. The latter also does not agree with the thermodynamics data (see above). In article [95], starting from the assumption that iron atoms implanted in a In_2Te_3 and Ga_2Te_3 matrix are neutral, a scale of isomeric shifts δ was constructed as a function of the electron density on the Fe nucleus, calculated according to [106] for different electron configurations of iron atoms by the Hartree–Fock method, though taking into account relativistic corrections [107]. In constructing the scale the values of δ were used for neutral Fe^0 atoms localized in the cavities of a loose lattice of zeolites [108], and neutral iron atoms implanted in a matrix of solidified inert gases [104]. In the first of these materials the iron state is characterized as $3d^8$, and in the second as $3d^6 4s^2$. The aforementioned calculations show that the iron state in In_2Te_3 and Ga_2Te_3 may be very convincingly interpreted as a $3d^7 4s$ state. Of course, as in zeolites, the change in the electron state of a neutral iron atom compared to its state in a free Fe atom should be associated with a 'compression' of the electron shell of the atom by the matrix in which it is introduced.

Thus, Mössbauer spectroscopy of both tin and iron gives results that are in full agreement with the assumed neutrality of impurity atoms in crystals of In_2Te_3 and Ga_2Te_3. However, on account of the closeness of the experimental values of the isomeric shift corresponding to the ionized species Sn^{2+} and Fe^{2+}, and unionized Sn^0 and Fe^0, there is no longer a clear choice between these two variants. Data on the temperature dependence of quadrupole splitting provide more specific evidence of the absence of chemical bonding between the impurities and the matrix.

In the aforementioned articles [95, 96] the temperature evolution of the specified two NGR iron doublets is investigated. It was found that the 'internal' doublet substantially decreases in intensity on lowering the temperature, the process being completely reversible. The activation energy of this process is measured in [96], and was found to be extremely small (1×10^{-2} eV). The authors of [96] explain this effect by migration of iron atoms between nonequivalent positions, assuming that such a low migration activation energy of an impurity atom may exist only in the absence of a chemical bond between the impurity atom and matrix. The surprising ease with which iron volatilizes from doped samples during prolonged annealing, which is reflected in a decrease in the intensity of the NGR spectra, is also noted in [96]. This is also evidence of an extremely weak bonding of iron atoms in In_2Te_3 and Ga_2Te_3 lattices.

Other spectroscopic investigations of the doping of In_2Te_3 and Ga_2Te_3 crystals have been carried out, which also unequivocally point to the absence of chemical bonding between impurity atoms and matrix atoms.

X-ray emission spectra of In_2Te_3 and Ga_2Te_3 doped with tin are compared with a number of tin compounds (SnO_2, SnTe, β-tin) in article [109]. It was found that the chemical shifts L_{α_1} and L_{α_2} of the tin lines in In_2Te_3 and Ga_2Te_3 are coinciding and exceed the values of the chemical shifts for SnO_2 and SnTe. In SnO_2, which may to a good approximation be regarded as an ionic compound, Sn has a charge of +4. Tin in SnTe formally has a charge of +2, though since the degree of ionicity in this compound is less than 50%, the effective Sn charge is ≤ 1. The chemical shift for tin dissolved in In_2Te_3 and Ga_2Te_3 is substantially greater than for tin in SnTe, which indicates that the degree of charge transfer from tin is substantially less than unity. On the basis of these data it may be asserted that the state of tin in In_2Te_3 and Ga_2Te_3 is at least close to the state of a neutral atom that has not lost its valency electrons.

In [110] a study is made of the IR absorption of In_2Te_3 doped with various impurities (Cu, Fe, Mg, Mn, Co, superstoichiometric

In) in different concentrations in the limits of the homogeneity regions of the corresponding alloys. The authors [110] showed that, with introduction of the impurities, the lattice absorption maxima are weakly though uniformly displaced, demonstrating that the bonds in the In_2Te_3 matrix are distorted during insertion of impurities, due to elastic displacements. However, absorption bands corresponding to Te-impurity atom bonds or indium of a different valency do not appear. The bond distortion that is observed in IR absorption experiments is obviously the result of local changes in the In–Te bond energies in the In_2Te_3 matrix, as a consequence of distortions of the lattice in the vicinity of the interstitial impurity atoms (see above).

Photoelectron spectra of In_2Te_3 are investigated in article [72]. It was found that the photoelectron spectrum of indium during doping of In_2Te_3 with iron and tin is displaced by 0.15 ± 0.06 eV, which corresponds to a decrease of this magnitude in the binding energy of an electron. This experimental result is thus in qualitative agreement with the IR spectroscopy data [110] and that obtained by thermodynamic calculations (Section 2.4). It is important that new bands compared to In_2Te_3, which might indicate the presence of some new electron states of indium, are not discovered in the photoelectron spectra after doping.

An investigation of IR spectra of alloys from a system of solid solutions of $CuInTe_2-In_2Te_3$, in which copper is knowingly present in substitution positions and is chemically bonded to tellurium atoms [69], was also carried out in [110]. It was found that the IR spectra of alloys with bonded copper differ completely from the spectra for alloys where copper is inserted in the In_2Te_3 as an independent impurity. Using these data as a basis, the authors [110] maintain that impurities introduced into In_2Te_3 as individual impurities (over the cross-section of the ternary system In_2Te_3—impurity) do not participate in chemical bonding with tellurium and are present in a nonionized, atomic state. It was noted that the anomalous properties in the IR absorption of In_2Te_3 with impurity magnesium are probably connected with the nonequilibrium state of the investigated alloy.

In an investigation of positron annihilation carried out by Dekhtyar and Rustamov [111], it was shown that only a small proportion of impurity copper in In_2Te_3 is apparently charged. This fraction is of the order of 0.1% of the total number of impurity atoms introduced in the crystal, the remaining impurity atoms being uncharged.

As mentioned above, the data used to demonstrate the dependence of thermodynamic dissolution parameters on the atomic radii of impurity atoms in In_2Te_3 and Ga_2Te_3, as well the presented data of various types of spectroscopy, merely demonstrate that impurity atoms do not chemically react with matrix atoms. These data do not exclude the possibility of chemical interaction between the impurity atoms themselves. There are a number of experimental facts that indicate such an interaction apparently takes place. This was suggested for the first time by the authors of article [112] when investigating EPR spectra in In_2Te_3 with excess indium.

Data on the temperature dependence of the magnetic susceptibility of Ga_2Te_3 [113] containing excess superstoichiometric gallium ($\sim 1.5 \times 10^{26}\,m^{-3}$) and antimony as impurity ($\sim 5 \times 10^{25}\,m^{-3}$) showed that only a small fraction of these atoms give a paramagnetic response ($\sim 10^{23}\,m^{-3}$), and the overwhelming proportion of introduced impurity atoms do not contribute. The authors [113] associate this experimental result with a charge transfer of gallium in the lattice and with a compensation effect. However, as already mentioned above, data on the thermodynamics of dissolution as well as on the scattering of charge carriers indicate the absence of any compensation effects. Meanwhile, this very interesting result [113] may be interpreted as a result of the interaction of superstoichiometric gallium or antimony atoms with organized clusters of impurity atoms with Ga−Ga or Sb−Sb bonds, accompanied by the coupling of uncompensated spins of *p*-electrons. The experimentally determined paramagnetic particles are isolated Ga^0 and Sb^0 atoms. Obviously, the binding energy between impurity atoms localized in two adjacent vacancies is very small and its contribution to the total internal energy of the crystal may be ignored. At the same time, the magnetic properties of doped samples are largely determined by the formation of such two-electron bonds. Evidence of interaction between impurities and the formation of clusters may also be obtained from the result discussed in [58, 72, 82], where it is shown that ferromagnetism is detected up to a temperature of 810 K in the α-phase of $In_2Te_3Fe_x$ doped with iron ($x = 0.07$). The formation of similar clusters is a fairly common phenomenon in covalent semiconductors [114]. Although no specific investigations on the formation of impurity clusters in In_2Te_3 and Ga_2Te_3 have been carried out, the available results evidently point to the existence of such clusters.

The combination of experimental and theoretical data thus provides a basis for maintaining that the overwhelming proportion of impurity atoms and superstoichiometric atoms are localized in stoichiometric

vacancies of In_2Te_3 and Ga_2Te_3 crystals in an unionized, atomic state, in which connection the formation of clusters of impurity atoms is possible. The fact that the principal dissolution mechanism in In_2Te_3 and Ga_2Te_3 is determined by the localization of impurity atoms in SV in an atomic state obviously does not exclude, as shown in [77] (*see* Section 2.2), manifestations of other equilibrium mechanisms involved in solubility. It should be noted at the same time that even neutral impurity or superstoichiometric atoms, without introducing additional electrons (or holes), of course produce distortions in the lattice, and by destroying its periodicity lead to the appearance of permitted local states in the energy gap. The formation of traps of this type is investigated in [115].

In [95] it was shown that a fairly weak though stable signal corresponding to the iron state Fe^{3+} is detected in the NGR spectra of In_2Te_3 and Ga_2Te_3 doped with iron. The question arises of the mechanism of formation of Fe^{3+} during In_2Te_3-Fe and Ga_2Te_3-Fe cross-section doping of the corresponding ternary systems. One of the possible variants from the crystal-chemistry aspect is insertion of ions in interstitial positions or in SV. Such a variant would however conflict with the fact that impurity conduction does not occur in this connection. It is most likely that a small proportion of the iron impurity replaces trivalent indium (or gallium), in which connection indium (gallium) atoms displaced from their sites are localized in SV as if they were superstoichiometric.

The compounds Ga_2Se_3 and Ga_2S_3, which are similar as regards crystal chemistry to In_2Te_3 and Ga_2Te_3 and have, like the latter, one-third SV in the cation sublattice, have been studied in much less detail than indium and gallium tellurides.

With regard to Ga_2Se_3 it has been shown [64] that, irrespective of the purity of the reactants from which this compound is synthesized, its electrical resistivity is very high. However, the temperature dependence of the latter shows that intrinsic conduction starts above 500 K. It was demonstrated qualitatively in [64] that whatever assumptions are made concerning the depth of the impurity energy levels in the energy gap and with any reasonable assumptions concerning the concentration of uncontrolled impurities, such a low electrical conduction and its closeness to the intrinsic conduction cannot be ensured if all the impurity atoms form chemical bonds with the matrix and can supply electrons (or holes). Thus, the electrical activity of the impurities is substantially suppressed in Ga_2Se_3. On the other hand, it is clear that some of the impurity atoms in Ga_2Se_3

are undoubtedly ionized. In article [116] the authors provide evidence from EPR data of the presence of ionized impurity iron in Ga_2Se_3, though they do not give any estimate of the proportion of these states relative to the total amount of introduced impurities.

The doping of Ga_2S_3 crystals has hardly been studied at all. The authors of article [117] interpret the iron NGR spectra obtained by them in Ga_2S_3 as Fe^{2+}. A specific analysis of the possible state Fe^0 was not given. The number of centres producing a spectral signal was also not estimated. EPR spectra of manganese in Ga_2S_3 obtained in [117] were also interpreted as Mn^{2+}. Such an interpretation is probably reasonable, though it should be borne in mind that the spin states of Mn^0 and Mn^{2+} are identical, and it is therefore difficult to draw an unambiguous conclusion. It is striking that the superfine structure of the EPR spectrum of manganese in Ga_2S_3 is already detected at $T = 300$ K. This possibly points to a decrease in the spin-phonon coupling, which might occur when *d*-electrons are screened by *s*-electrons of the outer Mn shell, if Mn^0 keeps its *s*-electrons.

The electrical and optical properties of doped Ga_2S_3 crystals, which could help to provide an estimate of the concentration of ionized centres, have not yet been investigated.

Thus, it should be regarded as established that in crystal of Ga_2Se_3, Ga_2S_3 and even In_2Te_3 and Ga_2Te_3, at least a certain proportion of the impurities is ionized. This is a direct consequence of the result [77] (cf. Section 2.5), according to which if various dissolution mechanisms are possible, then all necessarily exist, and the relative amount of impurities localized in the lattice according to one or other mechanism depends very critically on the internal energy of the corresponding type of defect.

Comparing tellurides, selenides and sulphides with SV, three important facts should be noted. Firstly, the crystal-chemistry sizes of the SV are greatest in tellurides. Secondly, the values of the dielectric-constant ε are also greater in In_2Te_3 and Ga_2Te_3 compared to Ga_2S_3 and Ga_2Se_3. Finally, the shear modulus G of tellurides is less than in sulphides and selenides. From a theoretical examination [76] (Section 2.3) it follows that, with an increase in R_0, a decrease in G and an increase in the dielectric constant, the energy corresponding to localization of a neutral atom in a vacancy decreases, and the energy of the ionized (Mott) centre increases.

In In_2Te_3 and Ga_2Te_3 the difference in the energy of inserted unionized atoms and the energy of the Mott centres is therefore large, since in accordance with [77] (*see* expression (2.10)), the equilibrium concentration of the latter is vanishingly small. In gallium selenide (Ga_2Se_3), and particularly in gallium sulphide (Ga_2S_3), the energy of the inserted atom increases, while the energy of the ionized atom decreases. In accordance with (2.10) this leads to an increase in the fraction of ionized impurities in Ga_2Se_3 and Ga_2S_3 compared to In_2Te_3 and Ga_2Te_3.

To conclude this section, we would point out that impurity atoms not involved in chemical bonding with atoms of the crystal matrix are detected also in other crystal bodies. An anomalously weak dependence of the electrical conduction on the concentration of impurities was noted in article [118], in which the semiconductor Sc_2S_3, which has a sodium chloride crystal lattice with SV in the cation sublattice, was doped. It was shown that in the equilibrium state, the impurity iron atoms do not form chemical bonds with the matrix atoms and are present in an unionized state in zeolites [119], where very large free cavities exist in the crystal lattice. It was also shown that hydrogen atoms, which have an extremely small crystal-chemistry size, are localized in interstitial positions in germanium and silicon, and remain in an atomic state [120]. In all other cases known to us impurity atoms in crystals are either ionized or form chemical bonds with matrix atoms.

It is known that the intrinsic conduction is preserved in semiconductor glasses doped with impurities. We do not intend to provide an analysis of the various models of this phenomenon, but would mention that one of the probable mechanisms is the localization of impurities in an unionized atomic state in cavities present in the matrix of semiconductor glasses [76, 121].

3. COMPOUNDS WITH LAYER STRUCTURE

3.1 Layer Structures and Physical Chemistry of Intercalation

Layer-type crystals, a classic example of which is graphite (see reviews [122–124]), are included among loose crystal structures. The structure of many crystalline compounds with a layer-type lattice may also be interpreted in terms of stoichiometric structural vacancies ($(Cd\square)I_2$, $(Pb\square)I_2$, $(Nb\square)Se_2$, $(Ta\square)S_2$, $Tl_2(S\square)$, $Ag_2(F\square)$, $(Bi_2\square)Te_3$, etc.). Compared to crystals of $(In_2\square)Te_3$, $(Sc_2\square)S_3$, $Y_2(\square O_3)$ and structures similar to the latter, where SV are distributed — ordered or disordered — but necessarily three-dimensionally among the sites of the cation or anion sublattice, SV in crystals of the type PbI_2, NbS_2 or Bi_2Te_3 comprise vacant layers unfilled by atoms. Each such SV layer is split up into three-layer packets (I–Pb–I or Tl–S–Tl), or five-layer packets (for example Te–Bi–Te–Bi–Te), since strong ion-covalent bonding, and very often also metallic bonding, exists within the packets, whereas only weak van der Waals forces act between the packets, i.e. through the layer of stoichiometric vacancies. In addition to the aforementioned types of layer structures, compounds with four-layer packets also exist (for example GaS, where bonding between metal atoms occurs in the packet S–Ga–Ga–S). The simplest and most comprehensively studied layer structure is graphite, which has single-atom packets and comprises a network of covalently bonded carbon atoms separated by van der Waals spaces. The quasi-two-dimensional structure of the packets results in a number of particular features in the electron and lattice vibration spectres (see [122]). In the present review we shall mainly discuss the phenomena resulting from the structural looseness of layer-type compounds, which is most clearly expressed in the intercalation effect.

An investigation of the interaction of such layer-type crystals with molecules (organic and inorganic), atoms and ions of different chemical natures showed that foreign molecules and atoms in equilibrium are localized in inter-layer gaps of the layer-type crystals [124–127]. The penetration of foreign molecules in interlayer spaces accompanied by the formation of an ordered structure with a corresponding increase in the lattice parameter perpendicular to the layers of the initial crystal is known as intercalation, and the resultant compounds are known as intercalation compounds or interstitial compounds. As in other structures with SV, foreign molecules and atoms are accordingly localized in lattice cavities. The similarity of the behaviour of foreign molecules in layered structures compared to crystals, where the SV are distributed over the volume of the crystal, is apparently confirmed by this, generally speaking, important analogy. In actual fact, the distribution of isolated impurity atoms or molecules in interlayer spaces is energetically unfavourable compared to their localization in the form of an ordered phase. This is illustrated by the diagram in Figure 19. Figure 19(a) corresponds to the case of molecules individually localized in an interlayer space, while Figure 19(b) corresponds to the case where they are localized in the form of a compact ordered phase. Figure 19(b) also illustrates the process of intercalation by penetration of molecules into interlayer spaces already in the form of a 'finished' phase, which constitutes a half-plane incorporated in the crystal, and the transition region from the undistorted initial crystal to the also undistorted region of the intercalation compound (length λ) is analogous to a dislocation line with Burger's vector of the order of the size of the inserted molecule. We shall evaluate the elastic energy of the system in cases (a) and (b), ignoring anisotropy of the shear modulus G. According to [128] the energy per unit length of the linear dislocation centre is $W_d = Gb/4\pi(1-\nu)$, where ν is Poisson's coefficient (~ 0.3) and b is Burger's vector, which in the present case is identical to the linear size of the incorporated molecule. With a length λ of the 'forced' packing of intercalation molecules in the crystal (Figure 19b), then if it is assumed that the regular distance between the intercalation molecules in the ordered phase is la (where a is the interatomic spacing in the initial layer crystal and l is an integer), the total number of molecules in an interlayer gap in a crystal 1 cm wide is $\lambda/(la)^2$. If the molecules are also distributed individually in the interlayer space, producing elastic stresses, then their total energy in the layer is, using (2.13), expressed as $W_i = 8\pi Gb^2\lambda/3l^2a^2$. The ratio of the two energies is

$$W_i/W_d = \frac{32\pi^2\,(1-\nu)}{l^2}\cdot\frac{\lambda}{a} \gg 1.$$

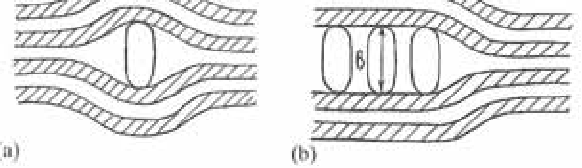

Figure 19 Incorporation of intercalating molecules in layer-type matrix: (a) deformation of lattice caused by single molecule in interlayer space; (b) deformation of lattice at boundary of intercalation phase front.

Of course, the expression for W_d is applicable only for macroscopic values $\lambda \gg a$. The evaluation made above indicates unequivocally that individual penetration of intercalation molecules into interlayer spaces is disadvantageous, and only insertion in the form of an ordered intercalation phase may occur. The above evaluation is preserved in the case where the intercalation species form chemical bonds with the matrix. In fact, as investigations have shown [129], the increases in mass and changes in volume of single crystals of the layer-type material PbI_2 that occur during implantation of intercalation molecules do not obey diffusion equations. The conclusion that the penetration of foreign molecules into a layer-type matrix occurs not by diffusion of individual molecules, but by the advance of the ordered intercalation phase front over interlayer spaces, is also confirmed in a number of investigations by X-ray analysis and spectroscopy methods, as well as with the aid of microstructure investigations and direct observation of the propagation front of the phase [129–132]. This process is very similar to the effects of surface flow and the formation of phases by surfactant substances [133]. Both polycrystalline and monocrystalline samples of layer-type materials disperse in a similar way to that which occurs in the interaction of surfactant substances on solid-state materials during intercalation [26, 127, 129]. In [129] it was found that a very small pressure of the order of 200–400 kPa on layer-type single crystals suppresses the penetration of intercalation molecules in the interlayer gaps, which can be interpreted in terms of the known Griffith's model with the formation of cracks during the advance of the intercalation phase front.*

Intercalation occurs during accommodation of the matrix being placed into a gaseous or liquid medium containing molecules of intercalants. When the intercalation phase front reaches the boundary of the crystal, filling the whole available interlayer space, stresses are absent in the layer-type packets. From what has been said above it is clear that, from the point of view of minimizing the internal energy in the equilibrium intercation structure, the formation of an ordered layer is advantageous compared to the insertion of isolated molecules.

---

* If the applied uniaxial pressure is above the critical value and penetration into the interlayer gaps is forbidden, the formation of an equilibrium intercalated phase proceeds via the extraction of fragments of the matrix material. This phenomenon is termed exteralation [129]. Another unusual effect, connected with the interaction of layer-type crystals with molecules capable of intercalating the latter, has also been discovered and is discussed in the same paper.

Since equilibrium exists between the medium and the intercalation compound being formed, the condition of equilibrium is determined by equality of the chemical potentials of the intercalant in the medium μ_m and in this compound μ_i. Assuming that the coefficient of activity in the medium is equal to unity, we have

$$\mu_i = \mu_m = \mu_m^0 + RT \ln N_{th} \qquad (3.1)$$

where μ_m^0 is the standard chemical potential and N_{th} is the mole fraction of the intercalant in the medium when equilibrium exists between the medium and the intercalation compound. From (3.1) it is obvious that, when the concentration of intercalant molecules in the medium is below the threshold value

$$N_{th} = \exp\,[(\mu_i - \mu_m^0)/RT] \qquad (3.2)$$

intercalation cannot take place, and starts only after the aforementioned threshold concentration value is reached. Such an intercalation concentration threshold has in fact been detected by means of IR and UV spectroscopy, in the example of PbI_2 intercalated from solutions of various amines in benzene [134]. The temperature dependence of N_{th} has been investigated, thus enabling the intercalation enthalpy and entropy of a number of compounds to be determined, since under isobaric–isothermal conditions $\mu_i - \mu_m^0 = (H_i - H_m^0) - T(S_i - S_m^0)$, where H_i, H_m^0, S_i, S_m^0 are the molar enthalpy and entropy of the intercalant in the solid intercalation phase and in the liquid amine respectively. Some examples: for aniline in PbI_2, $\Delta H = -30 \pm 2$ kJ/mole, $\Delta S = -81 \pm 6$ J/mole·K; for the compound PbI_2·pyridine, $\Delta H = -9 \pm 2$ kJ/mole and $\Delta S = -12 \pm 7$ J/mole·K; for the intercalation compound PbI_2 with piperidine, $\Delta H = -36 \pm 11$ J/mole and $\Delta S = -73 \pm 33$ J/mole·K. Matching values are also obtained from data on the deintercalation threshold, as well as from thermogravimetric data. The existence of a threshold concentration N_{th} also shows that the intercalation phase is formed immediately during incorporation.

Thus, the nature of the incorporation of foreign atoms and molecules in loose layer-type structure lattices is in principle different from that of lattices with a volumetric distribution of cavities; the intercalation of layer-type structures is associated with the formation of intercalation compounds. Intercalation by electron-donor atoms (metals) and molecules (amines, amino acids, dimethyl sulphoxide, etc.) has been studied most [126, 127, 135, 136].

Electron-donor molecules form intercalation compounds with layer matrices of the type MeX_2 (NbS_2, TaS_2, TiS_2, $NbSe_2$, VS_2, HfS_2, PbI_2, BiI_3, etc.). Equilibrium intercalation (without involvement of external factors) of such matrices by electron-acceptor molecules evidently does not take place. In [137, 138] it is shown that Ag_2F and Tl_2S matrices with three-layer packets reversed compared to MeX_2, where the atoms confining the packet are metal atoms, in fact form equilibrium intercalation compounds with electron-acceptor molecules (benzonitrile, nitrobenzene, tetracyanoquinodimethane, tetracyanoethylene).

Graphite is seemingly a unique matrix, in which both electron donors and electron acceptors can be successfully intercalated [139]. Layer-type matrices may be metals (NbS_2, TaS_2, Ag_2F, etc.) or by semiconductors (ZrS_2, HfS_2, Tl_2S, etc.), though the capacity of matrices for acceptor or donor intercalation is determined only by the structure of the packet, i.e. Me_2X or MeX_2. A classification of layer-type intercalated matrices is given in the review [140].

During intercalation the packets (matrix−host layers) preserve their structure or, at least, the structure changes only slightly. Molecules or atoms implanted in the interlayer spaces increase the lattice parameter perpendicular to the layers, according to their crystal-chemistry sizes.

For example, in the intercalation of TiS_2 by steramide molecules the lattice parameter increases by 50 Å [127]. The increase in the lattice parameter in the direction perpendicular to the layers is the most characteristic structural manifestation of intercalation. Intercalation sharply increases the conduction anisotropy [141].

Single crystals of intercalation compounds can be successfully grown [138, 142]. The formation of intercalation compounds is controlled by the formation of chemical bonds between the guest molecules and layers of the host matrix. In this connection, in the case of intercalation by electron-donor molecules charge transfer from the latter to the matrix occurs. This is manifested in an increase in the concentration of free charge carriers in the conduction band [143, 144], changes in the vibration frequencies of the active electron-donor amino groups (IR spectroscopy of intercalation semiconductors [145]), inelastic scattering of neutrons in the intercalation layer-type metals TaS_2 and NbS_2 [146], and in the luminescence spectra of intercalation semiconductors [147]. It was shown that, during incorporation of electron-donor intercalants into graphite, the intercalants donate electrons, while the electron-acceptor molecules remove electrons from the matrix [124]. Crystal-chemistry evidence of charge transfer from the donor intercalant to the matrix also exists. For example, in article [148] it is shown that the increase in the interlayer gap in the intercalation compounds $Me_{0.5}NbS_2$ (where Me = Ti, V, Cr, Mn, Fe, Co, and Ni) accurately corresponds to the ionic radii of the implanted intercalants in the valency state (2+). Such a simple crystal-chemistry analysis is complicated in the case of intercalation of organic molecules since the latter tend to contact the host matrix layer through an active donor group (for example a pair of electrons on the nitrogen atom in the amino group), and accordingly in a number of cases intercalated aliphatic molecules are arranged at an angle to the matrix layer.

Molecules in the interlayer space can interact not only with the matrix, but with one another. At small intercalant interspacings this interaction leads to the occurrence of covalent bonding between the incorporated molecules (*see* [126]), and the formation of hydrogen bonds in the intercalation of PbI_2 has been detected [149]. At large intercalant interspacings in a given interlayer space, as well as in the case of interaction of intercalants via the matrix layer, there is no overlapping of the wave functions of the intercalated molecules and the comparatively weak long-range forces play a major role.

3.2 Superlattices and Electron Properties of Intercalation Crystals

In principle, it is important to calculate the interaction of intercalants, since in fact this leads to ordering of the latter and essentially determines the stoichiometric compositions of the intercalation compounds. In each given matrix−intercalant system several intercalation compounds with different stoichiometric concentrations of intercalants in the matrix may exist. These intercalants, being arranged in an ordered manner, may form a two-dimensional superlattice in the plane of the layers, with a period na, where a is the lattice parameter and n is an integer [136, 150, 151]. In another ordering variant the intercalants are not arranged in every interlayer gap, but instead in alternate spaces, every two spaces, etc. (so-called intercalation 'steps').

Several examples of ordering in intercalation compounds are shown in Figure 20. Various observable distributions of unfilled interlayer spaces and spaces filled by molecules are shown in Figure 20(a) with the example of graphite, in which periodic alternation — one-dimensional ordering — exists (*see* [124]). Figure 20(b) illustrates

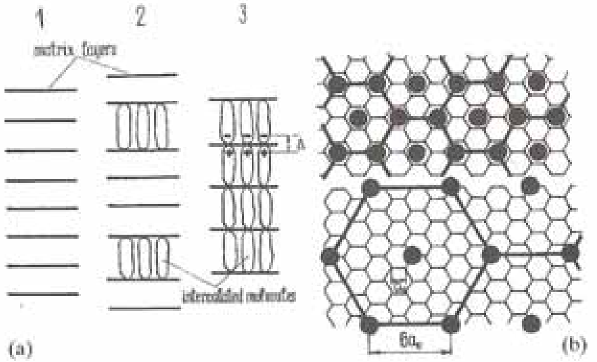

Figure 20 Examples of one-dimensional ordering of intercalated molecules for case of graphite (a) and two-dimensional case of intercalated compound PbI_2 (b).

the two-dimensional ordering of intercalation molecules with the example of the layer-type compound PbI_2 (*see* [136]).

Saphran, in article [152], investigated theoretically for the first time the matrix–intercalant phase diagram for the case of a matrix with metallic conduction, similar to graphite or $NbSe_2$, involving the occupation of various interlayer spaces. In his investigation Saphran employed the model Hamiltonian to construct the aforementioned phase diagram

$$H = -\mu \sum_i \sigma_i - 1/2\, U_0 \sum_i \sigma_i^2 + 1/2 \sum_{i,j} V_{ij}\sigma_i\sigma_j, \qquad (3.3)$$

where μ is the chemical potential; the second term describes the weak attraction of intercalation atoms or molecules arranged in the *i*th layer with occupancy number σ_i; the third term in (3.3) describes the weak repulsion between intercalants present in different layers *i* and *j*. The potential $V_{ij} \sim Z_{ij}^{-\gamma}$ (where Z_{ij} is the distance between the layers, $\gamma = 2$ or 4) should describe elastic repulsion. The numerical calculation made in [152] showed the existence of phases with superlattice periods $2a_0$, $3a_0$, $4a_0$ and $5a_0$. In this model it was found that the phase concentration regions are very narrow. This is connected with the fact that the principal contribution to the internal energy of the system, namely the formation of an intercalant–matrix chemical bond, is not taken into account in the Hamiltonian (3.3). If intercalation of a semiconductor or dielectric layer-type matrix is involved, then the extremely strong Coulomb interaction between the charges transferred from the intercalant to the matrix over the whole volume of the crystal also have to be taken into account, since in non-metallic matrices there is a no screening by free carriers. As demonstrated in article [153], during adsorption as a consequence of repulsion of parallel dipoles formed as a result of charge transfer, the transferred charge itself decreases. This obviously leads to a decrease in the bonding energy of each given adsorbed molecule with the surface, but is compensated by an increase in the number of molecules on the surface.

The above effects have been taken into account in the relevant theory [154, 155]. The Hamiltonian of the system is written in the form

$$H = \sum_i [E_{ch}(q_i) - \mu]\sigma_i + 1/2 \sum_{i \neq j} V_{ij}q_iq_j\sigma_i\sigma_j, \qquad (3.4)$$

where q_i is the magnitude of the transferred charge of the intercalant in the *i*th layer; $E_{ch}(q_i)$ is the energy of the ionic–covalent chemical bond of the intercalant with the layer, which naturally depends on the degree of charge transfer; V_{ij} is the energy of the electrostatic interaction of charges *i* and *j*:

$$V_{ij} = \frac{2e^2}{\varepsilon a_0}\left[\frac{1}{R_{ij}} - \frac{1}{R_{ij} + \Delta/a_0}\right], \qquad (3.5)$$

where R_{ij} is the distance between intercalation molecules *i* and *j* in units of a_0, *e* is the charge of an electron, ε is the dielectric constant of the material, and Δ is the distance between the electron density maxima of the positive and negative charges after charge transfer from the electron-donor intercalant to the matrix (Figure 20(a)).

The Hamiltonian (3.4) is formulated within the framework of the one-dimensional Ising model, though since all the principal contributions to the energy of the system are taken into account in this model, this treatment qualitatively maintains its significance for the two-dimensional case of ordering in the plane of the layers.

The solution of the self-consistent field equations according to Khachaturiyan [156], obtained using a computer and assuming that σ_i are periodic functions of period na_0 with cyclic boundary conditions with $n = 12$, has enabled a schematic phase diagram of the matrix–intercalant system to be constructed (Figure 21).

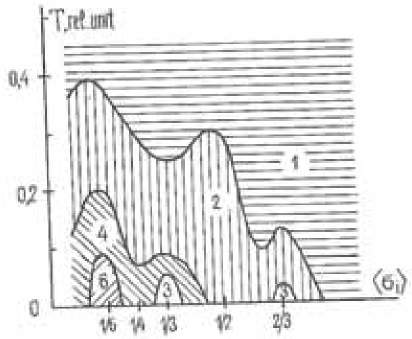

Figure 21 Phase diagram in intercalated system (T, temperature, $\langle\sigma_i\rangle$, occupation number of permitted crystallographic positions by intercalant molecules, corresponding to concentration of intercalant referred to number of possible positions). 1 = phase with $a = a_0$, 2 = phase with $a = 2a_0$, etc.

The main conclusion of this model is that fairly broad homogeneity regions exist, based on ordered phases with a superlattice period of $2a_0$, $3a_0$, $4a_0$, $6a_0$, etc. A computer simulation also showed that phase transitions between commensurate phases (for example the transitions $n = 4 \rightarrow n = 2$ or $n = 2 \rightarrow n = 1$) constitute second-order transitions, whereas transitions between non-commensurate lattices, for example $n = 6 \rightarrow n = 4$, being first-order transitions, take place via a completely disordered state, namely 'melting' of the system of molecules within one layer. As in adsorption phenomena, a decrease in the fraction of the transferred charge from the donor molecule to the matrix is observed during intercalation, when the stoichiometric concentration of the intercalant in the given system increases. This is shown by IR spectroscopy experiments on intercalant molecules in PbI_2 [132] and from X-ray spectroscopy data in intercalated TiS_2 [157]. The clearest demonstration of the dependence of the degree of charge transfer on the concentration of intercalant in the layer may well be the results given in article [150] where, taking the example of the layer-type compound TaS_2 intercalated by various metals, it is shown that at comparatively small concentrations of intercalants in the layer the intercalants are ionized, and at large concentrations the transferred charge is apparently equal to zero. In this connection, a covalent or metallic bond is probably formed between the intercalants. The absence of a chemical bond between implanted atoms and the matrix should be compared with the effect of the insertion of unionized impurity atoms in a lattice of the type In_2Te_3 [74], described in the previous sections (see Section 2.2). A similar effect was also observed by Bogomolov [119] in connection with the incorporation of tin, gallium and mercury under pressure in the free channels of loose zeolite lattices.

The theoretical constructions in articles [154, 155] are also in agreement with the experimental fact of the existence of several ordered phases in the given intercalant–matrix system [129, 140, 141], in which connection in fact the regions of homogeneity of the phases are fairly substantial [132]. In the PbI_2–quinoline system at a temperature of 223 K the intercalation crystal, which has a superlattice period of $4a_0$ at room temperature, undergoes a second-order phase transition, with an increase in the superlattice period to $8a_0$ [158, 159]. The transition between commensurate phases in accordance with the theory is in fact a second-order transition.

One of the most interesting consequences of the formation of two-dimensional superlattices in intercalation crystals is the formation of a long-period potential relief that modulate the intrinsic periodic potential of the matrix. The resultant quasi-two-dimensional potential wells with linear dimensions equal to the period of the corresponding superlattice should result in a dimensional quantum effect of the electron in a two-dimensional well. This has been demonstrated by Koshkin and Katrunov in article [160], where it was shown that the displacement of the edge of the fundamental optical absorption band (corresponding to a valence-condition zone transition) that occurs due to intercalation of PbI_2 is in fact determined by the quantum size effect. The short-wave length displacement ΔE of the edge of the optical absorption band due to intercalation of piperidine, aniline, quinoline, nonylamine, dimethylcetylamine and decylamine, has been investigated. The plane superlattice parameter a for all these intercalation compounds was previously determined in article [136]. It was found that the dependence of ΔE on the quantity a^{-2} is linear and is described by the empirical equation

$$\Delta E = 100a^{-2} + 0.13 \tag{3.6}$$

where ΔE is expressed in eV, and the superlattice parameter a in Å. This dependence has a natural interpretation if it is assumed that the potential walls formed by the superlattice are fairly high. The permitted energy values of an electron in a square well under an isotropic two-dimensional dispersion law are

$$E_{n_x n_y} = \frac{\hbar^2}{8m^*}\frac{1}{a^2}\left(n_x^2 + n_y^2\right), \tag{3.7}$$

where n_x, n_y are integers, $\hbar$ is Planck's constant and m^* is the effective mass of the charge carriers.

The size effect is of course manifested in the quantum valency band as well as in the conduction band.

The lowest permitted state for an electron is raised above the bottom of the conduction band by the amount

$$E_{11}^{(c)} = \frac{\hbar^2}{4}\frac{1}{m_1}\cdot\frac{1}{a^2}. \tag{3.8}$$

The upper permitted state for holes is lowered relative to the ceiling of the valency band by the amount

$$E_{11}^{(v)} = \frac{\hbar^2}{4}\frac{1}{m_2}\cdot\frac{1}{a^2}, \tag{3.9}$$

where m_1 and m_2 are the effective masses of electrons and holes respectively in the plane of the layers of the PbI_2 matrix. Considering equations (3.8) and (3.9), it can easily be seen that the light quantum energy required to transfer an electron from the upper permitted state in the valency band to the lowest permitted state in the conduction band is

$$E_g' = E_g^0 + E_{11}^{(c)} + E_{11}^{(v)} = E_g^0 + \frac{\hbar^2}{4}\frac{m_1 + m_2}{m_1 m_2}\frac{1}{a^2},$$

where E_g^0 and E_g' correspond to the edge of the fundamental absorption band in the non-intercalated and intercalated semiconductor respectively. It is clear that the short-wave length shift of the edge of the absorption band is

$$\Delta E = E_{11}^{(c)} + E_{11}^{(v)} = \frac{\hbar^2}{4}\frac{m_1 + m_2}{m_1 m_2}\frac{1}{a^2}. \tag{3.10}$$

The value of the reduced mass of the electron in PbI_2, viz. $m_1 m_2/(m_1 + m_2) = 0.8$, can easily be obtained from measurements in independent experiments on the superlattice parameter a and quantity ΔE.

A short-wave length shift of the edge of the fundamental absorption band was discovered for the first time by Rybalka and Miloslavskii [161] in connection with the intercalation of PbI_2 films by pyridine. Although the structural parameters were not determined in [161], the detected effect can possibly be explained by the same reasons. Similar phenomena are also observed in the intercalated layer-type semiconductor BiI_3 [162].

The independent from superlattice parameter term in expression (3.6) may be interpreted as the manifestation of a dimensional quantization in the direction perpendicular to the plane of the layers. In this case the width of the well is the 'thickness' of the three-layered packet I–Pb–I, and the magnitude of the shift of the edge of the fundamental absorption band due to intercalation should be written taking into account the three-dimensional quantization

$$\Delta E = \frac{\hbar^2}{4}\frac{m_1 + m_2}{m_1 m_2}\frac{1}{a^2} + \frac{\hbar^2}{8d^2}\left(\frac{1}{m_{z_1}} + \frac{1}{m_{z_2}}\right), \tag{3.11}$$

where m_{z_1} and m_{z_2} are the effective masses of electrons and holes in the direction perpendicular to the layers. Since the thickness d of the packet naturally does not change during intercalation, it is appropriate to relate the second term in (3.11) to the independent term in expression (3.6). This is confirmed by the fact that, in particular, by the intercalation of piperidine, when a two-dimensional lattice is not formed ($a = \infty$), and the first term in Equations (3.6) and (3.11) is equal to zero, the experimental value of the shift of the band edge (0.13 eV) accurately corresponds to the free term in Equation (3.6). The fact of the appearance of a shift ΔE during intercalation, when a flat superlattice is not formed, indicates that before intercalation there is a non-zero overlapping of the wave functions via van der Waals spaces in PbI_2. The magnitude of this overlapping is such that the corresponding electron delocalization reduces the electron energy compared to the isolated layer by not less than 0.13 eV. Undoubtedly, this is characteristic also of other layer-type crystals. The incorporation of molecules in the interlayer spaces removes this overlapping, resulting in a shift in the edge of the fundamental band, independent of the period of the flat superlattice. Since size quantization occurs in each of the cells of the superlattice of the intercalation compound, discrete energy quantum levels in this periodic structure are formed in the band. Such an approach is, generally speaking, more appropriate for a crystal. The origin of such bands may also be considered in the weak bond approximation (see, for example, [163]). The appearance of a long-period modulating potential of a superlattice with period na_0 leads to an n-fold reduction of the corresponding Brillouin zones, and a minor-zone energy spectrum of electrons in the conduction band and of holes in the valency band is thus created. This aspect of the interpretation of changes in the electron spectrum during intercalation was examined for the first time in article [164] and then in more detail in [159], where the change in the minor-zone spectrum during a phase transition with a change in the period of the superlattice in the intercalation crystal PbI_2–quinoline was also studied. The reduction in the Brillouin zones was also detected during phase transition in the metallic crystal $NbSe_2$ intercalated by iron. The structural phase transition in this material is also associated with the formation and transformation of two-dimensional superlattices [165].

4. EQUILIBRIUM POINT DEFECTS IN CRYSTALLINE COMPOUNDS WITH LOOSE STRUCTURE

4.1 *Equilibrium Defects in Solids*

At a temperature other than 0 K, all crystalline bodies contain point defects. Two types of such defects have been studied, namely Schottky vacancies and Frenkel defects, which constitute a pair of defects — vacancy and atom — presenting in an interstitial position (*see* [43, 87]).

In order to determine the concentration of thermal defects in equilibrium at a given temperature, it is necessary to determine first of all the free energy of the crystal as a function of the defect concentration.

The free energy per unit volume of a crystal with N_S Schottky defects or N_F Frenkel defects is respectively

$$\Delta F_S = E_S N_S - T\Delta S_S \tag{4.1}$$

$$\Delta F_F = E_F N_F - T\Delta S_F, \tag{4.2}$$

where E_S, E_F are respectively the energies of formation of Schottky vacancies and Frenkel pairs, and ΔS_S and ΔS_F are the entropies of their distributions.

The entropy N_S of defects distributed over N lattice sites is

$$\Delta S_S = k\ln\,(N!/N_S!(N - N_S)!) \tag{4.3}$$

The entropy N_F of vacancies and N_F of interstitial atoms, if they are distributed independently of one another, is

$$\Delta S_F = k\ln\{(N!/N_F!(N - N_F)!)\,(M!/N_F!(M - N_F)!)\}, \tag{4.4}$$

where M is the number of equivalent interstitial positions in the crystal, and k is Boltzmann's constant.

The equilibrium concentrations N_S and N_F corresponding to the free energy minimum are, in a linear approximation,

$$N_S = N\exp(-E_S/kT) \tag{4.5}$$

$$N_F = (NM)^{1/2}\exp(-E_F/2kT), \tag{4.6}$$

E_S and E_F are the equilibrium energies of formation of defects, which are substantially less than the characteristic energy required to rupture chemical bonds during the formation of a vacancy, since after bond rupture the crystal lattice around the vacancy that has formed relaxes and the defect energy decreases. The quantity E_F includes two parts, namely the energy of formation of the vacancy and the excess energy of the interstitial atom (ion), which distorts the lattice about itself. This latter term is normally very large. We shall examine its contribution to the energy of formation E_F, assuming that the lattice distortion energy in the vicinity of an incorporated interstitial atom ΔE_F may be described in terms of the theory of elasticity, as is the case with inserted impurity atoms (Section 2.3):

$$\Delta E_F = 16\pi G R_0(r - R_0)^2/3, \tag{4.7}$$

where R_0 is the effective radius of the cavity in the lattice in which an ion of radius r is inserted. If we disregard zeolite crystals and crystals of similar structure, where the sizes of the cavities may reach tens of ångströms, then in the overwhelming majority of other crystals, whose structure may in one way or another be described in terms of the packing of ion spheres, the sizes of the cavities R_0 is less than the radius of the intrinsic ions, i.e. normally $R_0 < r$ (*see* Section 1.3). Accordingly the value ΔE_F decreases with an increase in R_0 (naturally becoming zero at $R_0 = r$). From this it follows that Frenkel pairs may be the predominant type of equilibrium lattice defects only in loose structures, where the effective sizes of the cavities are fairly large. In fact, Frenkel equilibrium defects have been reliably recorded at the present time only for crystals with loose structures, in particular in superionic conductors, for example of the AgI type.

An important characteristic of point defects is the activation energy required to displace them from a given position in the lattice to a neighbouring, crystallographically equivalent position. This parameter, termed the migration energy U_m, has a value greater than, or of the order of, 1 eV [166–168] for vacancies, whereas for intrinsic interstitial atoms the value of U_m is substantially less and is 0.05–0.2 eV [167–169].

In the examination of Frenkel defects it is assumed that an atom displaced from its site beyond the limits of the first coordination sphere reaches a potential well and may then recombine with a vacancy only after having overcome the potential barrier U^i_m. It is shown below that interaction between a vacancy and an interstitial atom, just like interaction of any other defects in a crystal lattice, leads to the formation in the vicinity of each defect of an instability zone (IZ) for another defect, the size of which zone may in certain circumstances substantially exceed the interatomic spacing, and an interstitial atom that for example finds itself within the confines of such a zone will in fact recombine with 'its' vacancy in an activationless manner with a probability equal to unity and at any low temperature. The existence of IZ was detected for the first time in computer simulation models of radiation damage [170].

4.2 *Defect Instability Zones in Crystals*

The physical nature of IZ has been investigated in various publications [171–174].

Let us consider a one-dimensional model of a crystal. We shall assume that the crystal contains a vacancy 'v' and an interstitial atom 'i', the interaction energy of which is $U_{iv}(r)$, where r is the distance between v and i. The energy of an interstitial atom in the periodic field of a crystal lattice may be represented in the form

$$U_{oi} = \frac{U^i_m}{2}\cos\left(\frac{2\pi}{a}r\right) + A, \tag{4.8}$$

where a is the interatomic distance and A is that part of the energy i in the crystal matrix that is independent of r.

The total potential energy of the interstitial atom is (Figure 22)

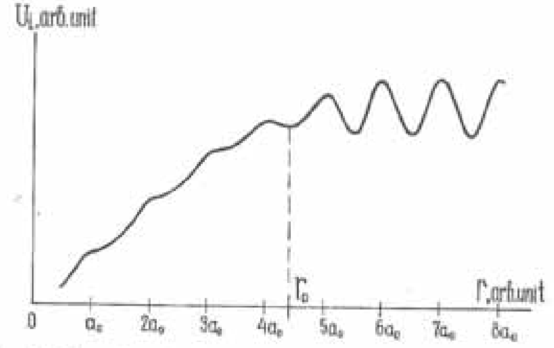

Figure 22 Dependence of total energy of mobile atom (ion) in lattice on distance r between latter and interacting fixed atom (ion).

$$U_i(r) = U_{iv}(r) + \frac{U^i_m}{2}\cos\left(\frac{2\pi}{a}r\right) + A \tag{4.9}$$

In the region of values of r where $U_i(r)$ increases monotonically, an interstitial atom remote from a lattice site recombines in an activationless manner with its vacancy. Accordingly the size of IZ is determined by the least value of r at which the oscillation function (4.9) has a maximum. The size of the IZ is thus determined by the smallest positive root of the equation $dU_i(r)/dr = 0$.

For the case of an i–v Coulomb interaction ($U_{iv} = -Z_iZ_ve^2/\cdot\varepsilon r$, where Z_ve, Z_ie are respectively the charge of a vacancy and of an interstitial atom, e is the charge of an electron, ε is the dielectric constant), we have

$$\frac{Z_iZ_ve^2}{\varepsilon r_0^2} - \frac{2\pi}{a}\frac{U^i_m}{2}\sin\left(\frac{2\pi}{a}r_0\right) = 0. \tag{4.10}$$

The IZ radius is, to an accuracy of one interatomic spacing

$$r_0 = \alpha\left(\frac{Z_iZ_ve^2a}{\varepsilon U^i_m}\right)^{1/2} \tag{4.11}$$

The coefficient α is associated with the specific form of the potential. In the case of the simplest sinusoidal potential (4.8) the value $\alpha =$

$\pi^{1/2}$. For any other choice of the potential U_{oi} the values of α are also close to unity.

Under an elastic interaction between i and v ($U_{iv} = G\Delta V_i \Delta V_v r^{-3}$, where G is the shear modulus, ΔV_v, ΔV_i are respectively the change in the volume of the crystal due to the introduction in the latter of a single vacancy or a single interstitial atom [175]):

$$r_0 = (3Ga\Delta V_i \Delta V_v / U_m^i)^{1/4} \tag{4.12}$$

(Here the elastic potential r^{-3} is employed, and not r^{-6}, which is characteristic of dilatation centres, since a real point defect always creates distortion of a lattice with local anisotropy.) Evaluations of a 'Coulomb' IZ according to (4.11) for $U_m^i = 0.05$ eV, $a = E$ Å, and $\varepsilon = 2$, which is characteristic of ionic crystals, gives $r_0 = 20$ Å; for the value $\varepsilon = 8$, characteristic of semiconductors, $r_0 = 10$ Å. These evaluations are in good agreement with experimental data for a number of metals [167, 176] for the ionic crystals KCl, KBr [177], MgO [178] and also for silicon [179].

It should be noted that IZ are formed not only in the vicinity of point defects. A detailed examination of these effects is given in [180]. For example, in dielectrics and semiconductors in the case where dislocations in the latter are charged (linear charge density σ), any charged point defect interacts with a dislocation, with the formation around the latter of a cylindrical IZ of radius

$$r_{DP} = 2\alpha^2 e^2 \sigma a / \varepsilon U_m^i \tag{4.13}$$

Under an elastic interaction of a dislocation and point defect

$$r_{DP} = \alpha \left(\frac{1}{3\pi} \frac{1 + \nu}{1 - \nu} Gba \frac{|\Delta V \sin\theta|}{U_m^i} \right)^{1/2}, \tag{4.14}$$

where G is the shear modulus, b is Burger's vector, ν is Poisson's coefficient, and ΔV is the change in the volume of the crystal due to the existence of a single point defect. If $\Delta V \sin\theta < 0$ and the interaction corresponds to an attraction, then in this half-space vacancies for example are attracted and interstitial atoms are repelled, and vice versa for $\Delta V \sin\theta > 0$. The IZ accordingly corresponds either to the absolute activationless capture cross-section of a defect by a dislocation, or to the cross-section of its absolute displacement, but in any case a region depleted in point defects appears in the vicinity of the dislocation in the cylinder of radius r_{DP} (IZ).

Two parallel interacting dislocations also form an IZ, interacting with a force [128] $F = Gb_1 b_2 / 2\pi\gamma r$, where $\gamma = 1$ for edge dislocations

and $\gamma = 1 - \nu$ for screw dislocations. The radius of the IZ calculated in a similar way according to (4.14) is, in this case,

$$r_{DD} = \alpha^2 G b_1 b_2 a^2 / 2\pi\gamma U_p, \tag{4.15}$$

where U_p is the Peierls barrier.

For parallel charged dislocations the IZ radius is

$$r_{DD} = 2\alpha^2 e^2 \sigma_1 \sigma_2 a^2 / \varepsilon U_p. \tag{4.16}$$

Of course, instability of the dislocations is manifested only in crystals with a small barrier U_p, i.e. in metals and ionic crystals. In covalent materials, in particular in semiconductors, the value $r_{DD} \approx a$, and IZ hardly play any role in plastic effects. However, in ductile metals and alkali halide crystals IZ should play a substantial role in plastic deformation and hardening processes. In the vicinity of macroscopic inclusions in crystals IZ are formed for point defects as well as for dislocations.

Thus, when the amplitude of the periodic migration potential of whatever defects there may be in the crystal is small and these defects interact with other defects (in particular with one another), a region (IZ) is always formed around one of the defects, where mobile defects are unstable and in the stationary state are absent from this region.

The effects of instability zones are manifested in a number of cases that are decisive in the physics of equilibrium and radiation point defects.

4.3 Equilibrium Unstable Vacancy–Atom Pairs in Interstices

The presence of a vacancy–atom IZ in an interstitial position predetermines the possibility of formation of a particular type of equilibrium point defect in crystals, namely vacancy (v)–interstitial atom (i) unstable pairs (UP), examined for the first time by Koshkin *et al.* in articles [10, 181]. In origin UP are similar to Frenkel pairs, though as will be shown below Frenkel pairs and UP differ in a number of principal characteristics, which means that UP have to be regarded as an independent type of defect.

If as a result of thermal fluctuations an atom leaves its lattice site but its distance from 'its' resultant vacancy is less than the IZ radius, then this atom should in fact recombine with this vacancy. If however the interstitial atom has moved beyond the confines of the IZ, a conventional stable Frenkel pair is formed. Of course, conventional Frenkel pairs whose components are mobile may also recombine, though the characteristic lifetime of Frenkel defects essentially depends on the temperature and at a sufficiently low temperature may be any large value, since in order for defects to propagate they must overcome the migration barrier U_m, and indeed in this context it is appropriate to term Frenkel defects stable pairs.

As regards UP, their lifetime practically does not depend on temperature.

We shall evaluate the characteristic lifetime of UP [181]. Assume that an atom i that has left its site stops at a distance R from the resultant vacancy and then, being within the confines of a IZ, moves back under the action only of the i–v Coulomb interaction, which is the strongest of the possible interactions. A time $\tau = \int_R^{\rho} \mathrm{d}r/u(r)$, where $u(r)$ is the velocity at the point with coordinate r, is required for the return of i to v, up to a distance ρ from the centre of the latter. Let the effective charges of i and v be q, and the mass of i be M. Then, having calculated $u(r)$ from the total kinetic energy $Mu^2(r)/2 = q^2/(r - q^2)/R$, we have

$$\tau = -\frac{1}{q}\sqrt{\frac{M}{2}}\left\{R\rho\sqrt{\frac{1}{r_0} - \frac{1}{R}} - R^{3/2} \arctan \sqrt{\frac{R}{\rho} - 1}\right\} \quad (4.17)$$

When ρ tends to zero, we obtain $\tau = (\pi\sqrt{M}/2\sqrt{2}q)R^{3/2}$.

For $M \sim 10^{-25}$ kg and $R \sim 10^{-9}$ m, we obtain $\tau \sim 10^{-12}$ s. From this evaluation it is clear that for relatively large values of R, the lifetime of a UP exceeds by only one order of magnitude the vibrational relaxation time of the lattice. If a partial relaxation of the lattice in the vicinity of the resultant defect and the creation of a dielectric screening effect are taken into account, the lifetime of the UP increases. In fact, the above evaluation also does not take account of the fact that an interstitial atom moving towards its vacancy exchanges its energy with its neighbours. The detailed diffusion model for the return of i to v within the limits of an IZ, developed in [182], gave however an evaluation of this order of magnitude.

Despite the fact that UP constitute extremely short-lived excitations, their equilibrium concentration should be absolutely finite and may be calculated.

The contribution to the free energy of a crystal with the simultaneous presence in the latter of conventional Frenkel pairs (N_F per unit volume) and UP (N_{UP} per unit volume) is:

$$\Delta F = N_F E_F + N_{UP}\bar{E}_{UP} - T\Delta S, \quad (4.18)$$

where E_F is the energy of the formation of Frenkel pairs, and $\bar{E}_{UP}$ is the energy of the formation of UP, and

$$\Delta S = k\ln w = k\ln(w_i w_v),$$

where w is the total number of possible states of the system, and w_v and w_i are respectively the number of possible vacancy states and interstitial atom states.

$$w_v = \frac{N!}{(N - N_F - N_{UP})!N_{UP}!N_F!)} \quad (4.19)$$

$$w_i = f_0^n \frac{(M - f_0 N_{UP})!}{(M - f_0 N_{UP} - N_F)!N_F!} \quad (4.20)$$

In (4.20), in contrast to conventional calculations of the configuration entropy, the number of possible states of interstitial atoms in an IZ,

$$f_0 = \frac{4\pi}{3}\left(\frac{r_0}{a}\right)^3,$$

has been introduced.

Substituting (4.19) and (4.20) in (4.18) and employing Stirling's formula, from the equilibrium conditions $\partial\Delta F/\partial N_{UP} = \partial\Delta F/\partial N_F = 0$ we find the following equations for the equilibrium concentrations of UP and Frenkel pairs:

$$N_F = (N - N_F - N_{UP})^{1/2}\frac{[M - (f_0 + 1)N_F]^{(f_0+1)/2}}{(M - f_0 N_F)^{f_0/2}} \exp\left(-\frac{E_F}{2kT}\right) \quad (4.21)$$

$$N_{UP} = f_0(N - N_F - N_{UP}) \exp\left(-\frac{\bar{E}_{UP}}{kT}\right) \quad (4.22)$$

Introducing the concentration of defects in the form $n_F = N_F/N$ and $n_{UP} = N_{UP}/N$, taking $M = \beta N$ (where β is of the order of several units), and assuming $f_0 n_F \ll 1$, to a first approximation we obtain

$$n_F = \beta^{1/2}\exp(-E_F/2kT) \quad (4.23)$$

$$n_{UP} = f_0 \exp(-\bar{E}_{UP}/kT). \quad (4.24)$$

From (4.24) it is clear that the equilibrium concentration of unstable pairs grows with an increase in the size of the IZ. In this approximation n_F does not depend on the radius r_0. In the following approximation it is found that n_F decreases with an increase in f_0 [181].

In contrast to Frenkel pairs, the annihilation of which is determined by thermoactivation diffusion processes and random encounters of interstitial atoms and vacancies, the interstitial atoms and vacancies belonging to UP recombine in fact with the same partner with which they were associated in their birth, and the act of recombination is activationless. The characteristic lifetime of Frenkel pairs essentially depends on the temperature, and at sufficiently low temperatures may be extremely long. In contrast, as demonstrated above, the lifetime of a UP is short and practically does not depend on temperature. UP as it were 'flare up' and are 'extinguished' at the point where they are generated. In this sense, it is appropriate to call such defects 'flickering' pairs. The above analysis shows that the sets of possible positions of v and i in crystals in the case of Frenkel pairs and unstable pairs are substantially different: for Frenkel pairs these states are independent, whereas in the case of UP the possible i and v states are closely correlated. This factor determines the substantial difference in the statistical sum in (4.19) and (4.20).

The above features of UP reveal that they are an independent, third type of point defect in crystals in addition to Frenkel defects and Schottky defects. They constitute a type of defect in crystals between harmonic vibrations of the lattice and point defects, also involving vibrations of atoms about their position in a regular lattice, though with a very large amplitude, which may be of the order of the interatomic spacings, and accordingly it is not possible in principle to describe such vibrations as harmonic, even with small nonlinear corrections. It was precisely for this reason that it proved appropriate to introduce UP as an independent type of lattice defect.

The physical meaning of the energy of the formation $\bar{E}_{UP}$ requires comment. $\bar{E}_{UP}$ has the meaning of an average energy over the ensemble, since for example in the case of Coulomb interaction between v and i, which in UP is substantial, for each UP the energy of excitation is of course different, depending on the distance r_{iv} by which the interstitial atom moves from its vacancy. In the case of Frenkel pairs, where the average distance between the components is large, interaction between the latter may be ignored. If for the purposes of the evaluation it is assumed that the relaxation of the lattice in Frenkel pairs and in UP is identical, it is not difficult to obtain the ratio between E_F and $\bar{E}_{UP}$ in the case of charged i and v:

$$\bar{E}_{UP} = E_F - q^2/\varepsilon\bar{r}_{iv}, \tag{4.25}$$

where $\bar{r}_{iv}$ is the average i−v distance.

The ratio of the concentrations is

$$\frac{n_{UP}}{n_F} = \frac{4\pi}{3}\left(\frac{r_0}{a}\right)^3 \exp\left[\frac{1}{2kT}\left(\frac{2q^2}{\varepsilon\bar{r}_{iv}} - E_F\right)\right] \tag{4.26}$$

From (4.26) it is clear that for $E_F \leq 2q^2/\varepsilon\bar{r}_{iv}$, UP should be the predominant type of defect in the crystal.

In evaluations according to (4.26) it should be remembered that the value of the dielectric constant for small r_{iv} is, generally speaking, less than its macroscopic value if we are talking about the lattice polarizability of the crystal matrix [183], whereas if the main contribution to ε is provided by the electron polarizability, as is the case in crystals with substantially covalent bonds, then such a high-frequency value of ε may be used in the evaluations.

4.4 *Unstable Pairs and Chemical Bonding in Crystals*

From what has been said in Section 4.3 it is clear that the existence and equilibrium concentration of UP are essentially determined by the size of the IZ. The IZ radius is in turn determined by the type of i−v interactions that actually take place, and is clear from (4.11), (4.12) that the largest value of IZ corresponds, under otherwise equal conditions, to a Coulomb i−v interaction. In this section we shall investigate the charge state of i and v during the escape of an interstitial atom from its site.

In article [184] it was shown that the degree of ionicity rises with an increase in the interatomic distance in a molecule with an ionic–covalent bond. This is connected with the fact that the covalent interaction energy decreases rapidly and exponentially with distance, whereas the ion−ion interaction energy decreases only slowly with distance.

We shall examine the process of rupture of a bond in an ionic–covalent molecule, whose state we shall write in the Heitler−London model with the wave function in Pauling's representation.

Let (1) and (2) be the coordinates of two electrons in the two-electron stationary wave function of the molecule. Two purely covalent states and two purely ionic states are described by the wave functions

$$\begin{aligned} \psi_{C_1} &= \psi_A(1)\psi_B(2) + \psi_A(2)\psi_B(1) \\ \psi_{C_2} &= \psi_A(1)\psi_B(2) - \psi_A(2)\psi_B(1) \\ \psi_{i_1} &= \psi_B(1)\psi_B(2) \\ \psi_{i_2} &= \psi_A(1)\psi_A(2) \end{aligned} \tag{4.27}$$

The total wave function of the system is

$$\psi = a\psi_{C_1} + b\psi_{C_2} + c\psi_{i_1} + d\psi_{i_2}, \tag{4.28}$$

where a, b, c and d are variation parameters.

In the case of a principally covalent bond the lowest state of the system is described by an almost pure wave function ψ_{c1}, corresponding to a bonding orbital, and the first excited state is described by an almost pure wave function ψ_{c2}, corresponding to an antibonding orbital. Both ionic states with localization of both electrons on the more electronegative atom B or electropositive atom A correspond to higher excitations. With an increase in the degree of ionicity and a decrease in the energy of the lowest state the energy of the state with ψ_{i1} decreases, since at some value $\lambda_{\min}$ this ionic state in fact becomes the first excited state of the system. According to the Landau–Zener criterion [185], during dissociation of a molecule the probability that the charge state of the atoms is preserved as in the unexcited molecule increases with an increase in the scattering velocity of the two atoms. In the case of a covalent bond this would correspond to the flight of neutral atoms. However, this probability becomes substantial only at very high energies of the atoms (of the order of 10^4–10^5 eV). Such energies are excluded under thermal excitation, and the probability of preservation of a charge state coinciding with the state in the molecule is very small at small energies of the first excited state. In such slow processes, at the moment of scattering the pristine molecule transfers with a high degree of probability to the first excited state. Accordingly, at an ionicity value $\lambda > \lambda_{\min}$ dissociation of a molecule in the form of ions is most probable. A calculation [186] performed on the basis of this model for crystals showed that the escape of an interstitial atom from its site in the form of an ion is overwhelmingly more probable even with very low degrees of ionicity in ionic–covalent crystals. It should be noted that the scattering probability in the charged state corresponding to the first excited state rapidly decreases with an increase in the energy gap between the ground state and first excited state of the crystal, since if the energy gap is large, which is typical of ionic crystals, the escape of interstitial atoms from sites in a charge state coinciding with the ground state becomes fairly likely.

Accordingly, in the overwhelming proportion of nonmetallic crystals even with a small degree of ionicity of the bonds an interstitial atom is charged at the moment of its formation, and a Coulomb IZ is formed in the vicinity of the vacancy.

4.5 Equilibrium Unstable Pairs in Semiconductors with Stoichiometric Vacancies

If a crystal in which Frenkel defects or Schottky vacancies are the main type of defect is rapidly quenched from a high temperature, these defects may be frozen in the matrix in concentrations close to what were the equilibrium concentrations at the high temperature. This is governed by the fact that the lifetime of each of these defects increases exponentially with a decrease in temperature, since the processes of their annihilation or escape to sinks (surface, dislocations, grain boundaries) are associated with migration over the crystal and with the surmounting of the migration energy barriers. Accordingly rapid quenching preserves that concentration of Frenkel and Schottky defects that was the high-temperature equilibrium concentration, but which is not the low-temperature equilibrium concentration. Rapid quenching of defects is in fact one of the main methods of investigating defects using subsequent isochronous or isothermal annealing, which enables many of their characteristics to be determined (see, for example, [187]). The behaviour of UP should be substantially different. Since they recombine in an activationless manner, their lifetime practically does not depend on the temperature and remains extremely short (*see* Section 4.3). Accordingly, UP should be unquenchable.

As demonstrated above (cf. Section 4.3), it is most likely that UP are in fact the predominant type of equilibrium defect in loose crystal structures. Quenching experiments on In_2Te_3 and Ga_2Te_3 crystals were accordingly carried out in [11]. Germanium, cadmium telluride (CdTe) and zinc telluride (ZnTe), which have a diamond-type crystal structure similar to In_2Te_3 and Ga_2Te_3 but not so loose (without SV), were subjected to parallel quenching experiments. In order to ensure an identical quenching rate of materials with different thermal conductivities, the sizes of the samples were chosen on the basis of the Fourier thermal criterion. Close relative temperatures (in relation to the melting point of the corresponding materials) were chosen as the starting temperatures for the quenching, the rate of which, as shown by calculations, was not less than 100 K.s^{-1}. The concentration of frozen defects in the case where activationless recombination was absent, evaluated in accordance with Lomer's equation [188], would be of the order of 10^{23} m^{-3} (10^{-3}%).

Experiments showed that the resistivity, concentration of charge carriers and their mobility, as well as the value of the coefficient of thermo-e.m.f. of In_2Te_3 and Ga_2Te_3 crystals measured at room temperature remained practically unchanged after quenching. The same parameters for Ge, ZnTe, CdTe changed very markedly, in full accordance with the literature data [166], which indicates that point defects in these crystals were frozen. An investigation of the temperature dependence of the electrical conduction of In_2Te_3 and Ga_2Te_3 quenched in liquid nitrogen and in water shows that, at least at a temperature higher than 260 K, the conduction is intrinsic conduction, just as before quenching. An investigation of the thermo-stimulated conduction of samples quenched in nitrogen showed that defects are formed in In_2Te_3 during quenching, which remain stable up to $T < 260$ K, though their concentration is estimated to be 10^{15}–10^{17} m^{-3}, which is at least 6–8 orders of magnitude less than the concentration of quenched defects in conventional, nonloose structures.

A possible reason for the stabilization of a small number of defects in lattices where the principal type of equilibrium defect is UP may be connected with the fact that minority types of defects in very small concentrations present in the equilibrium (*see* Section 4.3), and in fact become frozen. Other possible reasons will be analysed in more detail in Section 5. However, experiments show that without any doubt the overwhelming proportion of defects in In_2Te_3 and Ga_2Te_3 loose structures are unquenched, which is evidence that the principal type of defect in such lattices is unstable pairs.

In crystals where the predominant type of equilibrium defect is UP, a completely different diffusion mechanism should be involved. Two diffision mechanisms are known, namely an interstitial mechanism in which the diffusion activation energy coincides with the migration energy, and a vacancy mechanism, where the diffusing atom moves to the adjacent vacancy. In the latter case the diffusion activation energy is the sum of the energy of formation of the vacancy and the migration activation energy of the atom located at

the lattice site. In the conventional vacancy mechanism the coefficient of diffusion is determined by the probability that the vacancy is in a position directly adjacent to the atom that has to move to the vacancy. The total number of lattice sites frequented by all the Frenkel pairs in the crystal per unit time is $Z_F = N_F/\tau_F$, where N_F is determined according to (4.21) and $\tau_F = \tau_1 \exp(U_m/kT)$. In the case of UP the number of sites frequented by vacancies classified as short-lived (flickering) pairs is $Z_{UP} = N_{UP}/\tau_{UP}$, where N_{UP} is determined from (4.22), and the lifetime τ_{UP} of the UP is determined according to (4.17) and exceeds by only 1–2 orders of magnitude the vibration time of the lattice (10^{-13} s). Accordingly, despite the fact that the UP and its components do not manage to migrate over the lattice, the number of lattice sites in the crystal that they visit is very large. The calculation of the coefficient of diffusion made in article [189], when the diffusing atoms are 'served' by vacancies belonging to the UP, gives

$$D = \frac{4\pi}{9}\frac{r_0^3}{a}\frac{1}{\tau_{UP}} \exp\left(-\bar{E}_{UP}/kT\right), \qquad (4.29)$$

if it is assumed that the magnitude of the elementary jump of an atom is equal to the interatomic spacing a. If it is also assumed that the value of the elementary jump of the diffusing atom coincides with the size of the instability zone, then

$$D = \frac{4\pi}{9}\frac{r_0^5}{a^3}\frac{1}{\tau_{UP}} \exp\left(-\bar{E}_{UP}/kT\right) \qquad (4.30)$$

In (4.29) and (4.30) it should, generally speaking, be borne in mind that an interstitial atom belonging to a UP competes with a diffusing atom for the 'right' to occupy the vacancy, and to the extent that the mean distance between the vacancy and its interstitial atom ($\bar{r}_{iv}$) and the mean distance between the vacancy and the diffusing atom are related, a coefficient of less than unity should be introduced in (4.29) and (4.30). An overlapping of instability zones is essentially involved, which will be examined in more detail in Section 5.

The most important feature of UP diffusion is that in this case the diffusion activation energy coincides with the energy of formation of the UP.

Experiments [190, 191] on self-diffusion of indium and tellurium in In_2Te_3, as well as of cadmium and zinc in these crystals, using radioisotope investigation methods gave the following results in a wide temperature range: for indium and tellurium total coincidence between the coefficients of diffusion $D_{In(Te)} = 4.3 \times 10^{-7} \exp(-1.0eV/kT)$ m^2/s, for cadmium $D_{Cd} = 2.6 \times 10^{-5} \exp(-1.0eV/kT)$ m^2/s and for zinc $D_{Zn} = 3.5 \times 10^{-7} \exp(-1.0eV/kT)$ m^2/s. To a high degree of accuracy, diffusion activation energies in In_2Te_3 do not depend on the respective individual characteristics of the diffusing atoms. This is in accord with the conclusions of the model, and is yet further confirmation that unstable pairs are the predominant equilibrium-type defect in loose crystal structures with stoichiometric vacancies.

4.6 Equilibrium Unstable Pairs in Superionic Crystals

A very broad group of compounds with an extremely high ionic conductivity normally manifested as a jump following a phase transition associated with disordering of one of the sublattices (cationic or anionic) has been discovered in ionic crystals. This class of substance is termed superionic crystals (SIC). These substances include for example silver and copper halides, triple phosphate salts ($Na_3Sc_2(PO_4)_3$), silver sulphide, PbF_2, Ag_2HgI_4, Ag_4RbI_5, Ag_3AsS_3, AgSI, and mixed crystals, where in addition to inorganic ions, organic ions (for example pyridinium) are involved as cations in some of these crystals. These substances, which have completely different crystal lattices, exhibit a common property: all superionic structures are loose, which predetermines the formation of Frenkel pairs in them and furthermore ensures a high ionic conduction in the lattice and its percolation coherence.

Several excellent reviews on the chemistry and physics of superionic conductors exist [192, 193], where detailed information may be obtained on experimental data and currently existing theoretical models of SIC. Here we shall concentrate on a recently formulated model that provides a description of all the principal properties of SIC, including the thermodynamics of phase transitions in the superionic state, as well as transfer phenomena in SIC.

It was found that all the properties of SIC basically depend not only on the existence of Frenkel pairs in the crystals, as was previously assumed, but on the concentration of unstable pairs [10, 180, 181], and interaction between the latter is, in principle, important. A theory of superionic phase transitions that takes this interaction into account has been formulated in [194, 195].

As demonstrated in Section 4.3, even with a small degree of ionicity the UP components are charged. A dipole with an arm $\bar{r} \sim a$ is accordingly produced during the formation of a UP, and the mean dipole moment d of the UP is $d = q\bar{r}/2$. Such unstable short-lived dipoles interact with one another over the whole volume of the crystal. If a fluctuating configuration of dipoles is formed such that the concentration x_1 of interstitial ions ejected from their lattice sites in any direction is greater than their concentration x_2 in the opposite direction, then a directed self-consistent field of unstable dipoles will be formed, with which each of the dipoles will interact. Using the mean field approximation to describe the collective interaction UP, the energy ΔW associated with one defect may be expressed as follows:

$$\Delta W = (x_1 + x_2)\bar{E}_{UP} - \phi(x_1 - x_2)^2, \qquad (4.31)$$

where ϕ is the total electrostatic field of all the dipoles if these dipoles were situated in each of the N lattice sites; $(x_1 + x_2)$ represents the total concentration of UP. The second term in (4.31) represents the energy $(x_1 - x_2)$ of the dipoles, i.e. that fraction of all the dipoles that produce the directed field. The field intensity may be calculated in the same way as for the collective interaction of a system of static dipoles in ferroelectrics $E = \mu q\bar{r}(x_1 - x_2)N/2$, where μ is the Lorentz factor [196]. Since each unstable dipole interacts with this field, the interaction energy of all $(x_1 - x_2)N$ dipoles has a value $(-\mu q^2\bar{r}^2(x_1 - x_2)N^2/8)$, and a value of $(-\mu q^2\bar{r}^2(x_1 - x_2)N/8)$ per lattice site. Accordingly, in (4.31) $\phi = \mu q^2\bar{r}^2 N/8$.

The entropy of a system consisting only of unstable pairs is, in accordance with expression (4.20) but taking into account the fact that the directions of the dipoles are opposite ($N_1 = Nx_1$, $N_2 = Nx_2$):

$$\Delta S = k\ln[(f_0N_1)!f_0^{N_2}N!/(N - N_1 - N_2)!N_1!N_2!] \qquad (4.32)$$

Here, in contrast to (4.20), we have taken $2f_0 = 4(r_0/a)^3/3\pi$ in order to take into account individually states of interstitial species ejected in two opposite directions. The equilibrium concentrations of UP with oppositely aligned dipoles correspond to the minimum of Helmholtz free energy $\Delta F = \Delta W - T\Delta S$, and are calculated from the system of equations $\partial\Delta F/\partial x_1 = \partial\Delta F/\partial x_2 = 0$. It is convenient to introduce other variables in place of x_1 and x_2: $u = x_1 + x_2$, which represents the total concentration of UP, and $z = (x_1 - x_2)/(x_1 + x_2)$, which represents the relative proportion of those interstitial species that produced dipoles along a given direction. It is clear that the parameter z has the physical meaning of an orientational order parameter of the unstable dipoles in the system.

The equations for minimizing ΔF lead to the following transcendental equations connecting u and z.

$$u = (2\gamma\beta z)^{-1}\ln(1 + z/(1 - z)) \tag{4.33}$$

$$\ln(1 + z/(1 - z)) = 4\gamma\beta f_0 z\exp(-\beta/\sqrt{1 - z^2}) + 2f_0\exp(-\beta), \tag{4.34}$$

where $\beta = \overline{E}_{\mathrm{UP}}/kT$, $\gamma = 2\phi/\overline{E}_{\mathrm{UP}}$. Equations (4.33) and (4.34) have different solutions for different values of β and γ. An analysis of these solutions, given in article [194], shows that three different dependences of the total concentration of UP (u) and order parameter (z) on the temperature are possible in a system of interacting unstable pairs. At comparatively small values of the parameter γ, which corresponds to a relatively small value of the interaction energy of UP compared to their formation energy, there is no ordering at all of the short-lived 'flickering' dipoles (order parameter $z = 0$), and the total concentration u increases monotonically with temperature and does not exhibit a jump-like behaviour (Figure 23a). At large values of γ, exceeding some critical value, two-phase transitions take place in the system, the high-temperature one of which is necessarily a second-order transition. The dependence $u(\beta)$ and $z(\beta)$ in the case where both phase transitions are second-order transitions is illustrated in Figure 23(b), and the case where the low-temperature transition is a first-order transition is illustrated in Figure 23(c) (the phase-transition points are denoted by C_1 and C_2 in Figure 23). In both cases the order parameter z, which differs from zero, appears in a certain temperature range, which corresponds to ordering of the short-lived dipoles, and the appearance of their self-consistent field leads in accordance with (4.31) to a reduction in the effective energy of formation ΔW of the unstable pairs and to an increase in their concentration. This corresponds to a break at the low-temperature phase-transition point in Figure 23(b) and to a sharp jump in the total concentration u at the first-order phase-transition point (Figure 23c). Just such a sequence of phase transitions actually occurs in many superionic crystals [192], and the theory provides an explanation of this fact.

The theory [194] enables the temperature of the phase transitions to be evaluated for characteristic values of the parameters. For example, for $E_F = 1$ eV, $U_m = 0.05$ eV, $a = 5$ Å, $\varepsilon = 7$ and $\mu = 4\pi/3$, we obtain $\gamma = 1.1$.; $f_0 = 200$, the temperature of the first phase transition ≈ 300 K, and of the second-phase transition ≈ 2500 K. It should be noted that only one phase transition is observed in a number of crystals undergoing transformation to the superionic state. It is likely that the second, high-temperature transition does not occur since the crystal has already melted.

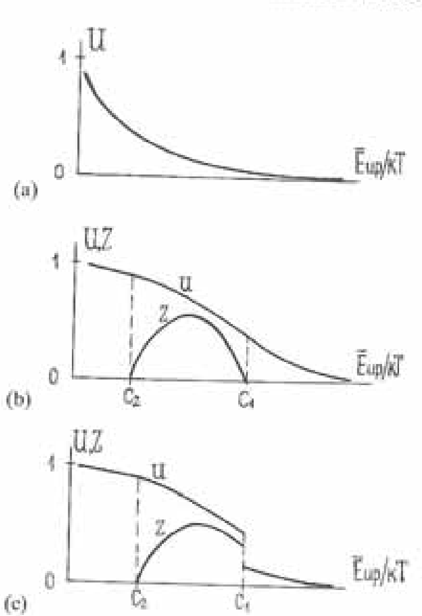

Figure 23 Temperature dependence of total concentration of unstable pairs u and order parameter z on temperature T ($\overline{E}_{\mathrm{UP}}$ is the average energy of formation of unstable pairs) (for explanation see text).

Apart from the correspondence between the overall thermodynamic picture and the experimentally observed phase transition in superionic crystals, there is also very clear microscopic evidence that unstable pairs play a principal role in the thermodynamic properties of superionics. In articles [197–199], which describe neutron diffractometry structural investigations of a typical superionic crystal, namely silver iodide, it is shown that the ions very rarely move large distances from their lattice sites, though they execute strongly anharmonic vibrations of large amplitude in the vicinity of the sites. This is direct observation of unstable pairs, which are 'intermediate' defects between vibrations in the vicinity of the lattice site and a Frenkel defect, corresponding to the vibrational amplitude when the atom already vacates its site and goes beyond the confines of the instability zone [200].

It has been shown in several articles that domains exist in the superionic state [201]. In the investigation of neutron scattering in Ag_2S, it was discovered that these domains are nonstationary, and their lifetime is $\sim 5 \times 10^{-11}$ s, which is close to the lifetime of a UP. Moreover, although the formation of domains in the average field approximation adopted in the formulation of the theory [194] cannot be obtained strictly, such a close correspondence between the experimentally determined lifetime of the domain and the theoretical estimate of the UP lifetime (*see* Section 4.3) may also serve as confirmation of the predominant role of UP in the formation of the superionic state. For $\gamma > 2$, when the collective interaction energy of the UP exceeds the mean energy of formation of the UP, static displacements of ions from their sites with the formation of dipoles becomes energetically favourable only with respect to the internal energy, and instead of dynamic unstable dipoles static displacements are produced, which correspond to a conventional ferroelectric ordering of stationary displacements for $T = 0$, $z = 1$, and $u = 1$. Of course, in this case the physical meaning of u is no longer the concentration of defects but the total number of displacements, which coincides with the overall number N of sites of, for example, the cationic sublattice. Thus, in this limiting case the model [194] no longer describes the superionic state but instead the ferroelectric state. The meaning of the concentration of defects in such a ferroelectric phase acquires the value $(1 - u)$. Consequently, the theory [194] based on the concept of interacting UP enables the interrelationship between superionic and ferroelectric states in crystals to be investigated.

The parameter $\gamma = 2\phi/\bar{E}_{UP}$, which determines the ordering of the dipoles, depends on temperature. Using (4.25) for the average energy of formation of UP and the expression for the self-consistent value of the energy of a given dipole in the electrostatic field of all 'flickering' dipoles (see above), we obtain

$$\gamma = \frac{\mu q^2 N \varepsilon}{4} \left(\frac{\bar{r}^3}{E_F \varepsilon \bar{r} - q^2} \right) \tag{4.35}$$

Since the average value of the i−v distance increases with temperature $(\partial \bar{r}/\partial T > 0)$, then assuming that E_F and ε for a given crystal do not depend to a first approximation on the temperature, we find that $\partial \gamma / \partial T > 0$. Accordingly, crystalline materials may exist in which superionic conduction $(\gamma < 2)$ exists at a comparatively low temperature, while at elevated temperatures, when the value of γ exceeds the critical value $(\gamma = 2)$, the crystal transforms to the ferroelectric state. Such crystals have in fact been discovered [202–204].

Experimental investigations of absorption of electromagnetic radiation by a number of superionic crystals in the microwave range [205] have revealed discontinuities at frequencies of 2–20 cm^{-1}, with anomalously large damping. In articles [205, 206] the physical meaning of these oscillators is qualitatively interpreted as the manifestation of 'ions jumping forwards and then immediately backwards' within the limits of an elementary cell at just these frequencies. The meaning of this qualitative explanation quite obviously coincides with a strict understanding of unstable pairs. The theory of absorption of electromagnetic radiation based on the UP model has provided a complete quantitative description of these experimental phenomena [207].

The theory of interacting unstable pairs thus enables a wide range of phenomena in superionic crystals to be described. However, the presence only of UP cannot explain the high static conduction of superionic crystals, which is their principal distinguishing feature. In actual fact, since an interstitial ion belonging to UP actually recombines with the vacancy that it escaped from at the moment of formation, charge transfer by means of ions belonging to UP is, in principle, impossible. Charge transfer to SIC in low-frequency and static fields may occur only by means of transfer of interstitial ions that have left the IZ of their vacancies, i.e. those that belong to conventional Frenkel pairs. Thus, on the one hand, as demonstrated above, the transition to the superionic state is determined by UP, and on the other hand, the high static conduction produced by the jump at the instant of this phase transition is determined by Frenkel pairs, the concentration of which therefore also increases in a jump-like manner under the superionic phase transition. This indicates that the energy of formation of Frenkel pairs decreases under a phase transition. The qualitative interpretation of this fact is obvious.

According to (4.25), $E_F = \bar{E}_{UP} + q^2/\varepsilon r$, and $\bar{E}_{UP}$, as shown above, sharply decreases in the self-consistent field of ordered unstable dipoles. Accordingly, as a result of the superionic phase transition determined by the interaction of UP, the energy of formation of Frenkel pairs sharply decreases, resulting in the formation of a large concentration of mobile charge carriers. A more detailed examination of the effect of the decrease in E_F in the presence of 'flickering' UP dipoles in a crystal is given in article [194]. It is assumed that the short-lived dipoles 'solvate' the free ions and charged vacancy. This effect is similar to the solvation of electrolytes in liquids having a fairly marked short-range order, for example in water. Solvation in such structured liquids, which is examined in [208], leads to two competing effects. On the one hand the energy of the system decreases when the dipoles become ordered in accordance with the Coulomb field of the ion, while on the other hand this ordering destroys the degree of arrangement of the molecules in the solvent (or UP dipoles in the self-consistent field). Calculations performed in [194] for superionic crystals showed that the energy of the system due to such a dynamic solvation may, generally speaking, decrease as well as increase. However, in superconductors with a large UP concentration the decrease in energy predominates; hence the energy of formation of Frenkel pairs decreases, which agrees with the result of the simple evaluation given above.

The influence of UP on the static conduction of superionic crystals is however determined not only by the reduction in E_F and, accordingly, by the increase in the concentration of free ions, i.e. current carriers. Their role in charge-transfer processes is also substantial [195]. 'Jump' models of ion transfer in superionic crystals are inapplicable. Since the mean free path time of an ion is close to (and may even exceed) its lifetime in the settled state, it is more appropriate to employ the Drude model of free carriers in order to describe the conduction σ, using the concept of the mean free path λ of ions having a thermal velocity $v = (3kT/m)^{1/2}$, where m is the mass of the ions

$$\sigma = q^2 n_F N\lambda/(3mkT)^{1/2} \tag{4.36}$$

Unstable pairs will influence the mean free path of an ion since the latter, in turn, is determined by the annihilation of mobile interstitial ions with vacancies belonging to both UP and Frenkel pairs. Such an examination has been performed in article [195].

Superionic crystals may be subdivided into two groups according to the magnitude of their conduction. The first group is characterized by comparatively small values of σ and fairly large values of the conduction activation energy E_σ in the superionic phase. Crystals of the second group have a very low resistivity. To start with, we shall examine the conduction of the first of the aforementioned groups, in which the UP concentration $Nn_{UP} \ll r_0^{-1/3}$, i.e. the IZ do not overlap. If a free ion reaches the IZ of any vacancy then, because of annihilation with the latter, it is naturally not involved in ion transfer. Accordingly, the annihilation cross-section of an interstitial species at vacancies belonging to Frenkel pairs is πr_0^2, and the path length relating to this process is $\lambda_1 = (\pi r_0^2 N n_F)^{-1}$. When a free ion encounters a vacancy belonging to a UP, this ion competes for the 'right of recombination' with the interstitial ion belonging to the UP in question. Consequently, it is annihilated only in the case where it is at a distance less than $\bar{r}$ from the vacancy. The mean free path of an ion in this process is accordingly $\lambda_2 = (\pi \bar{r}^2 N n_{UP})^{-1}$. For the total path length we have: $\lambda^{-1} = \lambda_1^{-1} + \lambda_2^{-1}$.

Using (4.36) we obtain

$$\sigma = \frac{q^2}{\pi r_0^2 \, (3mkT)^{1/2}} \left(1 + \frac{n_{UP}\,\bar{r}^2}{n_F r_0^2}\right)^{-1} \tag{4.37}$$

For $n_{UP}\bar{r}^2 \gg n_F r_0^2$ we have

$$\sigma = \frac{q^2}{\pi r_0^2 \, (3mkT)^{1/2}} \exp\,(-E_\sigma/kT), \tag{4.38}$$

where the electrical conduction activation energy $E_\sigma = q^2/\varepsilon\bar{r} - E_F$. As we saw above, provided that $n_F \ll n_{UP}$ the value $E_\sigma > 0$, in which connection this may be a fairly substantial quantity, as is observed in comparatively high-resistance superionics [192, 193].

Evaluations of values of $\bar{r}$ using experimental data on σ and E_σ carried out in [209] give values of $\bar{r}$ that are in fairly good agreement with the interatomic distances in superionic crystals, where the temperature dependence of the conduction involves large values of E_σ.

In high-conducting superionic crystals the temperature dependence of σ is very weak. In these crystals the concentration of UP is so large that the instability zones overlap. If in this connection it happens that not only $(nN)^{-1/3} < r_0$ but $(nN)^{-1/3} < \bar{r}$, then ions belonging to UP do not differ from free Frenkel ions as regards the possibility of escaping from their own vacancy, which would correspond to the Drude model, except for the fact that the scattering cross-sections become equal to $\pi\bar{r}^2$ for any vacancies, and the concentration of free ions is $n_P + n_{UP}$. In this case

$$\sigma = \frac{q^2}{\pi\bar{r}^2 (3mkT)^{1/2}} \tag{4.39}$$

For $\bar{r} = 2\,\text{Å}$, $m = 10^{-25}$ kg, $T = 500$ K, and the value $\sigma \sim 10^3$ ohm$^{-1}\cdot$m^{-1}. Expression (4.39) however gives a very small, though negative, value of $d\sigma/dT$. Under a more strict examination that takes into account the fact that the activation energy $\bar{E}_{UP}$ remains nonzero also in superionic crystals with a very high electrical conduction, the difference in the ion fluxes in the direction of the external electric field and in the opposite direction is calculated, which is determined by the existence of asymmetry in the electric field of the activation energy of those unstable pairs in which $r_0 \geq (n_{UP}N)^{-1/3}$. The expression for the electrical conduction in this computation is

$$\sigma = A\frac{\sqrt{3}\, q^2 (Nn_{UP})^{2/3}}{(mkT)^{1/2}}, \tag{4.40}$$

where A is a constant that includes the quantities $(nN)^{-1/3}$, r_0, a and the value of the effective dielectric constant corresponding to small vacancy–ion distances in the interstitial position, and accordingly is difficult to determine numerically [182].

For reasonable values of the parameters, the values of σ are the same as in the initial evaluation, namely of the order of several kohm. This value is very close to the limiting values of the conductivity observed experimentally in superionic crystals with a high conduction.

Unstable pairs are thus the determining type of equilibrium defect in loose crystal structures with a superionic phase transition.

5. RADIATION PROPERTIES OF CRYSTALLINE COMPOUNDS WITH LOOSE STRUCTURE

5.1 *Radiation Defects in Crystals*

The development of nuclear energy has inevitably led to a comprehensive detailed study of the action of ionizing radiation on crystalline materials. When solids are irradiated by high-energy particles, defects are produced, the mechanisms of formation and characteristics of the influence of which on the physical parameters of crystals have been comprehensively investigated. These results may be found in the relevant monographs (see, for example, [167, 210, 211]), and we shall restrict ourselves here to a brief outline of the main concepts and principles of radiation physics of solids.

The primary act of interaction of a particle (of energy E_1) with an atom in a lattice consists in the transfer of energy and momentum to the latter. If the mass of the incident particle is m and the mass of an atom in the crystal is M, then the magnitude of the transferred energy in frontal collision is

$$E_{tr} = \frac{4mM}{(m+M)^2} E_1 \tag{5.1}$$

An electron with an energy of the order of 1 MeV transfers energy of several tens of eV to an atom having a mass of the order of 50 atomic units. During irradiation by γ-quanta, the mechanism of radiation damage also reduces to interaction between atoms of the material and electrons of the same energy formed as a result of the nuclear photoeffect, Compton effect, generation of electron–positron pairs, and the action of recoil nuclei formed at fairly high γ-quanta energies (see, for example, [167]).

During irradiation with fast neutrons of 1 MeV energy, an energy of the order of 10 keV is transmitted to the initially knocked off atom according to (5.1). Electrons of high energies may, on account of their large relativistic mass, also transfer a significant amount of energy during collisions with atoms of the lattice.

In addition to the impact mechanism of formation of defects, ionization is also a significant mechanism during irradiation with charged particles. A detailed analysis of mechanisms of radiation defect generation is included in the reviews [167, 210].

In all cases the simplest radiation defect in a crystal consists of an atom that has been ejected from its site and the vacancy formed as a result, namely a Frenkel pair. The concept of the Seitz threshold energy E_d is introduced, which corresponds to the magnitude of the transferred energy required to produce a single Frenkel pair. Evaluations of E_d give values of the order of 10–70 eV, which generally speaking far exceeds the energy required to rupture all the bonds of the given lattice atom and the energy required to expel this atom, which has been freed from its bonds, beyond the limits of the first coordination sphere. The use of the IZ model described in Chapter 4 has enabled the Seitz threshold to be redefined as the value E_d necessary to remove an atom beyond the IZ limits [181, 212, 213]. The effective value of E_d provides an estimate of the total number of point defects produced under an impact mechanism of their formation, after impact of one ionizing particle (see [167])

$$\nu \sim E_{tr}/E_d \tag{5.2}$$

Sometimes the quantity ν is termed the cascade function, meaning that under the impact of a high-energy and heavy particle the energy transferred to the initially ejected atom may very greatly exceed the Seitz threshold E_d, and in this case the initially ejected atom on colliding with another atom in the lattice will eject it from its crystallographic position, this latter atom will eject the next one, and so on. A damage cascade is thus initiated, which is localized in the vicinity of that lattice site which was subjected to the initial impact of the fast particle. The cascade region is saturated with vacancies and interstitial atoms, the distribution of the latter being displaced towards the periphery of the cascade, whereas the centre of the cascade preferentially contains vacancies. The displacement of the distributions in the case of non-metals means that each of the interstitial ions removed to the periphery of the cascade exists in the Coulomb charge field of all the vacancies that have accumulated at the centre. An examination similar to that carried out in Section 4.2 showed [214] that, in this case, an instability macrozone is formed, the size of which is determined by the difference between the total charge of all the vacancies and all the interstitial ions in a sphere of radius equal to the distance from the centre of the cascade to the given interstitial ion. The region where practically all the energy of the fast particle is released is quite small and covers only 10^3-10^4 atomic volumes, since it is possible to regard it as a strongly heated-up section whose temperature is very high, although it rapidly equilibrates, in proportion to the thermal conduction, with the temperature of the whole crystal. Local melting of the material (so-called 'thermal spikes' [167] or 'θ-flashes' [215]) is possible in this region. So-called 'Brinkman displacement spikes', characterized by the appearance of dislocation loops, are formed at the end of the cascade when the mean free paths of the ejected atoms are of the order of interatomic distances. We shall not describe in detail the features of the mechanisms of formation of the various types of radiation damage (see, for example, the reviews [167, 210]), and for an overall evaluation of the radiation stability of materials we shall use the simple Kinchin–Pease model (5.2) to investigate elementary radiation damage sustained by interstitial atom–vacancy pairs.

An important parameter is the characteristic distance between an atom i ejected from its site and after it has stopped, and the formed vacancy v. If the periodic structure of the crystal is ignored, then in the solid spheres approximation [167] the average v–i distance after total dissipation of the energy is given by the expression

$$\bar{x} = 4\pi a_0 E_{tr}/(\pi a e)^2 (z_1 z_2)^{7/6} N_0, \tag{5.3}$$

where $a_0 = 0.529$ Å is the Bohr radius, N_0 is the number of atoms per unit volume, and z_1, z_2 are the atomic numbers of the constituent elements of the lattice of the diatomic crystal. Since atoms are scattered by large angles under mutual collisions, the value of $\bar{x}$ is small. For example, for $E_{tr} = 10$ keV the mean distance between vacancies and interstitial atoms in aluminium is 20 Å, and in copper is only 3 Å.

However, processes leading to the separation of an interstitial atom and the resultant vacant site by substantially greater distances, namely channelling and focusing phenomena, may occur in periodic structures. The first of these phenomena occurs only in the case of atoms with very high energy (not less than several hundred eV), in which connection, if the ejected atom escapes at a very small angle in the channel between the atomic rows (planes) that does not exceed some critical value characteristic of the given structure, then its mean free path may amount to hundreds and even thousands of ångströms. It may be shown that the fraction of such channelled atoms is very small under any type of external interaction.

The phenomenon of focusing (Silsbee [216]) of atomic collisions in periodic structures is considerably more likely during radiation influences, and may be described as follows.

Consider a long row of atoms, to the first of which is imparted momentum directed along the chain or at a small angle to its axis. If the energy of the first atom is sufficient to displace the neighbouring atom along the chain during a collision, then the first atom will occupy the position of the second atom, the second will occupy the position of the third, and so on. A vacancy remains at the site of the first atom, and the interstitial atom will be situated at the distance reached by the sequence of displacements. Such a chain or sequence of displacements is termed a dynamic crowdion. Energy dissipation during movement of a crowdion is relatively small, and accordingly its mean free path may amount to tens or even hundreds of ångströms, and thus the v–i distance as a result of the focusing of atomic collisions may be considerable.

The aforementioned phenomenon of focusing along a row of atoms occurs only along closely-packed crystallographic directions and depends to a very great extent on the angle of attack of the initially ejected atom relative to the direction of the chain. The limiting angle and maximum possible focusing energy increase sharply if the atomic row in which focusing occurs has in its first coordination sphere ('coordination cylinder') an environment with a high axial symmetry at each point along the length of the atomic row. In this connection the surrounding atoms restore to the focusing direction those atoms whose angle of attack exceeds the limiting angle for the aforementioned simple focusing. This phenomenon is similar to the action of lenses in optics, and the corresponding symmetrical (triangular and square) atomic environments are termed atomic lenses. They produce a so-called additional focusing (Nelson, Thompson) of atomic collisions, this latter focusing being more effective than simple focusing [217].

A large proportion of interstitial atoms and vacancies thus remain in a region close to the site where the initially ejected atom appears, though the distribution of interstitial atoms located at a large distance from this point is in fact determined by comparatively rare atomic collision focusing events.

As demonstrated in Section 4.2, in practically all solids instability zones are formed in the vicinity of vacancies, in which an interstitial atom cannot exist in a stationary state and is annihilated in an activationless manner with a vacancy. Accordingly, if an interstitial atom is in an IZ, self-healing of the radiation defect occurs. The accumulation of such defects with an increase in the radiation dose is thus substantially determined by the size of the IZ. The presence of the latter determines the kinetics of the growth of concentration of defects with an increase in the radiation dose: initially the number of defects grows with an increase in the dose, though when such a concentration is reached that the IZ of all the formed vacancies cover the whole volume of the crystal, any new interstitial atoms will, with a probability equal to unity, enter the IZ of any of the already existing vacancies [167].

Let the number of stationary defects introduced by the ionizing radiation be N_d per unit-volume. If we assume that all stationary defects are distributed strictly uniformly and ignore any probability of escape of new i and v to sinks, then under an increase in the overall concentration of stationary defects of $\chi d\phi$, where ϕ is the absorbed radiation dose and χ is the number of point defects introduced per unit absorbed dose, the increase dN_d is proportional to the fraction of the volume free from IZ:

$$dN_d = [1 - w_0 N_d]\chi d\phi, \tag{5.4}$$

where $w_0 = 4\pi r_0^3/3$ is the volume of an IZ, and N_0 is the number of atoms per unit volume of the crystal. Integrating (5.4) we obtain

$$N_d = \frac{1}{w_0}[1 - \exp(-w_0\chi\phi)] \tag{5.5}$$

From (5.5) it is clear that the concentration N_d tends towards saturation with an increase in the radiation dose, and the limiting concentration corresponds to coverage of the IZ of all stable N_d ($N_d w_0 = 1$). Evaluations for various materials give values of w_0 of the order of 10^2-10^3 atomic volumes, which corresponds to a number of defects per unit volume of the order of $10^{24}-10^{25}$ m^{-3} (*see* [176, 177]. Incidentally, the assumption that interstitial atoms and vacancies are uniformly distributed at the moment of formation does not reflect the actual situation. In fact, as discussed above, ejected atoms do not travel substantial distances from the formed vacancy [167], and the overwhelming proportion of interstitial atoms remain within the IZ limits of their vacancies, and recombine with the latter. Since IZ exist in practically all crystalline bodies and since normally the average distance between defects $\bar{x} < r_0$, the majority of crystals should, as it were, be radiation-stable as a consequence of the self-healing of radiation defects. Experiments however have demonstrated the reverse: the majority of crystals do not exhibit radiation-stable properties. The reason for this is the aforementioned focusing phenomenon, as a result of which an interstitial atom may be at a distance from its vacancy that exceeds the IZ radius. 'Self-healing' of such point radiation defects cannot take place without special annealing. There are also other reasons for the stabilization of radiation defects, which are analysed in the review is mentioned above as well as in Section 5.5.

The main task of radiation physics is to discover materials with a high radiation stability. The following paragraphs will discuss the possible existence of crystalline materials in which all defects formed during irradiation are unstable and self-healing.

5.2 *Crystal Chemistry of Radiation Stability*

From the comments in Section 5.1 it follows that the existence of IZ is simply a necessary but not sufficient condition for the self-healing of radiation defects at the moment and at the site of their formation. A sufficient condition would be the absence of focusing of atomic collisions in the crystal, or at least a mean free path of the dynamic crowdion l_t^{hkl} that was less than the IZ radius r_0^{hkl}, where h, k, and l are the Miller indices. These conditions have been formulated by Koshkin *et al.* in articles [12, 173, 218].

The focusing factor $\phi = a/2R(E)$ [167] (where a is the interatomic distance along a chain of atoms and R is the effective atomic radius) obtained in the approximation of solid spheres, assuming that the potential energy of repulsion in the Born–Mayer form is equal to the kinetic energy E_{tr} transferred to the atom, determines the possibility of focusing. If $\phi < 1$, focusing is possible, whereas if $\phi > 1$ it is prohibited. Accordingly, it is clear that focusing may exist only along closely-packed directions (with low crystallographic indices), in which the values a are relatively small. Dmitriev has carried out, in article [219] using the Nelson–Thompson method [217] and Born–Mayer potentials calculated according to the Urusov method [220], an analytical computation of simple and additional focusing parameters (focusing energy and path length of the dynamic crowdion) for various structures with cubic and hexagonal lattices in the crystallographic directions $<hkl>$, where $h, k, l = 0$ or 1. Crystal-chemistry types of diamond (Ge), sphalerite (CdTe), fluorite (CaF_2), rock salt (NaCl), copper (Cu), ReO_3, CdI_2, rutile (TiO_2), cuprite (Cu_2O) and the uniquely closely-packed structure BiF_3 have been investigated. BiF_3 represents the closest cubic packing of large bismuth ions, in which all octahedral and tetrahedral voids are occupied by small fluorine ions. For germanium, sphalerite, rock salt and copper the analytical results agree with the computer simulation results of radiation damage [221–223]. Focusing in other structural types by other methods was not studied. It was found that all the mentioned structures have symmetrical focusing atomic lenses along at least one of the crystallographic directions with small indices. Focusing therefore occurs in these structures. Several types of crystallographic structure, in which the focusing lenses and focusing directions are indicated, are illustrated in Figures 24(b) and 25(b). Calculations of the crowdion path lengths l_t^{hkl} show that along these directions $l_t^{hkl} \gg r_0^{hkl}$, since the radiation stability of similar crystals cannot in principle be large. This is in full agreement with numerous experimental data.

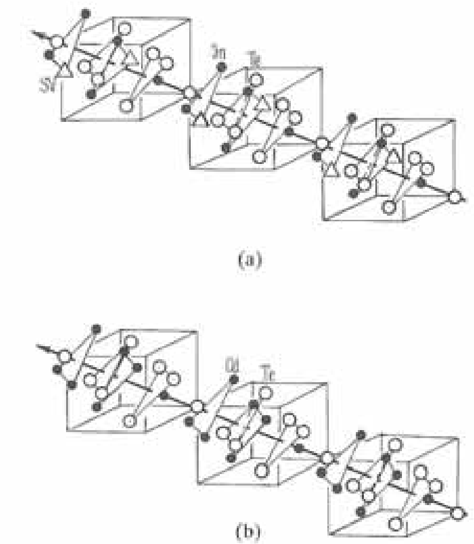

(a)

(b)

Figure 24 Focusing of atomic collision along direction <111> (a) in compounds of the type In_2Te_3; (b) in compounds of the type CdTe.

In loose crystal structures with stoichiometric vacancies in one of the sublattices, the conditions for simple focusing [12] as well as for additional focusing [218] are destroyed. In actual fact, along the crystallographic directions on which the SV are arranged, the distances between two nearest atoms in the row increases (at least by the value of the SV 'diameter'), which reduces the focusing factor. No less important is the fact that the appearance of SV at atomic sites destroys the symmetry of the atomic lenses, and converts the latter from focusing lenses into defocusing lenses (Figures 24(a) and 25(a)). This should lead to a disruption of chains of focused collisions.

In such structures, where collisions are no longer glancing collisions and the angles of attack deviate widely from the focusing axis, the

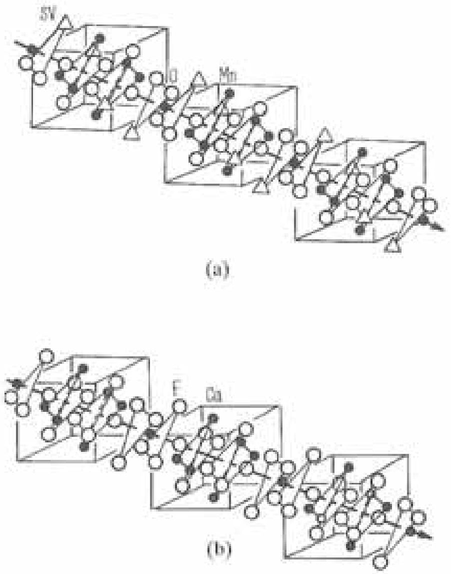

(a)

(b)

Figure 25 Focusing of atomic collisions along direction <111> (a) in compounds of type Mn_2O_3; (b) in compounds of type CaF_2.

momentum approximation used to calculate the focusing parameters is invalid. A computer simulation involving the common solution of the set of equations of motion of all the participating atoms for the four structures Ge and In_2Te_3, and CaF_2 and Mn_2O_3, was accordingly adopted in article [218] to investigate the possibility of focusing in crystals with SV. The choice of these particular structures to elucidate the role of SV in the focusing of atomic collisions is explained by the fact that, as demonstrated in Section 1.1, In_2Te_3 has the same type of lattice as germanium, and Mn_2O_3 the same type of lattice as fluorite, CaF_2. The sole difference is the presence of SV in In_2Te_3 and Mn_2O_3: in $(In_2\square)Te_3$ one-third of the cation positions are SV, while in $Mn_2(O_3\square)$ a quarter of the anionic positions are SV. A paired comparison of the results enables the influence of SV on the focusing to be established. This paired comparison approach is also adopted in the problem of the lattice energy of crystals with SV (*see* Section 1.2) and [37]), the problem of the anharmonicity of vibrations of atoms adjacent to SV (Section 1.4 and [41]), and problems of the experimental investigation of equilibrium defects [11] and radiation defects [10, 12] in crystals with SV. It was found that in germanium and sphalerite crystals chains of focused collisions are formed in the <111> direction (which is in agreement with numerous other calculations: *see*, for example, [221]). Under the same Born–Mayer potential parameters chains of focused collisions in In_2Te_3 and Mn_2O_3 already break after two collisions, and the atoms scatter by large angles. This is connected with the fact that an atom, on traversing a triangular lens (Figures 24(a) and 25(a)) destroyed by the presence of SV in this lens, is sharply deflected from the focusing axis, and a crowdion breaks off at this site. It is extremely important that this result is stable and is preserved under very wide variations in the parameters of the Born–Mayer repulsion potentials and when the existence of the Coulomb charge at the lattice atoms is taken into account.

Thus, although the values of the energy and critical angles of focusing, if such occurs, depend largely on the parameters of the interaction potential, the very fact of the existence or absence of focusing depends only slightly on the potential and is totally determined only by the lattice structure. Normally computer simulation of radiation defects gives a result that depends exclusively and strongly on the potential parameters. In the problem examined in article [218], numerical simulation enabled a strict result to be formulated that is practically independent of the potential parameters: in sphalerite and fluorite type lattices focusing of atomic collisions occurs, whereas in similar lattices of the $(In_2\square)Te_3$ and $Mn_2(O_3\square)$ type focusing is suppressed in all crystallographic directions on account of the presence of SV. A dynamic crowdion is not formed in these loose structures and the characteristic interstitial atom–vacancy distance may in these cases be evaluated according to (5.3), as in a noncrystalline body ('chaotic' model of the condensed state). The derivation of this strict result now enables crystals with destroyed focusing to be identified in a number of cases, and without computer simulation but simply from an analysis of the lattice geometry.

In loose crystal structures with destroyed focusing an ejected interstitial atom thus practically always remains within the limits of the instability zone of its vacancy, and accordingly point defects of radiation origin should basically be annihilated. This determines the anomalously high radiation stability of loose crystal structures. Thus, for the activationless, athermal annihilation of a vacancy and 'its' interstitial atom, i.e. for an ideal impurity-free crystal to have a particularly high radiation stability, a necessary and sufficient condition is the existence of an instability zone and the suppression of focusing of atomic collisions. A very broad criterion may thus be formulated: the inequality $r_0^{hkl} > l_f^{hkl}$ is a necessary and sufficient condition for a high radiation stability. This condition is satisfied in loose crystal structures, where focusing lenses in the immediate vicinity for any closely packed direction are destroyed.

5.3 Phenomenon of Anomalously High Radiation Stability of Semiconductors with Stoichiometric Vacancies

This phenomenon was revealed experimentally much earlier [8–10, 12, 224] than the formulation of the general criterion of radiation stability [218].

In 1969 Koshkin *et al.* discovered a class of semiconductor materials with stoichiometric vacancies having an outstanding radiation stability [8]. These and subsequent detailed investigations on crystals of In_2Te_3, Ga_2Te_3 and Ga_2Se_3 carried out by the same group of investigators [8–10, 12, 224–230] revealed the following.

The monocrystalline and polycrystalline materials In_2Te_3, Ga_2Te_3 and Ga_2Se_3 were irradiated with a flux of γ-quanta of 1.2 MeV energy up to a dose of $3 \times 10^{22}\,m^{-2}$, a flux of fast electrons of energy up to 100 MeV to a dose of $10^{23}\,m^{-2}$, and with a flux of mixed γ-neutron radiation in stationary and pulsed nuclear reactors up to a dose of 10^{23} fast neutrons per m^2. At the same time as the In_2Te_3-type samples, semiconductor crystals of CdTe, ZnTe, ZnS, Ge and Si, which have a similar crystal lattice but without stoichiometric vacancies, were irradiated under the same conditions. Irradiation was carried out at a temperature close to 350 K. Some of the irradiation experiments were performed at 200 K, and the samples were kept at liquid nitrogen temperature before measuring the radiation effects. Various physical and physicochemical parameters of the samples were investigated both before and after the irradiation, including their specific conduction, its temperature dependence, concentration and mobility of charge carriers, thermo-e.m.f. coefficients, coefficient of optical absorption in the vicinity of the edge of the fundamental band–band transition, transmission in the infrared wavelength region from 1 to 20 μm, the kinetics and spectral dependences of photoconduction, and the microhardness value. In the aforementioned investigations it was shown that all the investigated parameters of semiconductors with stoichiometric vacancies are preserved after the action of such large doses of ionizing radiation. It was also demonstrated that the parameters of conventional semiconductors without stoichiometric vacancies irradiated under the same conditions change very significantly after similar radiation doses, in full agreement with numerous investigations carried out by other authors.

Only two manifestations of radiation changes were discovered: the thermo-e.m.f. of the ordered α-phase of In_2Te_3 changes slightly as regards absolute value, which indicates disorder in the cationic sublattice, and investigations on thermo-stimulated conduction in Ga_2Se_3 after irradiation with fast neutrons in a dose of $2 \times 10^{21}\,m^{-2}$ reveal the formation of a very small concentration of shallow traps (10^{15}–$10^{16}\,m^{-3}$), which annealed at 280 K. An evaluation of the relative proportion of these stabilized defects gave a figure of 10^{-11}% of the total number of defects that could be generated in the crystal under the specified radiation doses.

Experiments were also performed in which the electrical conduction of the same crystals was measured during their irradiation in a nuclear reactor channel [12, 229]. During irradiation free charge carriers are naturally formed, and the nonequilibrium conduction due to the internal photoeffect was measured in these experiments. These experiments showed that, with an unchanged reactor output and set of exposure doses, these characteristics of In_2Te_3 and Ga_2Te_3 do not change, whereas the parameters of Ge and CdTe degrade (Figure 26).

The radiation stability effect of semiconductor crystals with stoichiometric vacancies discovered by the Kharkov group in the aforementioned investigations was confirmed in the experiments of the present authors [112], who discovered however the accumulation of a certain amount of radiation defects under low-temperature irradiation of In_2Te_3 with 1 MeV energy electrons. This is apparently associated with the technological features of the preparation of the samples used in the investigations [112], in which the authors synthesized strictly stoichiometric In_2Te_3, which is a two-phase system (Section 2). Evidently the small proportion of the second phase,

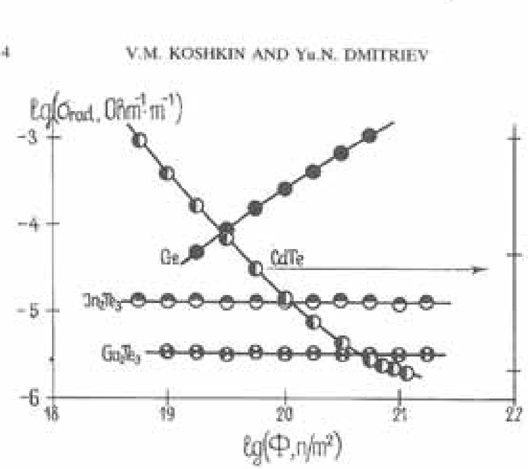

Figure 26 Dependence of specific electrical conduction of Ge, CdTe, In_2Te_3, Ga_2Te_3 on fast neutron flux, measured directly in nuclear reactor channel ($T = 190$ K).

which is not radiation-stable, leads to the appearance of some stable defects. This phenomenon has been analysed in [231]. The radiation stability of the electrical and photoelectrical parameters of In_2Te_3 has also been confirmed in [232].

Subsequently it was discovered that three-component semiconductors with stoichiometric vacancies also have a high radiation stability. In article [233] it was shown that the electrical conduction of the semiconductor $(Hg_3In_2\square)Te_6$, where one-sixth of the cationic sublattice sites constitutes stoichiometric vacancies, does not change after the action of a dose of γ-quanta of $2 \times 10^{22}\,m^{-2}$ and a reactor neutron flux of $10^{20}\,m^{-2}$. In article [233] it was shown that monocrystals of $(ZnIn_2\square)S_4$, which incidentally have a very high photosensitivity, preserve their electrical and optical parameters practically unchanged after the action of a 100 keV electron flux and a 1 MeV γ-radiation flux up to a dose of the order of $2 \times 10^{20}\,m^{-2}$.

Since all the members of the structural family of semiconductors with stoichiometric vacancies, i.e. $(ZnIn_2\square)S_4$, $(In_2\square)Te_3$, $(Ga_2\square)Te_3$, $(Ga_2\square)Se_3$, $(Hg_3In_2\square)Te_6$, are radiation-stable, it is clear that the property of radiation stability is determined by the overall features of their structure, namely the existence of SV and destroyed focusing, in full agreement with the mechanism described in Section 5.2.

5.4 *Radiation-Stable Dielectrics with Loose Structure*

In order to provide further experimental verification of the formulated general criterion of radiation stability, the authors of article [218] subjected powders of the materials specified in Table 3 to the action of various doses of reactor neutrons. Irradiation was carried out with fast neutrons in an atomic reactor channel at a temperature in the region of 300 K.

The diffuse reflection spectra in the range 350–900 nm were investigated. The coefficient of diffuse reflection R_d is spectrally analogous to absorption in monocrystalline materials [234]. The majority of investigated materials after irradiation do not exhibit pronounced new absorption bands in the visible region, though the R_d value of the majority of the materials did change fairly significantly after irradiation. The relative changes in R_d of a number of substances in the transmittance range at a fixed wavelength $\lambda = 700$ nm are given in Table 3. The same ratios of the quantities $\Delta R_d / R_{d_0}$ for these substances are naturally obtained for other wavelength values in the transmittance range ($\Delta R_d = R_d - R_{d_0}$), where R_{d_0}, R_d are respectively the values of the coefficient of diffuse reflection before and after neutron irradiation.

From Table 3 it is clear that the minimum value of $\Delta R_d / R_{d_0}$ corresponds to the compounds In_2O_3 and Y_2O_3 (Mn_2O_3 lattice with SV), while the value of $\Delta R_d / \Delta R_{d_0}$ for CdF_2 and PbF_2 crystals with the same fluorite lattice but without SV is considerably greater. Such radiation damage is observed in LiF and MgO with the NaCl

Table 3 Relative Changes in the Coefficient of Diffuse Reflection $\frac{\Delta R_d}{R_{d_0}} = \frac{R_d - R_{d_0}}{R_{d_0}}$ after Reactor Irradiation, $\lambda = 700$ nm

Compound	R_{d_0}(%)	$\Delta R_d / R_{d_0}$	
		$\Phi = 1 \times 10$[illegible] (n/m^2)	$\Phi = 1 \times 10^{20}$ (n/m^2)
In_2O_3	60.8	0.060	0.075
Y_2O_3	69.5	0.110	0.140
CdF_2	75.0	0.205	0.280
PbF_2	73.4	0.395	0.705
TiO_2	76.5	0.150	0.165
MgO	100.0	0.465	0.410
LiF	79.0	0.270	0.465
MoO_3	59.9	0.265	0.435

lattice, where there are two focusing directions, namely <100> and <111>, and in the MoO_3 structure, where in addition to the above focusing directions focusing also takes place in the <110> direction. TiO_2, in which there is only weak focusing in the <001> direction, occupies an intermediate position as regards radiation stability.

After irradiation in a nuclear reactor numerous strong absorption bands appeared in the infrared region of the spectrum in crystals without SV, whereas infrared absorption of In_2O_3 and Y_2O_3 crystals with SV remained unchanged [235, 236]. The fact that crystals of both In_2O_3 and Y_2O_3 belong to one structural type demonstrates that their radiation stability is determined by a common structural feature, namely the existence of stoichiometric vacancies, just like the radiation stability of crystals of the In_2Te_3 structural type.

In crystals with stoichiometric vacancies the atomic lenses are totally destroyed, and this fact determines their practically absolute radiation stability. However, even a comparatively small distortion of the symmetry of the atomic lenses, which normally occurs in crystals with a low-symmetry lattice, should also lead to destruction of the focusing and, consequently, to a decrease in the path length of the crowdions. Of course, this cannot lead to complete suppression of focusing, though it may be expected that crystals with distorted atomic lenses should have a higher radiation stability under otherwise identical conditions. This assumption was stated and experimentally proved in article [237].

5.5 Possible Mechanisms of Accumulation of Radiation Defects in Crystals with Suppressed Focusing

Naturally, when predicting the radiation stability of materials the features of annihilation in cascades, probability of capture of radiation defects at impurities and dislocations, change in valency, nonlinear effects at large intensities, etc., should of course be taken into account.

However, the instability zone and focusing, which determine the fate of each pair consisting of a vacancy and 'its' interstitial atom, play a fundamental role in the atomic mechanisms on which the radiation stability depends.

Meanwhile, there are at least three possible mechanisms that may lead to the stabilization of radiation-induced unstable pairs. These mechanisms have been investigated in article [238]. The first mechanism involves the possibility of formation of impurity atom–interstitial atom or impurity atom–vacancy complexes. In this case, when one of the partners of the unstable pair is captured and cannot recombine, conditions are created for the accumulation of radiation defects. It should be noted that the formation cross-sections of such complexes in In_2Te_3-type semiconductors, where impurities are preferentially in the atomic state (see Section 2.2), are undoubtedly substantially less than in crystals where the impurities are ionized. Accordingly, the presence of impurities in In_2Te_3 has a weak influence on the radiation stability. The second mechanism for stabilization of unstable pairs may be associated with the capture, by one of the components of the pair (within the limits of the lifetime of the pair), of an electron from the conduction band or a hole from the valency band. It is very likely that the very small concentration of small traps formed during low-temperature irradiation which anneal below 280 K is in fact determined by this mechanism [11]. The third possibility of the formation of stable Frenkel defects from unstable pairs arises at a very high concentration of the latter, when the instability zones of the defects are covered, even if partially. Then the probability appears that any interstitial atom that has left its site and that remains in the instability zone of 'its' vacancy simultaneously enters the instability zone of another vacancy and in fact recombines with the latter. If in this connection an interstitial atom belonging by origin to this second vacancy does not enter the instability zone of the first vacancy, then one Frenkel pair will be formed from two unstable pairs. A similar situation may arise under very high radiation intensities, as well as in collision cascades produced by fast neutrons, ion beams or very high energy electrons (for example energy greater than 10 MeV). The spatial separation of the distributions of interstitial atoms and vacancies in cascades may stimulate these phenomena.

The mechanisms of defect stabilization described in [238] may lower the radiation stability of a material, even if the latter satisfies the crystal-chemistry structural criterion of stability.

Very unusual radiation effects occur in crystals where polymorphic modifications are possible. Such modifications may include equilibrium modifications at higher temperatures compared to the irradiation temperature, as well as modifications that do not occur at all under equilibrium conditions, but appear as a result of the action of radiation. A similar problem is phase segregation under radiation influences, in which mass fluxes have to be taken into account in the theoretical description of the phenomenon [239, 240]. If there is not even a local change in composition, then radiation-stimulated phase transformations can be successfully described phenomenologically by means of systems of differential equations that take account of the probability of radiation-stimulated transitions between phases without the involvement of diffusion terms. Each of the phases may be considered as some structural state of the system, and their radiation transformations as strong excitations (cf. [241]) resulting in transitions from one discrete state to another. This program was developed in [242] (see also the review [180]), where it was shown in particular that the dose dependence of the volumetric fraction of one or other phase (under the existence of not less than three possible phase states) may be nonmonotonic. This is actually observed experimentally, for example in the irradiation of quartz [243]. In addition to a description of the evolution of the phase state with the aid of a system of differential equations, a description of the evolution of the phase state is also given in [180, 242] in terms of Markov chains, followed by the action of a defect-formation operator and a radiation annealing operator. We shall not compare the results of these two approaches here, but would merely point out that in the Markov description the state vector of the radiation-resistant phase is an eigenvector of the defect-formation operator.

6. TECHNICAL USES OF MATERIALS WITH LOOSE CRYSTAL LATTICE

In this section we shall give a brief review of those applications described of materials that are already industrially available, as well as those that may form the basis of technical applications in the near future.

6.1 Compounds of Layer-type Structure in Engineering and Technology

The extremely small critical stress needed to cleave layer-type compounds along the basal plane has long been used in technology. The so-called 'dry grease' for friction-compact surfaces is prepared from graphite and a number of other layer-type compounds (MoS_2 type).

Zeolites have been mentioned only in passing in this paper, since they are already described in detail in numerous monographs. Meanwhile, one of the principal applications of zeolites is connected with the utilization of their extremely high adsorption capability, due to the penetration of molecules into structural cavities in the lattice, which is similar to the phenomenon of intercalation.

One of the most conspicuous applications of the particular phenomenon of intercalation is the work of Wittingham [244] on the electrochemical intercalation of layer and chain compounds with metallic-type conduction. In [244–246] it was shown that, by using a layer metal of the TaS_2 type as cathode in an electrochemical cell with lithium ions as charge carriers in a liquid electrolyte, electrical batteries with an extremely high specific capacitance can be obtained. The latter is determined by the fact that the layered structure of the material ensures an extremely large effective surface available to the electrochemical reaction. Lithium ions, on intercalating a layered metal, accumulate electrical energy with a very high density, and such batteries are widely employed. The chief disadvantage of these batteries is the low charging and discharging currents, which is associated with the low mobility of lithium ions in the layered matrix. Batteries of this type are accordingly extremely good for supplying low-current electrical circuits, though they can hardly be used in their present form for high-power electrical systems. Nevertheless, the possibilities of improving the characteristics of such batteries are far from being exhausted.

An interesting development of Wittingham's idea has been suggested by Tributsch [247]. In article [247] it is shown, by the example of $ZrSe_2$, that light-controlled electrochemical batteries can be fabricated on the basis of semiconductor layer-type matrices. By exposing the sample to light and thereby changing the Fermi quasi-level in the latter, it is possible to alter the electron-acceptor capacity of the matrix. Thus, during illumination cathode photointercalation occurs, corresponding to charging of the batteries. Tributsch showed that a similar photointercalation system may serve as a solar battery, which is very convenient since the processes of charging the battery and storage of energy are combined in one working element, in which connection up to 10% of the solar radiation may be utilized.

In article [248] it was discovered that the material of the layered matrix changes colour during photointercalation, which suggests a possible use of this material for optical storage of information.

Exposure of the layer-type semiconductor PbI_2 to light in the presence of various amines (aniline, quinoline, etc.), which under equilibrium conditions without illumination are intercalated in this material, results in the sensitization of this compound to photolysis [249]. It was shown that photolysis and intercalation processes compete, and that in fact intercalation inhibits photolysis. This effect may be used in silverless photography. On the other hand, the discovered phenomenon enables PbI_2 and similar layered semiconductors to be used as the working body for sensors, enabling the presence of amines in various media to be detected [257].

The discovery of a minor-zone energy electron spectrum during intercalation of layered semiconductors [160, 164] (see Section 3.2) creates interesting possibilities for using these materials in electronic devices similar to those that operate on the basis of artificial superlattices developed initially by Esaki [250]. The fact that these superlattices, being equilibrium structures, are incomparably simpler from the technological point of view and are certainly more stable and do not undergo ageing effects, is clearly an important advantage of long-period superlattices in intercalation semiconductors. The choice of various intercalants for a given layered semiconductor, choice of 'crystal–host'/'molecule–guest' stoichiometric ratios and, finally, the choice of operating temperature range enable the period of the superlattice and consequently the structure of the minor-zone spectrum to be varied. Knowledge of the formation of long-period superlattices was used in article [251], in which the possibility of forming monochromators for neutron diffractometry based on various degrees of intercalation of graphite with the formation of the 'graphite–$SbCl_5$' intercalation compound was demonstrated.

Completely new potential applications were discovered by Vol'pin, Novikov *et al.*, who studied the catalytic properties of intercalated graphite [124, 252, 253]. These investigators established the principles of the purposeful, targeted selection and synthesis of catalysts for various types of reactions. It was shown above all that the catalytic activity of intercalation compounds of graphite is determined not by individual active centres, but by the whole electron system of this heterogeneous catalyst. It was established in particular that reactions proceeding according to an anionic mechanism, for example the polymerization of siloxanes, as well as the synthesis of ammonia from nitrogen and hydrogen, are accelerated in the presence of compounds of graphite intercalated with metals, which increase the concentration of electrons in the graphite layers. Reactions occurring according to a cationic mechanism (for example the oxidation of ethyl benzene) are catalysed by graphite intercalated with molecules of dichlorides of a number of metals ($CuCl_2$, $FeCl_2$). The latter are electron acceptors with respect to graphite and produce an excess concentration of holes which predetermines the enhancement of the acceptor capacity of graphite layers. The same authors discovered the possibility of converting graphite [254] into diamond at very low pressures and temperatures in the presence of iron-intercalated graphite as catalyst.

Fairly recently, great hopes were placed on the application of the phenomenon of intercalation of layer-type metals by organic molecules to raise the superconductivity transition temperature [127]. However, the discovery of high-temperature oxide superconductors by Bednorz and Müller in 1986 has possibly made research on intercalation less attractive. Nevertheless, it appears to us that layer-type structural motifs and loose superconducting oxide lattices presuppose the discovery of phenomena similar to those described in this paper.

6.2 Technical Potentialities of Semiconductors with Stoichiometric Vacancies

The independence of the electrical conduction of the semiconductor tellurides In_2Te_3, Ga_2Te_3, $CdIn_2Te_4$, $Hg_3In_2Te_6$ on the concentration of impurities creates a number of unique technical potentialities. The production of these crystals requires practically no further purification to remove uncontrollable impurities, and accordingly the fabrication of materials of this type is technologically much simpler compared to conventional semiconductors. However, the property of inertness of impurities in this type of semiconductor creates not only advantages but also disadvantages, since it is not possible to form junctions in such semiconductors and fabricate active electronic components. Accordingly the principal potential application is the production of a wide range of resistors sensitive to various external interactions.

1. Since the semiconductors In_2Te_3 and Ga_2Te_3 always have the same resistivity at a given temperature and by virtue of this are intrinsic semiconductors and have a sufficiently broad energy gap, the temperature coefficient of resistance of these materials is extremely large (up to 12%/K at room temperature). The above materials may therefore be effectively employed as sensitive thermoresistors [255].

2. The intrinsic nature of the conduction and, consequently, the small concentration of charge carriers predetermines the extremely high thermo-e.m.f. coefficient, which may reach values of more than 1 mV/K in In_2Te_3 [60]. This means that these materials can be used as thermoelectric temperature transducers.

3. The absence of localized charge carriers in the energy gap predetermines the high strain sensitivity of materials of this type. In actual fact, the change in resistance under the application of pressure is determined by the barometric coefficient of the width of the energy gap at a high electron state density in the valency band, in contrast to the low density of states when the conduction of the semiconductor is determined by impurities. This was demonstrated by Figotin in [256] by the example of the flexural deformation of In_2Te_3, in which the relative coefficient of strain sensitivity reaches 300, which exceeds the strain sensitivity values of conventional semiconductors.

4. The authors of articles [226, 232] refer to the possibility of producing photoresistors based on In_2Te_3 and Ga_2Se_3 for the near-infrared and visible regions of the spectrum.

All the enumerated technical potentialities of these materials are particularly attractive on account of the fact that all the aforementioned parameters are unaffected by the action of extremely high doses of ionizing radiation (see Section 5.3). The radiation stability of all the physical parameters of the semiconductors In_2Te_3, Ga_2Te_3, Ga_2Se_3, $Hg_3In_2Te_6$ exceeds by many orders of magnitude the effective radiation life of all known semiconductors. This creates possibilities of using technical devices based on the latter in conditions subject to the action of large and intense radiation fields.

The invariability of the physical parameters after irradiation does not of course exclude the occurrence of observable electron excitations during the action of the radiation. The conductivity of In_2Te_3 under the action of a pulsed intense beam of fast electrons of energy up to 300 MeV was investigated in article [227]. The dependence of the conduction σ_{rad} of a crystal under irradiation is illustrated in Figure 27. The calculated intensity distribution of the beam over time is shown by the dashed line. It is clear from the diagram that very large flux intensities of fast electrons can be measured with a good time resolution using a working element fabricated from In_2Te_3, all the parameters of the latter being preserved even under substantial flux doses.

The conductivity of Ga_2Se_3 at room temperature as a function of the γ-radiation dose from two different sources (^{60}Co and ^{137}Cs) was investigated in article [229]. The linear response with an increase in intensity in a very wide range of variations in the latter can be seen in Figure 28. Although the sensitivity threshold of the crystals can be improved by reducing the temperature, it is nevertheless absolutely clear that the sensitivity of Ga_2Se_3 to γ-radiation is many orders of magnitude less than in, for example, conventional scintillators. Meanwhile, in scientific and technological problems where large intensities have to be measured, radiation-stable semiconductors of the Ga_2Se_3 type are clearly in a class of their own.

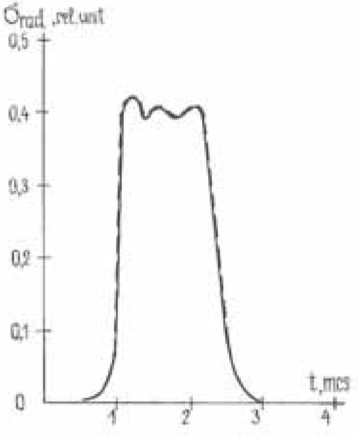

Figure 27 Dependence of radiation conductivity σ_{rad} in In_2Te_3 on time under action of pulsed fast electron flux.

The possibility of measuring the local energy release in an atomic reactor by means of semiconductor transducers based on In_2Te_3, Ga_2Te_3 and Ga_2Se_3 was also investigated in article [227], and is illustrated in Figure 29 with the example of the compound Ga_2Te_3. In the region of fairly low temperatures and large reactor output, when the conductivity excited by absorption of radiation exceeds the dark conductivity, the resistance of the transducer is determined by the radiation level in the reactor channel, which in turn is deter-

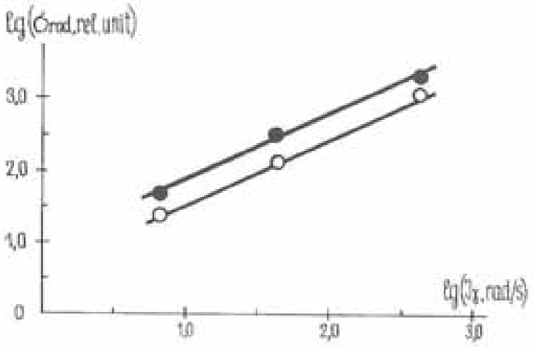

Figure 28 Dependence of radiation conductivity σ_{rad} in compound Ga_2Se_3 on radiation dose for two samples.

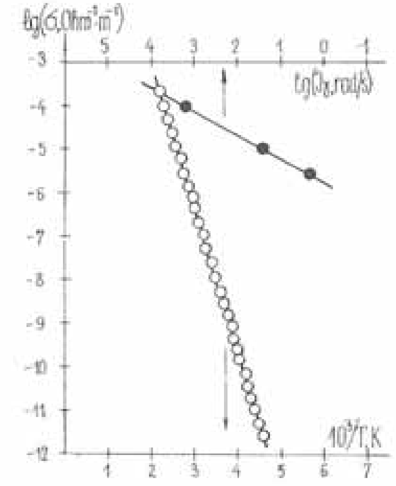

Figure 29 Dependence of dark conductivity of crystal Ga_2Te_3 on temperature, and dependence of the radiation conductivity of same crystal on γ-radiation dose in reactor.

mined by the local release of energy. At high temperature and low radiation power the dark conductivity of the transducer is determined by the temperature at that point in the reactor where the transducer is located, i.e. is also determined by the magnitude of the local energy release. Thus, depending on the local energy release, the same transducer operating under different regimes enables the magnitude of this local energy release to be determined.

The above examples cover the principal technical areas of use of materials with a loose crystal structure.

REFERENCES

1. Hahn, H. and Klingler, W. (1949) *Z. Anorg. Chem.*, **259**, 121.
2. Goryunova, N.A., Grigor'eva, V.S., Konovalenko, V.M. and Ryvkin, S.M. (1955) *Zh. Tekh. Fiz.*, **25**, 1675.
3. Zhuze, V.P., Sergeeva, V.M. and Shelykh, A.I. (1960) *Fiz. Tverd. Tela (Leningrad)*, **2**, 2858.
4. Zaslavskii, A.I. and Sergeeva, V.M. (1960) *Fiz. Tverd. Tela (Leningrad)*, **2**, 2872.
5. Zaslavskii, A.I., Sergeeva, V.M. and Smirnov, I.A. (1960) *Fiz. Tverd. Tela (Leningrad)*, **2**, 2885.
6. Zhuze, V.P. and Shelykh, A.I. (1965) *Fiz. Tverd. Tela (Leningrad)*, **7**, 1173.
7. Radautsan, S.I. (1966) Avtoreferat doktorskoi disssertatsii (Author's abstract of a Doctoral Dissertation). Leningrad.
8. Koshkin, V.M., Atroshchenko, L.V., Gal'chinetskii, L.P., Shakhovtsov, V.I. and Rudenko, M.I. (1970) Avtorskoe svidetel'stvo SSSR (USSR Inventor's Certificate No. 293395).
9. Gal'chinetskii, L.P., Koshkin, V.M., Kulakov, V.M., Kulik, V.N., Rudenko, M.I., Ryabka, P.M., Ulmanis, U.A. and Shakhovtsov, V.I. (1972) *Fiz. Tverd. Tela (Leningrad)*, **14**, 646.
10. Koshkin, V.M., Gal'chinetskii, L.P., Kulik, V.N., Minkov, B.I. and Ulmanis, U.A. (1973) *Solid State Commun.*, **13**, 1.
11. Dmitriev, Yu.N., Kulik, V.N., Gal'chinetskii, L.P. and Koshkin, V.M. (1975) *Fiz.-Tverd. Tela (Leningrad)*, **17**, 3685.
12. Koshkin, V.M., Gal'chinetskii, L.P., Kulik, V.N. and Ulmanis, U.A. (1975) *Radiat. Eff.*, **29**, 1.
13. Levin, A.A. (1974) *Vvedenie v Kvantovyuu Khimiyu Tverdogo Tela (Introduction to Quantum Chemistry of Solids)*. Moscow (in Russian).
14. Pauling, L. (1945) *The Nature of the Chemical Bond*. Ithaca.
15. Batsanov, S.S. (1962) *Elektrootritsatel'nost' Elementov i Khimicheskaya Svyaz' (Electronegativity of Elements and Chemical Bonding)*. Novosibirsk (in Russian).

16. Ovechkina, E.E., Koshkin, V.M. and Sysoev, L.A. (1969) *Zh. Strukt. Khim.*, **10**, 156.
17. *Poluprovodnikovye Veshchestva. Voprosy Khimicheskoi Svyazi (Semiconductor Materials. Questions of Chemical Bonding)* (1960) Moscow (in Russian).
18. Bokii, G.B. (1971) *Kristoallokhimiya (Crystal Chemistry)*. Moscow (in Russian).
19. Kitaigorodskii, A.I. (1971) *Molekulyarnye Kristally (Molecular Crystals)*. Moscow (in Russian).
20. Pines, B.Ya. (1961) *Ocherki po Metallofizike (Principles of the Physics of Metals)*. Kharkov (in Russian).
21. Schomaker, V. and Stevenson, D.P. (1941) *J. Amer. Chem. Soc.*, **63**, 37.
22. Palatnik, L.S., Komnik, Yu.F. and Koshkin, V.M. (1962) *Kristallografiya*, 7, 563.
23. Belov, N.V. (1947) *Struktura Ionnykh Kristallov i Metallicheskikh Faz (Structure of Ionic Crystals and Metallic Phases)*. Moscow (in Russian).
24. Ormont, B.F. (1973) *Vvedenie v Fizicheskuyu Khimiy i Kristallokhimyu Poluprovodnikov (Introduction to the Physical Chemistry and Crystal Chemistry of Semiconductors)*. Moscow (in Russian).
25. Goryunova, N.A. (1968) *Slozhnye Almazopodobnye Poluprovodniki (Complex Diamond-like Semiconductors)*. Moscow (in Russian).
26. Seraphin, B. (1954) *Z. Naturforsch.*, **9a**, 450.
27. Grimm, H. and Sommerfeld, A. (1926) *Zs. Physik*, **36**, 36.
28. Suchet, J.P. (1965) *Chemical Physics of Semiconductors*. London.
29. Goldshmidt, V. (1929) *Usp. Fiz. Nauk*, **9**, 811.
30. Palatnik, L.S., Koshkin, V.M. and Komnik, Yu.F. (1962) *Kristallografiya*, 7, 124.
31. Woolley, J.C., Gillett, G. and Evans, J.A. (1960) *J. Phys. Chem. Solids*, **16**, 138.
32. Woolley, J.C. and Ray, B. (1960) *J. Phys. Chem. Solids*, **16**, 102.
33. Woolley, J.C., Pamplin, B.R. and Evans, J.A. (1961) *J. Phys. Chem. Solids*, **19**, 147.
34. Palatnik, L.S., Koshkin, V.M. and Komnik, Yu.F. (1965) In *Khimicheskaya Svyaz' v Poluprovodnikakh i Tverdykh Telakh (Chemical Bonding in Semiconductors and Solids)*. Minsk (in Russian).
35. Newman, P.C. (1962) *J. Phys. Chem. Solids*, **23**, 19.
36. Street, R.A. and Mott, N.F. (1975) *Phys. Rev. Lett.*, **35**, 1293.
37. Koshkin, V.M., Manyukova, L.G. and Sysoev, L.A. (1968) *Izv. Akad. Nauk SSSR, Neorg. Mater.*, **4**, 1633.
38. Dmitriev, Yu.N. and Koshkin, V.M. (1976) *Raschet Postoyannykh Reshetki Kristallov s Razlichnoi Stepen'yu Zapolneniya Tetraedricheskikh i Oktaedricheskikh Pozitsii (Calculation of Lattice Constants of Crystals with Various Degrees of Filling of Tetrahedral and Octahedral Positions)* (in Russian). Cherkassy, N. 1049/76Dep.
39. Novikova, S.I. (1974) *Teplovoe Rasshirenie Tverdykh Tel (Thermal Expansion of Solids)*. Moscow (in Russian).
40. Sirota, N.N. and Berger, L.I. (1959) *Inzh. Fiz. Zh.*, **2**, 104.
41. Koshkin, V.M., Timan, B.L. and Gal'chinetskii, L.P. (1967) *Ukr. Fiz. Zh. (Russ. Ed.)*, **12**, 2065.
42. Koshkin, V.M., Gal'chinetskii, L.P. and Freiman, Yu.A. (1969) *Fiz. Tverd. Tela (Leningrad)*, **11**, 212.
43. Kittel, Ch. (1956) *Introduction to Solid State Physics*. New York.
44. Kontorova, T.A. (1956) *Zh. Tekh. Fiz.*, **26**, 20.
45. Grushka, G.G., Babyuk, T.I. and Parenyuk, I.A. (1987) *Izv. Akad. Nauk SSSR, Neorg. Mater.*, **23**, 410.
46. Gal'chinetskii, L.P. and Koshkin, V.M. (1969) *Ukr. Fiz. Zh. (Russ. Ed.)*, **14**, 54.
47. Abdurakhmanova, A.A. and Aliev, M.I. (1966) *Izv. Akad. Nauk SSSR, Neorg. Mater.*, **2**, 667.
48. Ambegaokar, V. (1959) *Phys Rev.*, **114**, 488.
49. Koshkin, V.M., Manyukova, L.G., Palatnik, L.S. and Gal'chinetskii, L.P. (1966) *Izv. Akad. Nauk SSSR, Neorg. Mater.*, **2**, 1138.
50. Grushka, G.G., Grushka, Z.M. and Gavaleshko, N.P. (1985) *Ukr. Fiz. Zh. (Russ. Ed.)*, **30**, 304.
51. Grushka, G.G., Grushka, Z.M. and Gavaleshko, N.P. (1988) *Ukr. Fiz. Zh. (Russ. Ed.)*, **33**, 1083.
52. Fistul, V.I. (1975) *Vvedenie v Fiziku Poluprovodnikov (Introduction to Semiconductor Physics)*. Moscow (in Russian).
53. Milnes, A.G. (1973) *Deep Impurities in Semiconductors*. New York.
54. Lishka, K. (1986) *Phys. Status Solidi B*, **133**, 17.
55. Glazov, V.M. and Zemskov, V.S. (1967) *Fiziko-khimicheskie Osnovy Legirovaniya Poluprovodnikov (Physico-chemical Principles of Doping of Semiconductors)*. Moscow (in Russian).
56. Kalyuzhnaya, G.A. and Kiseleva, K.V. (1987) *Trudy FIAN SSSR*, **177**, 5.
57. Koshkin, V.M., Gal'chinetskii, L.P. and Korin, A.I. (1971) *Fiz. Tekh. Poluprovod.*, **5**, 1983.
58. Ovechkina, E.E. (1978) Avtoreferat kandidatskoi dissertatsii (Author's abstract of Candidate's Dissertation). Kharkov.
59. Wright, H.C. and Newman, P.C. (1962) *Reports of Internat. Conf. on Phys. of Semiconduct., Exter*, 240.
60. Atroshchenko, L.V., Gal'chinetskii, L.P., Koshkin, V.M. and Palatnik, L.S. (1965) *Dokl. Akad. Nauk, SSSR*, **165**, 809.
61. Atroshchenko, L.V., Gal'chinetskii, L.P., Koshkin, V.M. and Palatnik, L.S. (1965) *Izv. Akad. Nauk SSSR, Neorg. Mater.*, **1**, 2140.
62. Atroshchenko, L.V., Gal'chinetskii, L.P. and Koshkin, V.M. (1967) *Izv. Akad. Nauk SSSR, Neorg. Mater.*, **3**, 777.
63. Dovletov, K., Ragimov, F., Nuriev, S. and Samokhatina, N.K. (1982) *Fiz. Tekh. Poluprovod.*, **16**, 1205.
64. Palatnik, L.S., Manyukova, L.G. and Koshkin, V.M. (1966) *Izv. Akad. Nauk SSSR, Neorg. Mater.*, **2**, 1031.
65. Atroshchenko, L.V. and Koshkin, V.M. (1970) *Problemy Prochnosti*, **6**, 95.
66. Atroshchenko, L.V. and Koshkin, V.M. (1969) *Izv. Akad. Nauk SSSR, Neorg. Mater.*, **5**, 265.
67. Bakumenko, V.L., Bonakov, A.K. and Grushka, G.G. (1983) *Elektronnaya Tekhnika*, Ser. 6, **2**, 175.

68. Palatnik, L.S., Komnik, Yu.F., Koshkin, V.M., Gal'chinetskii, L.P. and Manyukova, L.G. (1964) *Ukr. Fiz. Zh. (Russ. Ed.)*, **9**, 962.
69. Koshkin, V.M., Gal'chinetskii, L.P., Karas', V.R., Nesterova, T.N. and Sklovskaya, I.L. (1970) *Ukr. Fiz. Zh. (Russ. Ed.)*, **15**, 210.
70. Grushka, G.G., Gerasimenko, V.S. and Grushka, Z.M. (1983) *Zh. Neorgan. Khim.*, **7**, 1878.
71. Drabkin, I.A., Moizhes, B.Ya. and Sanfirov, Yu.Z. (1979) *Fiz. Tekh. Poluprovod.*, **13**, 134.
72. Nasredinov, F.S., Masterov, V.F., Saidov, Ch.S., Seregin, P.P., Troitskaya, N.N. and Tschirner, H.U. (1988) *Phys. Status Solidi A*, **107**, 291.
73. Koshkin, V.M., Freiman, Yu.A. and Atroshchenko, L.V. (1967) *Fiz. Tverd. Tela (Leningrad)*, **9**, 3120.
74. Koshkin, V.M., Atroshchenko, L.V. and Freiman, Yu.A. (1968) *Dokl. Akad. Nauk SSSR*, **183**, 83.
75. Ovechkina, E.E., Romanov, V.P., Zabrodskii, Yu. R. and Koshkin, V.M. (1977) *Zh. Eksp. Teor. Fiz.*, **72**, 329.
76. Koshkin, V.M., Zabrodskii, Yu.R. and Gerasimenko, V.S. (1980) *Fiz. Khim. Stekla*, **6**, 40.
77. Podorozhanskaya, N.M., Ovechkina, E.E., Kogan, Yu.M. and Koshkin, V.M. (1975) In *Monokristally i Tekhnika (Single Crystals and Technology)*, Vol. 11, p. 91. Kharkov (in Russian).
78. Atroshchenko, L.V. and Koshkin, V.M. (1971) *Izv. Akad. Nauk SSSR, Neorg. Mater.*, **7**, 773.
79. Atroshchenko, L.V., Gal'chinetskii, L.P. and Koshkin, V.M. (1972) *Izv. Akad. Nauk SSSR, Neorg. Mater.*, **8**, 685.
80. Koshkin, V.M. and Atroshchenko, L.V. (1970) *Monokristally i Tekhnika (Single Crystals and Technology)*, Vol. 1, 0.120. Kharkov (in Russian).
81. Koshkin, V.M. and Atroshchenko, L.V. (1970) *Izv. Akad. Nauk SSSR, Neorg. Mater.*, **6**, 714.
82. Ovechkina, E.E. and Kukol', V.V. (1982) *Izv. Akad. Nauk SSSR, Neorg. Mater.*, **18**, 939.
83. Fistul, V.I. (1967) *Sil'no Legirovannye Poluprovodniki (Highly Doped Semiconductors)*. Moscow (in Russian).
84. Atroshchenko, L.V. and Koshkin, V.M. (1966) *Izv. Akad. Nauk SSSR, Neorg. Mater.*, **2**, 405.
85. Lifshits, I.M. and Tanatarov, L.V. (1961) *Fiz. Met. Metalloved.*, **12**, 331.
86. Koshkin, V.M. and Atroshchenko, L.V. (1969) *Fiz. Tverd. Tela (Leningrad)*, **11**, 816.
87. Zhdanov, G.S. (1961) *Fizkika Tverdogo Tela (Solid State Physics)*. Moscow (in Russian).
88. Korol'kov, A.I. (1959) *Izv. Akad. Nauk SSSR, Met. Toplivo*, **5**, 123.
89. Atroshchenko, L.V. (1969) Avtoreferat kandidatskoi dissertatsii, (Author's abstract of Candidate's Dissertation). Kharkov.
90. Koshkin, V.M. and Atroshchenko, L.V. (1970) *Fiz. Tverd. Tela (Leningrad)*, **12**, 1536.
91. Koshkin, V.M. (1970) In *Nekotorye Voprosy Khimii i Fiziki Poluprovodnikov Slozhnogo Sostava (Questions Concerning the Chemistry and Physics of Semiconductors of Complex Compositions)*. Uzhgorod (in Russian).

92. Koshkin, V.M. and Manyukova, L.G. (1970) In *Monokristally i Teknika (Single Crystals and Technology)*, Vol. 2, p. 96. Kharkov (in Russian).
93. Conwell, E.M. and Weisskopf, V.F. (1950) *Phys. Rev.*, **77**, 388.
94. Koshkin, V.M., Ovechkina, E.E. and Romanov, V.P. (1975) *Zh. Eksp. Teor. Fiz.*, **69**, 2218.
95. Romanov, V.P., Ovechkina, E.E. and Koshkin, V.M. (1977) *Fiz. Nizk. Temp.*, **3**, 1489.
96. Anisimova, O.A., Godovnikov, S.K., Gubskaya, G.F., Menshikova, T.K., Ufimtseva, E.F. and Frolov, Yu.P. (1982) *Izv. Akad. Nauk SSSR, Neorg. Mater.*, **18**, 573.
97. Klee, C., McNab, T.K., Litturs, G.I. and Micklitz, H. (1974) *Z. Phys.*, **270**, 31.
98. Pivnichny, I.V. and Brinzinger, H.H. (1973) *Inorg. Chem.*, **12**, 2839.
99. Kumera, M., Kobayashi, N., Suzuki, M. and Shimizu, T. (1975) *Japan J. Appl. Phys.*, **14**, 172.
100. Laskin, V.N., Chepeleva, I.V., Zhilinskaya, E.A. and Chernov, A.P. (1975) *Phys. Status Solidi B*, **69**, 399.
101. Shpinel', V.S. (1969) *Rezonans γ-Luchei v Kristallakh (γ-Radiation Resonance in Crystals)*. Moscow (in Russian).
102. Bryukhanov, V.A., Delyagin, N.N. and Shpinel', V.S. (1964) *Zh. Eksp. Teor. Fiz.*, **47**, 80.
103. Micklitz, H. and Barrett, P.H. (1972) *Phys. Rev.*, **B5**, 1704.
104. Micklitz, H. and Barrett, P.H. (1972) *Appl. Phys. Lett.*, **20**, 387.
105. Chekin, V.V., Vinnikov, A.P. and Balkashin, O.P. (1967) *Fiz. Tverd. Tela (Leningrad)*, **9**, 2993.
106. Blomquist, I., Rovs, B. and Sundbom, M. (1971) *J. Chem. Phys.*, **55**, 141.
107. Trautwein, A., Harris, F.E., Freeman, A.I. and Deslaux, I.P. (1975) *Phys. Rev.*, **B11**, 4101.
108. Kumer, K., Porch, H. and Kaltseis, I. (1972) *Phys. Lett.*, **A40**, 59.
109. Zalyubovskii, I.I., Koshkin, V.M., Kulagin, N.A., Ovechkina, E.E. and Podus, L.P. (1980) *Fiz. Tekh. Poluprovod.*, **14**, 2081.
110. Gerasimenko, V.S., Grushka, G.G. and Sheremet, G.P. (1984) *Izv. Akad. Nauk SSSR, Neorg. Mater.*, **20**, 1323.
111. Dekhtyar, I.Ya. and Rustamov, Zh.A. (1981) *Fiz. Tverd. Tela (Leningrad)*, **23**, 2206.
112. Swenson, H., Locker, D.R., Meese, J.M. and Manthuruthil, J.C. (1974) *IEEE Trans. Nucl. Sci.*, **NS-21**, 40.
113. Drabkin, I.A. and Kvantov, M.A. (1980) *Fiz. Tekh. Poluprovod.*, **14**, 1821.
114. Omel'yanovskii, E.M. and Fistul', V.I. (1983) *Primesi Perekhodzykh Metallov v Poluprovodnikakh (Transition Metal Impurities in Semiconductors)*. Moscow (in Russian).
115. Anan'ina, D.B., Bakumenko, V.L., Grushka, G.G., Kurbatov, L.N. (1976) *Fiz. Tekh. Poluprovod.*, **10**, 6.

116. Tagiev, B.G., Sultanov, G.D., Niftiev, G.N., Ascerov, I.M. and Aslanov, G.K. (1984) *Phys. Status Solidi A*, **184**, K159.
117. Askerov, I.M., Mekhnabov, A.O., Aslanov, G.K., Tagiev, B.G. and Nakhmetov, S.M. (1988) *Phys. Status Solidi A*, **105**, K151.
118. Dismukes, J.P. (1971) *J. Phys. Chem. Solids*, **32**, 1689.
119. Bogomolov, V.N. (1978) *Usp. Fiz. Nauk*, **124**, 171.
120. Reiss, H. (1956) *J. Chem. Phys.*, **25**, 681.
121. Koshkin, V.M. (1971) Avtoreferat doktorskoi dissertatskii (Author's abstract of a Doctoral Dissertation). Kharkov.
122. Bulaevskii, L.N. (1975) *Usp. Fiz. Nauk*, **116**, 449.
123. Ioffe, A.D. (1976) *Chem. Soc. Rev.*, **5**, 51.
124. Novikov, Yu.N. and Vol'pin, M.E. (1971) *Usp. Khim.*, **40**, 1568.
125. Rudorf, W. and Zeeler, K. (1955) *Z. Anorg. Allg. Chem.*, **B279**, 8.
126. Schölhorn, R. (1980) *Physica*, **99B**, 89.
127. Gamble, F.R., Osiecki, I.H. and Gais, M. (1971) *Science*, **174**, 493.
128. Friedel, J. (1964) *Dislocation*. New York.
129. Koshkin, V.M. and Mil'ner, A.P. (1983) *Pis'ma Zh. Tekh. Fiz.*, **9**, 123.
130. Mühlberger, R., Butz, T. and Lerf, A. (1981) *Physica*, **105B**, 218.
131. Kaluarachi, D. and Frindt, R.E. (1983) *Phys. Rev.*, **28B**, 3663.
132. Gurina, G.I., Evtushenko, V.D., Muraeva, O.A., Ignatyuk, V.P. and Koshkin, V.M. (1985) *Ukr. Khim. Zh.*, **51**, 1154.
133. Likhtman, V.I., Schchukin, E.D. and Rebinder, P.A. (1962) *Fizikokhimicheskaya Mekhanika Metallov (Physicochemical Mechanics of Metals)*. Moscow (in Russian).
134. Gurina, G.I., Evtushenko, V.D. and Koshkin, V.M. (1985) *Zh. Eksp. Teor. Khim.*, **21**, 123.
135. Koshkin, V.M., Mil'ner, A.P., Kukol', V.V., Zabrodskii, Yu.R., Dmitriev, Yu.N. and Brintsev, F.I. (1976) *Fiz. Tverd. Tela (Leningrad)*, **18**, 609.
136. Koshkin, V.M., Mil'ner, A.P., Kukol', V.V., Zabrodskii, Yu.R. and Katrunov, K.A. (1977) *Fiz. Tverd. Tela (Leningrad)*, **19**, 1608.
137. Koshkin, V.M., Yagubskii, E.B., Mil'ner, A.P. and Zabrodskii, Yu.R. (1976) *Pis'ma Zh. Eksp. Teor. Fiz.*, **24**, 129.
138. Mil'ner, A.P., Zabrodskii, Yu.R., Yagubskii, E.B., Koshkin, V.M. and Guseinov, G.D. (1980) *Zh. Strukt. Khim.*, **21**, 93.
139. Novikov, Yu.N., Kazakov, M.V., Zvarykina, A.V. and Vol'pin, M.E. (1971) *Zh. Strukt. Khim.*, **12**, 486.
140. Koshkin, V.M. (1981) *Izv. Akad. Nauk Latv. SSR*, **6**, 90.
141. Tompson, A.H. (1973) *Solid State Commun.*, **13**, 1911.
142. Mil'ner, A.P., Koshkin, V.M. and Kukol', V.V. (1979) *Pis'ma Zh. Tekh. Fiz.*, **5**, 351.
143. Acrivos, J.V. and Salau, J.R. (1974) *Philos. Mag.*, **30**, 603.
144. Berthier, C. (1981) *Solid State Ionics*, **5**, 379.
145. Gurina, G.I., Evtushenko, V.D., Gritskaya, N.A. and Koshkin, V.M. (1986) *Zh. Neorg. Khim.*, **31**, 826.
146. Toffield, B.C. and Wright, C.J. (1977) *Solid State Commun.*, **22**, 715.
147. Katrunov, K.A., Koshkin, V.M. and Kulakov, V.M. (1982) *Ukr. Fiz. Zh. (Russ. Ed.)*, **27**, 226.

148. Rouxel, J. and Le Blanc, A. (1971) *Roy. Bull. Chim. Fr.*, **6**, 2019.
149. Zabrodskii, Yu.R., Tolmachev, D.V., Paivin, V.S., Mil'ner, A.P. and Koshkin, V.M. (1987) *Fiz. Tverd. Tela (Leningrad)*, **29**, 892.
150. Di Salvo, F.G., Hule, G.W., Schwarts, L.H., Voohoere, V. and Waszezak, Y.V. (1973) *J. Chem. Phys.*, **59**, 1922.
151. Rouxel, J. (1980) *Physica*, **99B**, 3.
152. Safran, S.A. (1980) *Phys. Rev. Lett.*, **44**, 939.
153. Bol'shov, L.A. and Napartovich, A.P. (1973) *Zh. Eksp. Teor. Fiz.*, **64**, 1404.
154. Zabrodskii, Yu.R., Katrunov, K.A. and Koshkin, V.M. (1983) *Fiz. Tverd. Tela (Leningrad)*, **25**, 908.
155. Zabrodskii, Yu.R., Katrunov, K.A. and Koshkin, V.M. (1984) *Poverkhnost'. Fiz., Khim., Mekh.*, **3**, 36.
156. Khachaturiyan, A.G. (1962) *Fiz. Met. Metalloved.*, **13**, 493.
157. Barinskii, R.P., Shevchenko, E.P., Kulikova, M.M., Golub', A.S., Novikov, Yu.N. and Vol'pin, M.E. (1984) *Dokl. Akad. Nauk SSSR*, **274**, 1381.
158. Zabrodskii, Yu.R., Tolmachev, D.V., Mil'ner, A.P. and Koshkin, V.M. (1987) *Ukr. Fiz. Zh. (Russ. Ed.)*, **32**, 273.
159. Zabrodskii, Yu.R., Kornienko, V.A., Tolmachev, D.V. and Koshkin, V.M. (1986) *Zh. Eksp. Teor. Fiz.*, **91**, 1702.
160. Koshkin, V.M. and Katrunov, K.A. (1979) *Pis'ma Zh. Eksp. Teor. Fiz.*, **29**, 205.
161. Rybalka, A.I. and Miloslavskii, V.K. (1976) *Opt. Spektrosk.*, **41**, 252.
162. Katrunov, K.A. (1985) Avtoreferat kandidatskoi dissertatsii (Author's abstract of Candidate's Dissertation). Kharkov.
163. Shik, A.Ya. (1974) *Fiz. Tekh. Poluprovod.*, **8**, 1841.
164. Katrunov, K.A., Koshkin, V.M., Mil'ner, A.P. and Shevchenko, S.I. (1978) *Fiz. Nizk. Temp.*, **4**, 531.
165. Zabrodskii, Yu.R., Zaporozhskii, V.D. and Koshkin, V.M. (1988) *Dokl. Akad. Nauk Ukr. SSR*, Ser. A, No. 4, 51.
166. *Atomic Diffusion in Semiconductors* (Ed. Shaw, D.) (1973) London–New York.
167. Thompson, M.W. (1960) *Defects and Radiation Damage in Metals*. Cambridge.
168. Orlov, A.N. and Trushin, Yu.V. (1983) *Energii Tochechnykh Defektov v Metallakh (Energies of Point Defects in Metals)*. Moscow (in Russian).
169. Saidoh, M. and Itoh, N. (1973) *J. Phys. Chem. Solids*, **34**, 1165.
170. Gibson, J.B., Goland, A.N., Milgram, M. and Vinejard, G.H. (1960) *Phys. Rev.*, **120**, 1229.
171. Koshkin, V.M. and Zabrodskii, Yu.R. (1974) *Fiz. Tverd. Tela (Leningrad)*, **16**, 3480.
172. Koshkin, V.M. and Zabrodskii, Yu.R. (1976) *Dokl. Akad. Nauk SSSR*, **227**, 1323.
173. Koshkin, V.M. and Ulmanis, U.A. (1979) *Radiation Defects in the In$_2$Te$_3$-type Semiconductors*, LAFI-016, Salaspils.
174. Koshkin, V.M., Zabrodskii, Yu.R. and Podorozhanskaya, N.M. (1979) In *Voprosy Atmonoi Nauki i Tekhniki (Questions of Nuclear Science and Engineering), Fiz. Radiats. Povrezhd i Radiats. Materia-*

loved, Vol. 3 (11), p. 21. Kharkov.

175. Kosevich, A.M. (1972) *Osnyovy Mekhaniki Kristallicheskoi Reshetki (Principles of the Mechanics of Crystal Lattices)*. Moscow (in Russian).
176. Biget, M., Rizk, R., Vaida, P. and Besis, A. (1975) *Solid State Commun.*, **16**, 949.
177. Balzer, R. (1970) *Z. Phys.*, **234**, 242.
178. Kuznetsov, A.S. (1976) *Trudy IF AN Est. SSR*, **45**, 101.
179. Smirnov, N.I. (1976) *Fiz. Tekh. Poluprovod.*, **10**, 1596.
180. Koshkin, V.M. and Zabrodskii, Yu.R. (1990). In *Modelirovanie na EVM Defektov v Metallakh (Computer Simulation of Defects in Metals)*, p. 185. Leningrad (in Russian).
181. Koshkin, V.M., Minkov, B.I., Gal'chinetskii, L.P. and Kulik, V.N. (1973) *Fiz. Tverd. Tela (Leningrad)*, **16**, 128.
182. Oksengendler, B.L. (1979) In *Vliyanie Nesovershenstv Struktury na Svoistva Kristallov (Influence of Structural Imperfections on the Properties of Crystals)*, p. 11. Tashkent.
183. Tolpygo, K.B. and Kucher, T.I. (1967) *Fiz. Tekh. Poluprovod.*, **1**, 77.
184. Koshkin, V.M. (1964) *Ukr. Fiz. Zh. (Russ. Ed.)*, **9**, 975.
185. Landau, L.D. (1971) *Sobr. Nauchn. Trudov (Collected Scientific Publications)*, Vol. 1. p. 81. Moscow (in Russian).
186. Koshkin, V.M., Zabrodskii, Yu.R. and Dmitriev, Yu.N. (1976) In *Khimicheskaya Svyaz' v Kristallakh i Tkh Fizicheskie Svoistv (Chemical Bonding in Crystals and Their Physical Properties)*, Vol. 1, p. 42. Minsk.
187. Damask, A.C. and Dienes, G.J. (1963) *Point Defects in Metals*. New York.
188. Lomer, W.M. (1959) *Progr. Metal Phys.*, **8**, 255.
189. Koshkin, V.M. and Ekkerman, V.M. (1974) *Fiz. Tverd. Tela (Leningrad)*, **16**, 3728.
190. Ekkerman, V.M., Gal'chinetskii, L.P. and Koshkin, V.M. (1974) *Fiz. Tverd. Tela (Leningrad)*, **16**, 1551.
191. Ekkerman, V.M., Koshkin, V.M., Gal'chinetskii, L.P. and Seredenko, T.N. (1972) In *Monokristally i Tekhnika (Single Crystals and Technology)*, Vol. 1, p. 144, Kharkov (in Russian).
192. *Fizika Superionnykh Provodnikov (Physics of Superionic Conductors)* (Ed. Salamon, N.B.). Riga (in Russian).
193. Gurevich, Yu.Ya and Kharkats, Yu.I. (1987) *Superionnaya Provodimost' Tverdykh Tel (Superionic Conduction of Solids)*. VINITI AN SSSR, 4 (in Russian).
194. Zabrodskii, Yu.R., Reshetnyak, Yu.B. and Koshkin, V.M. (1990). *Fiz. Tverd. Tela (Leningrad)*, **32**, 69.
195. Zabrodskii, Yu.R., Reshetnyak, Yu.B. and Koshkin, V.M. (1990) *Dokl. Akad. Nauk Ukr. SSR*, **7**, 57.
196. Strukov, B.A. and Levanyuk, A.P. (1983) *Fizicheskie Osnovy Segnetoelektricheskikh Yavlenii v Kristtalakh (Physical Principles of Ferroelectric Phenomena in Crystals)*. Moscow (in Russian).
197. Buhrer, W. and Halg, W. (1974) *Helv. Phys. Acta*, **47**, 27.
198. Wright, A.F. and Fender, B.E.F. (1977) *J. Phys. C*, **10**, 2261.
199. Cava, R.J., Reidinger, F. and Buensch, B.J. (1977) *Solid State Commun.*, **24**, 411.

200. Koshkin, V.M. and Zabrodskii, Yu.R. (1976) *Radioatsionnye Defekty v Poluprovodnikovykh Soedineniyakh (Radiation Defects in Semiconductor Compounds)*, Preprint KIYaI 76-22. Kiev (in Russian).
201. Cava, R.J. and McWhan, D.B. (1980) *Phys. Rev. Lett.*, **45**, 2046.
202. Stefanovich, S.Yu., Ivanova, L.A. and Astaf'ev, A.V. (1989) *Ionnaya i Superionnaya Provodimost' v Segnetoelektrikakh (Ionic and Superionic Conduction in Ferroelectric Materials)*. Moscow (in Russian).
203. Stefanovich, S.Yu., Kalinin, V.B. and Nogai, A. (1984) *Ferroelectrics*, **55**, 325.
204. Vorontsova, V.I. and Yanovskii, V. (1988) *Izv. Akad. Nauk SSSR, Neorg. Mater.*, **24**, 2062.
205. Volkov, A.A., Goncharov, Yu.G., Kozlov, G.V., Mirzoyants, G.I. and Prokhorov, A.M. (1986) *Dokl. Akad. Nauk SSSR*, **289**, 846.
206. Funke, K. and Schneider, H.J. (1984) *Solid State Ionics*, **13**, 335.
207. Zabrodskii, Yu.R., Reshetnyak, Yu.B. and Koshkin, V.M. (1990) *Ukr. Fiz. Zh. (Russ. Ed.)*, **35**, 611.
208. Koshkin, V.M. and Muraeva, O.A. (1987) *Chisla Sol'vatatskii (Solvation Numbers)*. UkrNIINTI, Dep. N. 2905-UK-87 (in Russian).
209. Reshetnyak, Yu.B. (1990) Avtoreferat kandidatskoi dissertatsii (Author's abstract of Candidate's Dissertation). Kharkov (in Russian).
210. Vinetskii, V.L. and Kholodar', G.A. (1979) *Radiatsionnaya Fizika Poluprovodnikov (Radiation Physics of Semiconductors)*. Kiev (in Russian).
211. Lehmann, Chr. (1977) *Interaction of Radiation with Solids and Elementary Defects Production*. New York.
212. Vinetskii, V.L., Entinzon, I.R. and Kholodar', G.A. (1979) *Fiz. Tekh. Poluprovod.*, **13**, 912.
213. Lapina, N.A., Mannanova, Kh.Kh., Oksengendler, B.L. and Yunusov, M.S. (1985) *Dokl. Akad. Nauk Uzb. SSR*, **10**, 21.
214. Geguzin, Ya.E., Zabrodskii, Yu.R. and Koshkin, V.M. (1979) *Fiz. Tverd. Tela (Leningrad)*, **21**, 1755.
215. Lifshits, I.M., Kaganov, M.I. and Tanatarov, L.V. (1979) *At. Energ.*, **6**, 391.
216. Silsbee, R.H. (1957) *J. Appl. Phys.*, **28**, 1246.
217. Nelson, R.S. and Thompson, M.W. (1961) *Proc. Roy. Soc.*, **259**, 458.
218. Koshkin, V.M., Dmitriev, Yu.N., Zabrodskii, Yu.R., Tarnopol'skaya, R.A. and Ulmanis, U.A. (1984) *Fiz. Tekh. Poluprovod.*, **18**, 1373.
219. Dmitriev, Yu.N. (1985) Avtoreferat kandidatskoi dissertatsii (Author's abstract of Candidate's Dissertation). Kharkov (in Russian).
220. Urosov, V.S. (1975) *Energeticheskaya Kristallokhimiya (Energy Aspects of Crystal Chemistry)*. Moscow (in Russian).
221. Akilov, Yu.Z. and Lenchenko, V.M. (1974) *Fiz. Tekh. Poluprovod.*, **8**, 30.
222. Anderson, G.S. (1962) *J. Appl. Phys.*, **33**, 2017.
223. Torrens, I.C. and Chadderton, L.T. (1967) *Phys. Rev.*, **159**, 671.
224. Gal'chinetskii, L.P., Koshkin, V.M., Kulakov, V.M., Kulik, V.N., Ulmanis, U.A. and Shakhovtsov, V.I. (1972) In *Monokristally i Tekhnika (Single Crystals and Technology)*, Vol. 6, p. 97. Kharkov (in

Russian).

225. Gal'chinetskii, L.P., Koshkin, V.M., Kulik, V.N. and Ulmanis, U.A. (1985) *Elektron. Tekh. Materialy*, **10**, 29.

226. Gal'chinetskii, L.P., Karas', V.R., Korin, A.I., Koshkin, V.M., Kulik, V.N., Ryabka, P.M. and Ulmanis, U.A. (1976) *Elektron. Tekh., Materialy*, **10**, 72.

227. Koshkin, V.M., Gal'chinetskii, L.P., Kulik, V.N., Gusev, G.K. and Gur'ev, V.R. (1977) *Prib. Tekh. Eksp.*, **3**, 66.

228. Koshkin, V.M., Usoskin, A.I. and Kulakov, V.M. (1977) In *Fizika i Khimiya Kristallov (Physics and Chemistry of Crystals)*, p. 48. Kharkov (in Russian).

229. Koshkin, V.M., Gal'chinetskii, L.P., Kulik, V.N., Gusev, G.K. and Ulmanis, U.A. (1977) *At. Energ.*, **12**, 290.

230. Gal'chinetskii, L.P., Katrunov, K.A., Koshkin, V.M. and Kulik, V.N. (1981) *At. Energ.*, **50**, 144.

231. Koshkin, V.M., Gal'chinetskii, L.P., Kulik, V.N. and Ulmanis, U.A. (1976) *Radiatsionnye Defekty v Poluprovodnikovykh Soedineniyakh (Radiation Defects in Semiconductor Compounds)*, Preprint KIYaI 76-22. Kiev (in Russian).

232. Anan'ina, D.B., Bakumenko, V.L., Grushka, G.G., Zaitov, F.A., Kurbatov, L.N. and Shalyapina, L.M. (1976) *Izv. Akad. Nauk SSSR, Neorg. Mater.*, **12**, 2074.

233. Turovič, A., Petrovič, B., Etlinger, B., Urei, N.B., Radautsan, S.I., Zhitar, V.F., Tiginyanu, I.M. and Machuga, A.I. (1985) *FZKAAA*, **17**, 7.

234. Volgin, Yu.N., Kovalev, V.P. and Ukhanov, Yu.I. (1970) *Fiz. Tekh. Poluprovod.*, **4**, 2400.

235. Tarnopol'skaya, R.A., Dmitriev, Yu.N. and Koshkin, V.M. (1984) *Ukr. Fiz. Zh. (Russ. Ed.)*, **29**, 469.

236. Dmitriev, Yu.N., Koshkin, V.M., Tarnopol'skaya, R.A. and Ulmanis, U.A. (1984) *Fiz. Tverd. Tela (Leningrad)*, **26**, 2497.

237. Dmitriev, Yu., Koshkin, V. and Ulmanis, U. (1988) *Phys. Status Solidi A*, **106**, K7.

238. Zabrodskii, Yu.R. and Koshkin, V.M. (1987) *Fiz. Tverd. Tela (Leningrad)*, **18**, 2857.

239. Slezov, V.V. and Sagalovich, V.V. (1987) *Usp. Fiz. Nauk*, **151**, 67.

240. Bakai, A.S., Zelenskii, V.F. and Neklyudov, I.M. (1983) *Voprosy Atomnoi Nauki i Tekhniki (Questions of Nuclear Sciences and Engineering), Fiz. Radiats. Povrezhd. i Radiats. Materialoved*, Vol. 5 (28), p. 3. Kharkov (in Russian).

241. Egorushkin, V.E., Panin, V.E., Savushkin, E.V. and Khon, Yu.A. (1987) *Izv. Vyssh. Uchebn. Zaved., Fiz.*, **1**, 9.

242. Koshkin, V.M. and Zabrodskii, Yu.R. (1991). In *Sil'novozbuzhdennye Sostoyaniya v Kristallakh (Highly Excited States in Crystals)*, p. 115. Tomsk (in Russian).

243. Sayapina, O.V. and Koshkin, V.M. (1990) *Pis'ma Zh. Tekh. Fiz.*, **16**, 58.

244. Wittingham, M.S. U.S. Pat., N 4 009.052 (1976), HO1M 35/02.

245. Wittingham, M.S. U.S. Pat., N 4 144.384 (1979), MKUHO 1M 4/58.

246. Wittingham, M.S. (1976) *Science*, **192**, 1126.

247. Tributsch, H. (1980) *J. Appl. Phys.*, **23**, 61.

248. Tributsch, H. and Butz, G. (1984) *J. Electrochem. Soc.*, **131**, 640.

249. Gurina, G.I., Evtushenko, V.D., Kobyakov, A.Yu. and Koshkin, V.M. (1985) *Zh. Teor. Eksp. Khim.*, **21**, 770.

250. Esaki, L. and Tsu, R. (1970) *IBM J. Res. and Develop.*, **14**, 61.

251. Eklund, P.C. and Smith, H.G. (1984) *J. Appl. Crystallogr.*, **17**, 400.

252. Novikov, Yu.N. and Vol'pin, M.E. (1981) *Physica*, **105B**, 471.

253. Novikov, Yu.N., Lapkina, N.D. and Vol'pin, M.E. (1976) *Kinetika i Kataliz*, **17**, 1537.

254. Kalashnikov, Ya.A., Farafontov, V.I., Novikov, Yu.N. and Vol'pin, M.E. (1979) *Izv. Akad. Nauk SSSR, Khim.*, **2**, 474.

255. Koshkin, V.M., Gal'chinetskii, L.P., Kulik, V.N. and Kulakov, V.M. (1974) In *Monokristally i Tekhnika (Single Crystals and Technology)*, Vol. 1, p. 114. Kharkov.

256. Figotin, L.I. (1980) In *Rost i Svoistva Kristallov (Growth and Properties of Crystals)*, Vol. 6, p. 129. Kharkov.

257. Koshkin, V.M., Gurina, G.I. and Savchenko, K.V. (1992) *J. Photochem. Photobiol. A., Chem.*, **64**, 369.

INDEX

(Continued from the inside front cover)

*ECU (European Currency Unit) is the worldwide base list currency rate; payment can be made by draft drawn on ECU currency in the amount shown or in local currency at the current conversion rate. The US Dollar rate is based on the ECU rate and applies to North American subscribers only. Subscribers from other territories should contact their agents or one of the offices listed below.

To order direct and for enquiries, contact:

Europe
Y-Parc, Chemin de la Sallaz
1400 Yverdon, Switzerland
Telephone: (024) 239 670
Fax: (024) 239 671

Far East (excluding Japan)
Kent Ridge, PO Box 1180
Singapore 9111
Telephone: 741 6933
Fax: 741 6922

USA
PO Box 786, Cooper Station
New York, NY 10276
Telephone: (212) 206 8900
Fax: (212) 645 2459

Japan
Yohan Western Publications Distribution Agency
3-14-9, Okubo, Shinjuku-ku, Tokyo 169
Telephone: (03) 3208 0181
Fax: (03) 3209 0288

License to Photocopy

Reprints of Individual Articles

Copies of individual articles may be obtained from the Publisher's own document delivery service at the appropriate fees. Write to: SCAN, PO Box 786, Cooper Station, New York, NY 10276, USA or Y-Parc, Chemin de la Sallaz, 1400 Yverdon, Switzerland. Special Fax Service — USA: (212) 645 2459 or Switzerland: (024) 239 671.

Distributed by STBS - Publisher's Distributor

Printed in the United States of America

May 1994